2016-08-05

Exploiting DNA Repair and ER Stress Response Pathways to Induce Apoptosis in Glioblastoma Multiforme: A Dissertation

Jessica L. Weatherbee
University of Massachusetts Medical School

EXPLOITING DNA REPAIR AND ER STRESS RESPONSE PATHWAYS TO INDUCE APOPTOSIS IN GLIOBLASTOMA MULTIFORME

A Dissertation Presented

By

JESSICA LEIGH WEATHERBEE

Submitted to the Faculty of the

University of Massachusetts Graduate School of Biomedical Sciences, Worcester

in partial fulfillment of the requirements for the degree of

DOCTOR OF PHILOSOPHY

August 5th 2016

INTERDISCIPLINARY GRADUATE PROGRAM

EXPLOITING DNA REPAIR AND ER STRESS RESPONSE PATHWAYS TO INDUCE APOPTOSIS IN GLIOBLASTOMA MUTIFORME

A Dissertation Presented
By

Jessica Leigh Weatherbee

This work was undertaken in the Graduate School of Biomedical Sciences

Interdisciplinary Graduate Program

The signature of the Thesis Advisor signifies
validation of Dissertation Content

_____

Alonzo Ross, Ph.D., Thesis Advisor

The signatures of the Dissertation Defense Committee signify
completion and approval as to style and content of the Dissertation

_____

Thomas Fazzio, Ph.D., Member of Committee

_____

Junhao Mao, Ph.D., Member of Committee

_____

Dannel McCollum, Ph.D., Member of Committee

_____

Brent Cochran, Ph.D., External Member of Committee

The signature of the Chair of the Committee signifies that the written dissertation meets
the requirements of the Dissertation Committee

_____

Miguel Sena-Esteves, Ph.D., Chair of Committee

The signature of the Dean of the Graduate School of Biomedical Sciences signifies
that the student has met all graduate requirements of the School.

_____

Anthony Carruthers, Ph.D.,
Dean of the Graduate School of Biomedical Sciences

August 5th, 2016

Dedication

For my family

Acknowledgements

It has been said that it takes a village to raise a child. Similarly, the development, progression, and culmination of this project and, more importantly, my growth as a scientist would not have been possible without:

Alonzo Ross, for giving me the freedom to explore multiple aspects of the project while teaching me to carefully and thoughtfully analyze data. More importantly, that it's ok to ask questions and not know the answers. Yulian Ramirez-Ellis, a sounding board for experiments, a second pair of eyes to check calculations and data, a listening ear for all things, and, most importantly, for the friendship and stories that began in the Diciest of times. Elizabeth Luna, whose key insights made me critically not only re-think data but also the best way to present it, an art she has skillfully mastered, and one I aspire to. Tara Smith, for her patient manner and invaluable guidance regarding staining and microscope work. Jean-Louis Kraus a patient collaborator who was truly excited to see the work progress. Richard Moser and the UMASS Tumor Bank for providing primary tumor samples used in the paper. To the UMASS FACS Core as well as the UMASS animal facility technicians Beverly and Luanne, for their help and friendship. To the IGP department, in particular Darla Cavanaugh, for her expert administrative assistance in navigating the myriad of required forms over these last seven years. To the BMP department for their financial support, in particular Bob Matthews and Tony Carruthers, as well as the invaluable administrative assistance provided by Karen Lekas and Elizabeth Hoyt. Past and present TRAC

members, Jean Marie Houghton, Miguel Sena-Esteves, Thomas Fazzio, Junhao Mao, and Dannel McCollum, for their time and guidance. To the DEC members, Miguel Sena-Esteves, Thomas Fazzio, Junhao Mao, Dannel McCollum, and Brent Cochran, for their insightful questions and for pushing me to think at a different level. Especially to Miguel Sena-Esteves, who has been a part of this journey from the qualifying exam to the defense, and who continually provided guidance, support, encouragement, and mentorship, making it possible to finish the last two miles of the marathon started seven years ago. Thank you.

The laughter, support, encouragement, and friendship of Kelly Hallstrom, Diane Golebiowski, Lorelei Stoica, Laura Deveau, Jennifer Cotton, Nomeda Girnius, Cassie Blanchette, Michelle Dubuke, Cara Weismann, and Dwijit GuhaSarkar made this process doable and that much more enjoyable. To Sebastian Mana-Capelli, for the many hours spent discussing science, politics and books. To William Monis, who listened to my science horror stories and always offered a helping hand, and to Karen Mruk, for buoying me through tough times, acting as an infinite reservoir of knowledge and support throughout paper and thesis writing and career decisions, thank you.

To the Sagerstrom lab, Priya Ghosh, Jennifer Maurer, Ozge Yildiz, Franck Ladam, Will Stanney, and Denise Zannino, for being my lab family, for listening, supporting, and patiently answering my many questions. More importantly, for your friendship, which made the bad science days not so bad.

To friends who are family, Michelle Colen, Mike “Connor” McGilvray, Maddie Pawlina, and Cat and Tristan Lubinski, for your endless support and encouragement over the last seven years.

To the Tidd family, for understanding last minute change of plans and absences at events. To Stephen Hequembourg, for being my steady and calming force through the good and the bad. Lastly, to my parents, Darlene and Charles Weatherbee, who listened tirelessly, supported and encouraged me relentlessly, celebrated my progresses, and helped me navigate my failures; I could not have done this without you.

Abstract

Glioblastoma multiforme (GBM) is a deadly grade IV brain tumor characterized by a heterogeneous population of cells that are drug resistant, aggressive, and infiltrative. The current standard of care, which has not changed in over a decade, only provides GBM patients with 12-14 months survival post diagnosis. We asked if the addition of a novel endoplasmic reticulum (ER) stress inducing agent, JLK1486, to the standard chemotherapy, temozolomide (TMZ), which induces DNA double strand breaks (DSBs), would enhance TMZ's efficacy. Because GBMs rely on the ER to mitigate their hypoxic environment and DNA repair to fix TMZ induced DSBs, we reasoned that DSBs occurring during heightened ER stress would be deleterious.

Treatment of GBM cells with TMZ+JLK1486 decreased cell viability and increased cell death due to apoptosis. We found that TMZ+JLK1486 prolonged ER stress induction, as indicated by elevated ER stress marker BiP, ATF4, and CHOP, while sustaining activation of the DNA damage response pathway. This combination produced unresolved DNA DSBs due to RAD51 reduction, a key DNA repair factor. The combination of TMZ+JLK1486 is a potential novel therapeutic combination and suggests an inverse relationship between ER stress and DNA repair pathways.

Table of Contents

Figure List

List of Copyrighted Materials

Material from the below open-access journal was used in the Abstract, Chapter II, and Chapter III:

Weatherbee JL, Kraus J-L, Ross AH. ER stress in temozolomide-treated gliomblastomas inteferes with DNA repair and induces apoptosis. *Oncotarget*. 2016.

Preface

Chapter II is published as follows: Weatherbee JL, Kraus J-L, Ross AH. ER stress in temozolomide-treated gliomblastomas inteferes with DNA repair and induces apoptosis. *Oncotarget*. 2016.

Chapter III TMZ+JLK1486 discussion was published in part in Weatherbee JL, Kraus J-L, Ross AH. ER stress in temozolomide-treated gliomblastomas inteferes with DNA repair and induces apoptosis. *Oncotarget*. 2016.

All experiments were performed and analyzed by Weatherbee, JL

JLK1486 was synthesized and provided by Kraus, J-L.

Figure 7: Annexin V vs. PI staining and sample running was performed by the UMASS Flow Cytometry Core. FlowJo data analysis and quantification was performed by Weatherbee, JL.

Figure 11 and 12: ATF4 sh control, shATF4 C1, and shATF4 E7 lentivirus was made by the UMASS shRNA Core Facility. Infections and generation of stable lines were performed by Weatherbee, JL.

CHAPTER I

Introduction to Glioblastoma Multiforme

Overview and rationale

Glioblastoma Multiforme (GBM) is a deadly grade IV brain tumor characterized by a heterogeneous population of cells forming a chemotherapeutic resistant, highly aggressive, and infiltrative tumor [1]. The development of comparative genomic hybridization (CGH) coupled with cDNA microarray analysis, fluorescent in situ hybridization (FISH), and completion of the cancer genome atlas (TCGA) has done much to identify and increase the understanding of mutations leading to GBM development and progression [2-4]. This knowledge will, hopefully, culminate in the development of effective, targeted therapies. At this time, the best treatment available for GBM patients is comprised of surgical resection, radiation therapy (RT) and the chemotherapeutic agent temozolomide (TMZ) [1] [5]. This provides GBM patients with a 12 to 14 months survival period post diagnosis, with only 6.9 months between treatment completion and tumor relapse [5]. This leaves much room for improvement.

Combination therapies are an attractive therapeutic approach as two pathways, critical for survival, can be inhibited. This may lead to decreased viability and delay tumor recurrence in patients. GBMs are solid tumors with viable cells maintained in extreme regions of hypoxia with decreased access to nutrients and glucose [6-9]. Such an unfavorable environment should activate the endoplasmic reticulum (ER) stress response pathway, resulting in cell death

[10]. However, glioma cells increase expression of pro-survival ER factors, turning this homeostasis mechanism into one that promotes cancer cell survival [11-15]. In addition to thriving in a state of chronic stress, glioma cells must prevent their highly unstable genomes from triggering apoptosis during replication. To circumvent this, GBMs increase the expression of DNA repair factors to promote homologous recombination (HR) [16-18]. The repair of deleterious DNA double strand breaks (DSB) keeps their fragile, aberrant genomes intact, supporting their viability.

Manipulating these pathways may exacerbate the fine balance of surviving ER stress and genomic instability, pushing the cell towards death. The work presented in this dissertation explores the combination of a DNA alkylating agent (TMZ) with a novel ER stress-inducing drug, JLK1486. We reasoned that induction of prolonged ER stress in the presence of increased DNA damage would be catastrophic. This work found that JLK1486 increased the efficacy of TMZ, resulting in decreased viability due to apoptosis [19]. Induction of apoptosis was the result of prolonged, unresolved ER stress promoting unrepaired DNA DSBs due to reduction of the key DNA HR factor, RADiation sensitive 51 (RAD51) [19]. To understand why the combination is detrimental to cells, we will address two themes: DNA repair and the ER stress response pathway.

WHO Classification of astrocytomas

The World Health Organization (WHO) categorizes astrocytomas into four grades, grade I being the least aggressive and grade IV the most [3].

Accumulation of genetic alterations drives grade progression and tumor aggressiveness [3].

Pilocytic astrocytomas, grade I brain tumors, are benign masses with slow growing, well-differentiated cells [20]. These tumors rarely progress and are considered curable as they can be surgically removed [20].

Astrocytomas, grade II brain tumors, are comprised of highly proliferative and infiltrative cells [21]. Because these cells infiltrate into normal brain, complete surgical resection is nearly impossible. One of the first genetic alterations associated with grade II are P53 mutations [20-21]. Mutations, usually in exons 5, 7 or 8, result in either missense or frameshifts that inactivate P53's DNA binding domain [21]. As P53 has been implicated in the regulation of over 2,500 genes, it is easy to understand how its loss would impact cell integrity [4]. The best-characterized target of P53, P21, is a cyclin dependent kinase (CDK) inhibitor responsible for initiating and maintaining a G1 to S cell cycle arrest [4] [21]. Therefore, P53 mutations result in loss of cell cycle arrest and increased proliferation due to decreased P21 transcription. In addition to P53 mutations, 30% of astrocytomas present with loss of heterozygosity (LOH) of chromosome 22q, the coding region for a pro-apoptotic member of the Bcl-2 family [3]. P53 and 22q LOH are early events that initiate astrocytoma development by generating a population of highly proliferative and apoptosis resistant glioma cells. These genetic alterations facilitate grade II to grade III progression.

Anaplastic astrocytomas, grade III tumors, contain grade II genetic alterations as well as LOH of 19q and deletion of tumor suppressor genes (TSGs) found on chromosomes 9p (P16), 11p,13q (retinoblastoma;RB), and 19q [20, 21]. Loss of P16 promotes CDK4/Cyclin D1 complex formation and kinase activity, resulting in phosphorylation of RB [21]. Phosphorylated RB is unable to bind E2F transcription factors, resulting in increased expression of G1 to S cell cycle progression factors. As P16 and RB function as cell cycle brakes, their loss allows aberrant cells to cycle.

Glioblastomas, grade IV brain tumors, are divided into two categories, progressive (secondary tumors) or de-novo (primary tumors) [22]. Progressive tumors are derived from lower grade astrocytomas, grade II and III, accumulating additional mutations over a 5-10 year span, leading to grade IV tumors [4] [20]. Conversely, de novo GBM patients lack clinical or histopathological evidence of a preceding tumor [1] [20]. Two characteristics distinguish de novo GBMs from secondary GBMs. First, 67% of secondary tumors contain P53 mutations in comparison to only 11% of de novo tumors, suggesting secondary GBMs depend on P53 mutations to promote tumorigenicity and progression [20]. Second, 40 to 63% of de novo tumors present with LOH of chromosome 10, resulting in loss of the phosphatase and tensin homolog (PTEN) TSG [1] [20] [22]. As secondary GBM tumors are less common than de novo ones, the genetic alterations that contribute to de novo GBM proliferation, angiogenesis, invasion, and apoptotic

resistance will be examined [1] [20]. Understanding these pathways leads to the development of smarter combination therapies for GBM patients.

Clinical and pathological presentations of GBMs

GBM patients initially present with symptoms of headache, memory loss, confusion, seizure, and changes in personality [1]. De novo GBMs are diagnosed in patients 50 years of age and older and are 40% more common in men than women [1]. MRIs indicate a brain mass associated with edema and central regions of necrosis surrounded by areas of hypoxia [1] [21]. These regions are comprised of proliferating glioma cells as well as endothelial cells [4]. As these tumors are highly infiltrative, surgeons must balance obtaining clean margins with quality of life after surgery [1] [21] [23].

De novo GBM genetic alterations: losses, translocations, and amplifications

CGH, FISH, and direct sequencing of grade IV GBMs identified large numbers of chromosomal aberrations [2,3]. CGH studies suggest GBMs have at least fourteen genomic amplifications and seventeen or more genomic losses and deletions that drive GBM development [2,4].

Loss of chromosomes 1, 10, 11, 13, 17, 19 and 22 are common and often associated with mutations in the CDKN2 and PTEN TSGs [2]. Correlation studies suggest loss of 1p occurs with loss of 19q, while gain of chromosome 7 occurs with loss of chromosome 10, and loss of chromosome 10 occurs with loss of 19q [2,3]. Gain of 8q was found to occur with loss of 9p while co-amplification of 3p

and 12p was correlated with loss of chromosomes 10 and 20 [3]. Recently, five novel regions containing TSGs including TOPR5, FANCG, and TP53BP1, were found to be deleted in GBMs [3]. This clearly illustrates how genome losses and amplifications result in a heterogeneously unstable genome. This unstable genome might be therapeutically exploited as inhibition of DNA repair factors may prevent glioma cells from maintaining their aberrant chromosomes.

In 2008, the Cancer Genome Atlas sequenced over 200 human GBMs, isolating candidate cancer genes as well as analyzing methylation status, DNA copy number variation, and non-coding RNAs in GBMs. This work suggests that mutations in cell cycle regulators and receptor tyrosine kinase pathways are key to GBM development [24].

PI3K / PTEN / AKT axis

Ablation of PTEN, occurring in 40-63% of GBM patients, is due to LOH of chromosome 10 [1] [20] [22]. This is problematic as PTEN negatively regulates receptor tyrosine kinases (RTKs) pathways that promote survival [4]. PTEN loss results in mitogen-activated phosphoinositide-3-kinases (PI3Ks) generating anionic phospholipids that turn on downstream survival kinase pathways, such as AKT [4]. AKT promotes cell cycle progression by sequestering the FOXO transcription factor in the cytoplasm, preventing transcription of p21, resulting in increased CDK/cyclin E complex formation and loss of G1 cell cycle arrest [4]. In addition to increasing RTK activity, PTEN loss decreases chromosomal stability, as it has been shown to bind to chromosome centromeres and facilitate DNA

repair [4]. As PTEN regulates processes ranging from cell division to DNA repair, it is easy to see how loss of this TSG impacts several pathways, resulting in genomic and cellular aberrations.

Epidermal Growth Factor Receptor amplification

The epidermal growth factor receptor (EGFR), a RTK that promotes proliferation and inhibits apoptosis, is amplified in 35 to 63% of de novo grade IV tumors [1] [4] [20] [22]. Amplification results in increased mRNA levels as well as protein levels [22]. Fifty percent of patients with amplified EGFR have deletions in exons 2-7, resulting in a constitutively active receptor due to partial loss of the extracellular binding domain [1]. This variant, VIII, increases proliferation and decreases apoptosis in comparison to full length amplified EGFR [4].

EGFR amplification and the VIII variant transmit cyto-protective measures through the PI3K/AKT and RAS/RAF/MEK/ERK signaling cascade [25]. VIII in particular leads to increased repair of DNA double strand breaks (DSBs) by increasing activation of DNA damage response (DDR) factors, including ataxia telangiectasia-mutated kinase (ATM) and RADiation sensitive 51 (RAD51) [25]. EGFR and MEK inhibitors decrease ATM and RAD51 mediated repair of DNA DSBs, increasing genomic instability, resulting in decreased viability [25]. Manipulation of DNA repair factors, in particular RAD51, may be a means to sensitize cells that have exploited RTK pathways to maintain their highly unstable genomes.

The VIII variant also promotes vasculature development *in vivo* [26]. Mice injected with VIII-expressing glioma cells versus amplified full length EGFR resulted in faster and larger tumor formation with increased vascular proliferation. This was due to increased expression and secretion of interluekin-6 (IL-6) elevating expression of vascular endothelial growth factor (VEGF), which induces the proliferation of endothelial cells [26]. Thus, targeting of the EGFR pathway may not only sensitize cells by preventing the repair of DNA DSBs, but may also decrease tumor vasculature, also decreasing tumor cell viability.

Increased expression of the Platelet Derived Growth Factor Receptor

In addition to EGFR over-expression, grade IV tumors also present with increased expression of the platelet derived growth factor receptor (PDGFR)[1] [3,4]. Increased expression of the receptor coincides with increased expression of PDGF alpha and beta-activating ligands, creating an autocrine loop [1] [4]. PDGFR activation promotes and supports glioma proliferation while inhibiting apoptosis by also signaling through the PI3K-AKT-mTOR pathways, again highlighting how loss of PTEN promotes tumorigenicity [1] [4].

Loss of cell cycle regulation

Although aberrant activation of RTKs promotes cell cycle entry and progression, the highly aberrant genome of glioma cells should trigger cell cycle arrest, leading to apoptosis. To prevent this, grade IV tumors use LOH of P16, resulting in loss of RB mediated G1 arrest, to allow S phase entry despite unrepaired single strand breaks, crosslinks, or mismatches [4]. Additionally, 15%

of grade IV tumors have amplified CDK4, circumventing wild type RB negative regulation of CDK transcription [2] [4].

Resistance to apoptosis

Increased resistance to apoptosis is primarily due to loss of PTEN's negative regulation of the PI3K / AKT signaling axis [4]. However, GBMs have evolved two additional mechanisms to evade apoptosis. First, to avoid extrinsic cell death mediated by TRAIL binding to death receptors 4 and/or 5 (DR4, DR5), glioma cells express death decoy receptors (DDcR) [4]. These DDcRs act as antagonistic receptors, preventing TRAIL from binding and initiating cell death through caspase effectors downstream of DR5. Secondly, glioma cells escape intrinsic mediated apoptosis by up-regulating the expression of Bcl-2 anti-apoptotic members, such as BAK, BAD, BID, BAX, and BCL-XL [4]. This shifts the ratio in favor of Bcl-2 pro-survival factors, preventing activity of pro-apoptotic Bcl-2 member from promoting mitochondrial mediated apoptosis through release of cytochrome C and cleavage of effector caspase 3. For example, the EGFR VIII mutation up-regulates Bcl-XL expression, correlating with chemotherapeutic resistance to and prevention of cell death caused by cross-linking agents such as cisplatin [4].

Solid tumors are at high risk of hypoxia-induced death. Normal brain oxygen levels range from 0.5 to 7%; however, 42% of gliomas present with severe hypoxia, defined as regions with oxygen levels less than 0.1% [9]. This is due to rapidly proliferating cells moving beyond the area oxygen can diffuse from

blood vessels. To alleviate this, glioma cells express high levels of angiogenic factors, such as VEGF, angiopietin 2, and PDGF [4] [8]. Although this promotes blood vessel formation, the resulting network is highly aberrant due to hyperplastic endothelial cells forming twisted, non-connected, and dead-end junctions [1] [4] [9]. In addition to malformed vessels, endothelial cells within the vessels do not form tight junctions, resulting in leaky, inefficient delivery. As pressure builds within the tortuous vessels, they often hemorrhage. Instead of promoting blood flow, the suboptimal network exacerbates hypoxic conditions as it is unable to efficiently deliver oxygen and nutrients to rapidly proliferating cells [4]. This results in necrosis, a pathological hallmark of GBMs [4] [8].

Although hypoxia-induced necrosis is lethal to some glioma cells, it promotes tumorigenicity by forming a population of chemotherapeutic and radiation resistant cells [4]. Radiation is only effective when oxygen generates free radicals to react with DNA, forming single and double stranded breaks. If oxygen levels are low, the formation of damaging free radicals is greatly reduced [69]. Additionally, abnormal blood vessel development impedes chemotherapeutics delivery, increasing resistance. Therefore, hypoxia selects cells capable of surviving and proliferating in an adverse environment, creating a sub-population of cells with increased tumorigenicity.

In addition to promoting chemo and radiation resistance, hypoxia promotes invasion, providing a mechanism for cells to exit unfavorable environments. For instance, GBMs increase expression of metalloproteases

(MMP) 2 and 9 that correlate with an invasive phenotype in response to hypoxia [4] [27]. Additionally, increased expression of cysteine proteases, in particular cathepsin beta, aids invasion by degrading the extracellular matrix (ECM) [4] [28].

The myriad of genetic alterations promoting proliferation, survival, angiogenesis, and apoptotic resistance generates a highly aggressive tumor that is difficult to treat. Although the fundamental genetic changes driving GBM progression and development have been identified, they have not yet translated into effective clinical treatments, leaving clinicians with three basic tools to treat GBM patients.

Treatment: surgical resection, radiation, and temozolomide

The majority of GBM patients undergo surgical debulking before radiation therapy [1]. However, surgical resection is limited by tumor location and infiltration [1] [5]. GBM patients receive fractionated RT every five days over a six-week time course, resulting in a total of 60 Gy. Addition of RT to surgery increases survival from 3-4 months to 7-12.1 months [1] [5]. The addition of nitrosourea chemotherapies, such as carmustine, only gave a 5% increase in survival, leading many to question their clinical use [5]. It was not until 2005 when Stupp et al published their landmark study reporting the combination of RT with temozolomide that significant treatment progress was made.

Temozolomide (TMZ) is an oral alkylating agent that efficiently crosses the blood brain barrier (BBB) [29, 30]. It breaks down to form the reactive

intermediate MTIC, which degrades to a methyldiazonium cation, resulting in alkylation of N7 guanine (70%), N3 adenine residues (9.2%), and O6 guanine residues (5%) [29]. The N7 and N3 adducts are not deleterious as either base excision repair (BER) or nucleotide excision repair (NER) recognizes and removes these methyl groups [29]. However, neither NER nor BER recognize and excise O6 alkylated guanine residues. Because the methyl group changes guanine's shape, the only base it can pair with during replication is thymine. A G-T pairing activates the mismatch repair response (MMR), resulting in excision of the thymine [29] [31]. However, as long as the O6 residue remains alkylated, the only base DNA polymerase can insert is thymine, resulting in futile cycles of MMR. To prevent replication fork collapse, the polymerase passes over the alkylated O6 guanine, generating a single strand break. The single strand break is converted to a double strand break during the next round of replication [32]. If these DSBs are not repaired, G2/M arrest occurs, resulting in apoptosis [29] [33].

The addition of TMZ to RT increased survival from 7-12.1 months to 14.6 months with the combination [5]. As a result of this study, the standard of care for GBM patients is surgery followed by RT with concomitant and adjuvant TMZ. A two-year follow up study of patients who received RT had a 10.9% survival while those who received RT+TMZ had a 27.2% survival. This trend continued to three (4.4% versus 12.1%), four (3.0% versus 9.8%), and five-year survival rates (1.9% versus 10.9%), with TMZ+RT patients consistently presenting at higher survival rates [34]. As exciting and encouraging as these 2005 results were, this

therapeutic triad has not changed or improved in over a decade. Furthermore, it is incapable of preventing tumor recurrence. After completing RT+TMZ, patient's tumors usually recur within 6.9 months [1]. Of these recurrent tumors, only 5.4% are sensitive to TMZ, and surgical debulking is limited by the preceding debulking [1]. There is a great need to improve time to recurrence and patient survival. To address this, we explored the use of a novel ER stress-inducing agent, JLK1486, with TMZ, to determine if this combination would decrease cell viability and delay recurrence.

Introduction to JLK1486

JLK1486, a bis-8-hydroxyquinoline substituted benzylamine (HQ motif), was synthesized with 15 other HQ analogs as potential cytotoxic agents to be used in a forward based chemical screen [35]. Of the 16 HQ motifs synthesized, seven exhibited levels of cytotoxicity in the KB3-1 human mouth epidermal cancer cell line [35]. Two of the seven HQ motifs, JLK1486 and JLK1472, had CC50's in the nanomolar range, leading to further study [35]. Initial characterization in the laboratory of Dr. Jean Louis Kraus (JLK), demonstrated that JLK1486 did not inhibit proteosome activity, but was capable of increasing caspase 3 and 7 activity [35]. This made it an attractive candidate to study as it suggested the drug was capable of initiating apoptosis.

Bis-8-hydroxyquinolines are highly reactive and fragment to form quinine methide (QM) reactive species [36]. JLK1486 QM species are not electrophilic enough to react with DNA, instead, they preferentially alkylate thiol residues [36,

[37]. JLK1486 alkylation of thiol residues blocks the formation of disulfide bonds required for protein tertiary structure [37[38]. This would lead to the accumulation of unfolded proteins in the endoplasmic reticulum (ER), triggering ER stress and subsequent activation of the unfolded protein response (UPR) [10] [39]. Microarray analysis of JLK1486 treated glioma cells, U87, confirmed this as ER stress response genes increased in response to JLK1486 treatment [36].

DNA damage and ER stress pathways crosstalk

Recent data suggests that sustained ER stress inhibits repair of DNA DSBs, resulting in decreased viability due to unrepaired DNA damage. Treatment of human lung cancer cells with the ER stress inducing agent tunicamycin leads to decreased expression of RAD51, a key DNA repair factor that promotes HR, resulting in unresolved DNA DSBs [40]. Hypoxia, a trigger of ER stress, was also shown to decrease RAD51 protein levels in breast cancer cell lines, leading to decreased viability [41]. Additionally, treatment of breast cancer cells with a PERK inhibitor, preventing activation of this ER kinase receptor, results in decreased DNA repair and increased sensitivity to RT [42]. Treatment of glioma cells with the 17AAG heat shock protein 90 (HSP90) inhibitor, prevented molecular chaperones from binding to and refolding unfolded proteins, and decreased RAD51 and BRAC2 protein levels, resulting in decreased HR [43]. The combination of 17AAG with a PARP inhibitor followed by RT further exacerbated DNA damage by preventing repair of single stranded breaks and double strand DNA breaks, decreasing proliferation and clonogenic survival [43].

During ER stress, unfolded and misfolded proteins within the ER are targeted for proteasomal-mediated degradation. Proteasomal inhibition triggers apoptosis as cells are unable to clear aberrant proteins. Treatment of glioma cells with bortezimib (Velcade ™), a proteosomal inhibitor, increases sensitivity to TRAIL mediated apoptosis [44]. Combination of Velcade™, with vorinostat, a histone deacetylase inhibitor, in glioma cells, decreases RAD51 protein, resulting in unresolved DNA DSBs [44]. Non small cell lung cancer cells treated with Velcade™, and exposed to RT underwent an 80-90% reduction in HR due to significant decreases in DNA repair factors FANCD2 and RAD51 [45].

These studies suggest inability to resolve ER stress results in delayed repair of DNA DSBs due to decreased HR. Although the exact mechanism is unknown, it is possible that sustained phosphorylation of eIF2 alpha leads to decreased translation of these HR factors. As TMZ alkylates DNA, resulting in the generation of DNA double strand breaks, and JLK1486 inhibits the formation of disulfide bonds, triggering ER stress, we reasoned that the combination of these two drugs would decrease GBM viability.

Summary

GBMs are genetically heterogeneous grade IV brain tumors [1]. Deletions, translocations, inversions, and amplifications promote glioma cell survival in adverse environments through receptor tyrosine kinase activation [2, 3] [24]. Furthermore, glioma cells alleviate hypoxia by increasing expression of angiogenic factors that promote blood vessel formation [8] [46,[46]. Although

these genetic alterations and adaptations serve as survival mechanisms, they can be therapeutically exploited. Because of their genetic aberrancies, gliomas heavily rely on their DNA damage repair response to maintain their genome while commandeering the ER stress response pathway to promote survival in highly unfavorable environments [39] [47]. We will focus on understanding how interference with DNA repair, specifically RAD51, and exacerbation of ER stress sensitizes GBM cells to the combination of TMZ and JLK1486.

Introduction to the DNA damage response pathway

Rationale

TMZ induces the formation of DNA DSBs [29]. These breaks must be repaired in order for the cell to avoid cell cycle arrest and / or apoptosis [33]. To do so, DNA damage response and repair factors must be activated, in particular ATM, CHK2, and RAD51 [48]. Understanding how these factors promote survival and why their inhibition is detrimental to cells provides the basis for the TMZ+JLK1486 combination treatment.

Overview of DNA damage repair: function, response, and key players

The DNA damage response (DDR) is the integrated network responsible for preventing genetically unstable cells from replicating [50, [49]. It maintains the genetic integrity of the organism, promoting homeostasis by reducing the risk of cellular transformation that leads to cancer development [50, 51].

The DDR is activated in response to a myriad of lesions, including inter and intra strand crosslinks, base pair mismatches, and DNA single strand (SSBs)

and DSBs [50]. Depending on the type of damage, the DDR activates specific pathways to recruit factors to the site of damage to mediate repair. For instance, the mismatch repair pathway (MMR) recognizes and removes mismatched bases while the nucleotide excision repair pathway (NER) detects and excises bulky DNA lesions [52]. Of the vast number of DNA lesions, the most deleterious are DNA DSBs arising from stalled replication forks, oxidative damage, or chemotherapeutic agents [33] [51]. DNA DSBs promote genetic instability through genomic and oncogenic translocations, inversions, and deletions, triggering mitotic catastrophe and cell death [17] [52]. This is of particular interest as temozolomide induces the formation of DSBs.

The cell utilizes two mechanisms to resolve DNA DSBs, non-homologous end joining (NHEJ) and homologous recombination (HR) [52]. NHEJ is traditionally viewed as an error-prone repair system in which two free DNA ends are simply ligated together [54]. Although this efficiently repairs the break, it results in loss of genetic material and translocations if two different chromosomes are fused together. Conversely, HR preserves genetic material and stability by using the sister chromatid of the damaged chromosome as a template to repair the DSB [54].

Signaling pathways activated by DDR converge to prevent damaged cells from propagating. Activation of cell cycle checkpoint kinases 1 and 2 (CHK1, CHK2) initiate either a G1/S or G2/M arrest, preventing damaged cells from replicating or undergoing mitosis [50] [52] [53]. This stall allows DNA repair

factors to localize to DNA DSBs and initiate HR, giving the cell time to repair damage. However, if the damage is not repaired, the cell is at risk of either entering a state of senescence or undergoing apoptosis. This clears the aberrant cell from the system, protecting the organism and promoting tissue homeostasis [50] [52] [55]. Cancer cells, GBM's in particular, hijack the DDR to promote survival despite severe genetic instability by increasing factors that mediate HR, allowing them to survive and proliferate despite stringent chemotherapeutic regimens [16] [17] [54] .

Detection of DNA DSBs: sensors, transducers, and effectors

Before catastrophic DNA DSBs can be repaired, the cell must detect them. DSBs activate the DDR sensors and alert the cell to the damage. Although poly-ADP-ribose polymerase (PARP) and the Mre11-RAD50-Nbs1 (MRN) complex are thought to be the primary initial sensors, a plethora of other DNA repair proteins can also fill this role [51, 52] [55]. Once the cell senses the lesion, transducers amplify the damage signal. PI3K like related protein, ataxia telengiectasia –mutated kinase (ATM), and the cell cycle checkpoint kinase 2 (CHK2) respond to DNA DSBs and activate the third class of DDR proteins - the effectors [52] [55]. Effectors are responsible for initiating cell cycle arrest and facilitating DNA repair. The most notable of these are BRAC1, BRAC2, Nbs1, P53, CDC25, and RAD51 [51]. The coordinated activation and signaling of sensors, transducers, and effectors enable cells to stall the cell cycle and repair DNA damage (Figure 1).

Resolution of DNA DSBs: histone modifications and ATM, CHK2, RAD51 activation

In response to detection of DSBs, the cell recruits DDR scaffolding factors to modify histones surrounding the break. PARP enzymes, in particular PARP1, covalently attaches poly-ADP-ribose (PAR) chains to lysine residues in the amino termini of histones [55]. This leads to chromatin re-modeling, promoting transcription of genes associated with DNA repair [56]. While PARP attaches PAR chains to histones, ATM kinase multimers dissociate into active monomers and phosphorylate the histone H2A.X variant on serine 139 (γH2A.X) [49] [56]. This triggers dephosphorylation of H2A.X tyrosine 142, allowing the mediator of DNA damage checkpoint protein 1 (MDC1) to bind γH2A.X [56]. Once bound to γH2A.X, MDC1 recruits the Mre11-Rad50-Nbs1 (MRN) complex to the DNA DSB through direct interaction with Nbs1 [57]. The MRN complex then recruits the ATM kinase to the DNA DSB site through ATM-Nbs1 interactions [58]. This tethers ATM to the DNA DSB site where it phosphorylates nearby H2A.Xs, amplifying the DNA damage signal [56]. The MRN complex, acting as an endonuclease, resects DNA DSBs to generate 3' single stranded DNA which is then bound by replication protein A (RPA) to prevent SS DNA cleavage [53] [58]. Scaffolding proteins, such as BRAC1 and BRAC2, are recruited to the DNA DSB and act as a recruitment platform for RAD51. After coating SS DNA to form a continuous nucleoprotein filament, RAD51 initiates the homologous chromosome

search [58-60]. Upon finding it, RAD51 hydrolyzes ATP and dissociates from SS DNA, allowing repair to occur [53] [60] (Figure 1).

To prevent a damaged cell from cycling before repair is complete, the DDR induces a cell cycle arrest mediated by ATM and cell cycle checkpoint kinase 2 (CHK2) [50] [52] [55] (Figure 1). ATM phosphorylates CHK2, which in turn phosphorylates the CDC25 phosphatase [51] [61]. This inactivates the phosphatase, preventing the dephosphorylation of CDC2 that results in G2 checkpoint release [50, 51]. CHK2 phosphorylation of CDC25 also inhibits Cdk2-Cdc45 complex activation, preventing chromatin loading and subsequent recruitment of DNA polymerase alpha [49]. Thus, CHK2 activation prolongs G2 arrest, providing time for the cell to repair breaks before entering M phase. In addition to inhibiting CDC25 activity, CHK2 promotes genome stability by phosphorylating P53 on serine 20 [51]. This prevents the MDM2 ubiquitin ligase from targeting it for degradation, allowing it to promote cell cycle arrest by inducing a P21 mediated G1 and G2 arrest [51]. Lastly, CHK2 enhances the repair of DNA DSBs by phosphorylating the scaffolding protein BRAC2, homing RAD51 to the DNA DSB site, facilitating HR [52].

It is through the coordinated activity of ATM, CHK2, and RAD51 that DNA DSBs are repaired, making it easy to envision how disruption of this signaling pathway, in particular RAD51, would be catastrophic to cell survival (Figure 1).

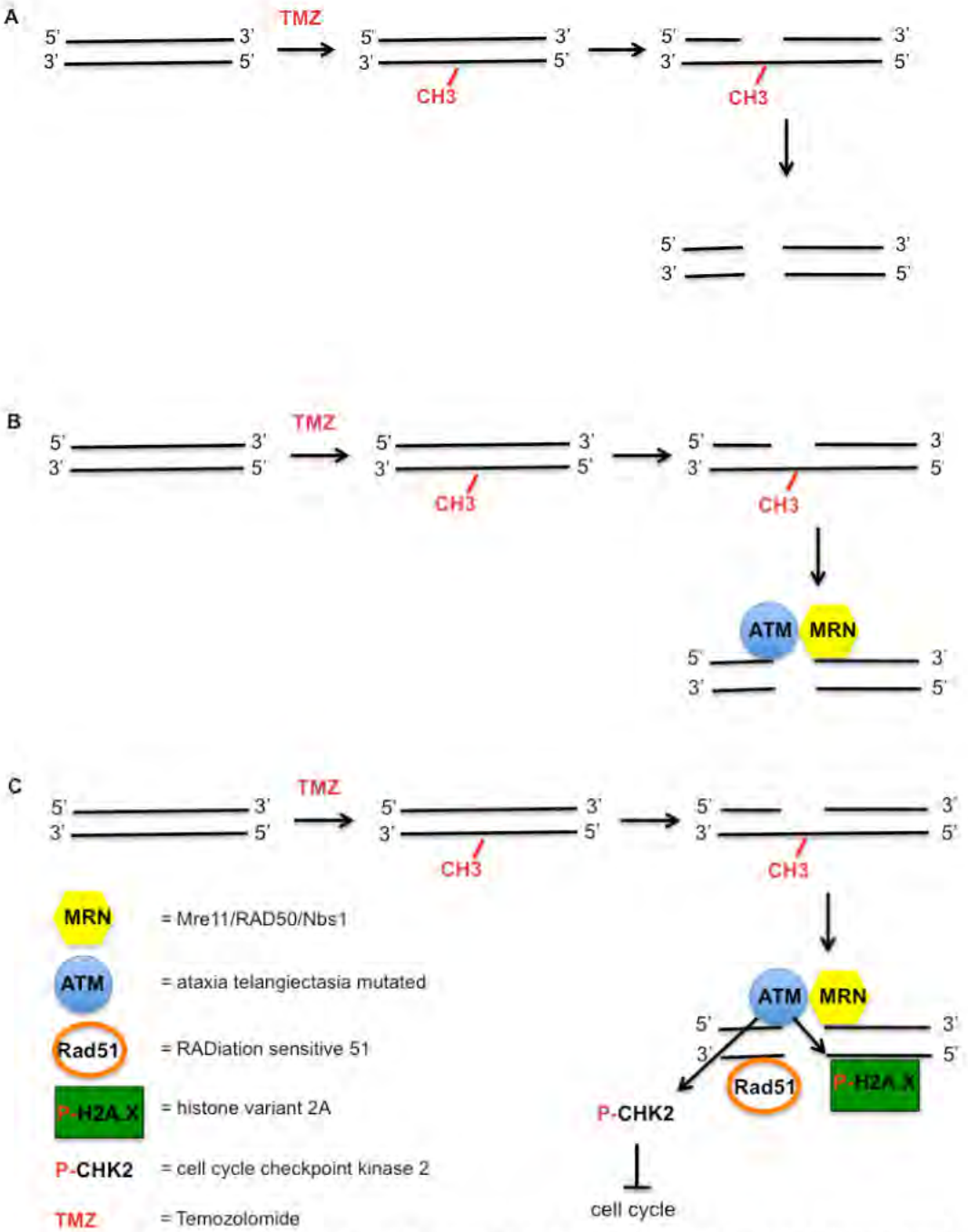

Figure 1: Sensors, transducers, and effectors regulate the response to DNA double strand breaks (DSBs). (A) TMZ induces DNA DSBs after two rounds of replication. **(B)** The MRN complex senses TMZ induced DNA DSBs and recruits the ATM transducer. **(C)** ATM phosphorylates H2A.X, recruiting the RAD51 effector to repair the DNA DSB via homologous recombination. Simultaneously, ATM phosphorylates CHK2, resulting in cell cycle arrest, preventing damaged cells from replicating.

RAD51 promotes cancer cell survival

Overview

Cancer cells are characterized by genomic aberrations due to mutations, translocations, amplifications, and deletions. When these cells enter and attempt to pass through the G2/M cell cycle checkpoint, their damaged and highly unstable genomes should trigger cell cycle arrest and initiate apoptosis. Glioma cells circumvent this by increasing expression of the DNA repair factor RAD51 [16] [59]. As RAD51 promotes the repair of DNA DSBs, increased expression leads to TMZ resistance and the maintenance of an unstable genome [16]. As TMZ+JLK1486 treatment decreases RAD51 expression resulting in cell death, how RAD51 acts as survival factor will be examined in detail.

Discovery and expression patterns

Genetic studies conducted in the 1960's suggested that the RecA factor was essential for *E. coli* survival after treatment with DNA damaging agents [53] [62]. It was proposed that RecA bound to single stranded DNA and promoted the search for the damaged DNA's homologous chromosome, resulting in homologous recombination [53]. In the early 1980's, a factor with similar properties and protein sequence to RecA was cloned in yeast [63]. Levels increased in response to X-rays during late G1 and early S phases of the cell cycle, suggesting it alleviated and resolved DNA damage similar to the RecA *E. coli* protein [64, 65]. Later studies confirmed that this eukaryotic DNA repair

factor, coined RAD51, performed the same function as the RecA predecessor and is essential for HR [53].

RAD51's highly conserved evolutionary sequence suggests it plays a vital role in maintaining genome stability. Higher eukaryotes have an 80% protein sequence homology with yeast RAD51 and maintain an ~50% similarity with its prokaryote RecA homolog [63]. Its expression is highest in the testis, ovary, spleen, and thymus, organs that rely on HR for their functionality [63]. Due to the essential role it plays during meiosis and recombination, it is not surprising that RAD51 knockouts are embryonic lethal [63].

RAD51 increased expression promotes cancer cell survival

As RAD51 binds to single stranded DNA and is responsible for initiating the search for homologous chromosomes, its expression is highest during the S/G2 phase of the cell cycle [17] [61, 62]. Cancer cells, however, aberrantly express RAD51 and maintain increased expression in G0 and early G1 [62]. Increased expression is not due to gene amplification but rather increased transcription [16].This enhances the repair of DNA damage accrued during chemotherapy and radiation, promoting resistance to both therapies [16]. As a result, it is not surprising that Rad51 expression is elevated in a variety of cancers, ranging from myeloid leukemia, T cell leukemia, cervical carcinoma, melanoma, colon and rectal cancer, and glioblastoma [16] [59] [66].

A twenty-two-year study of GBM patients found 58% of primary tumors show increased RAD51 expression versus normal temporal lobe tissue, as was

hypothesized [67]. However, counterintuitively, increased RAD51 expression correlated with increased survival while decreased RAD51 expression was associated with decreased survival [67]. This was unexpected as it was thought that decreased RAD51 expression leads to increased survival as tumor cells are unable to repair catastrophic DNA damage. A similar expression pattern also occurred in recurrent tumors, in that 70% of recurrent tumors had increased RAD51 expression compared to their corresponding primary tissue, and patients with increased RAD51 expression had prolonged survival (16 months) compared to patients' recurrent tumors with decreased RAD51 expression (4 months) [67]. As RAD51 mediates HR, it is expected that increased RAD51 would lead to increased proliferation, leading to decreased survival. However, no correlation between the proliferative Ki67 marker and RAD51 was found, suggesting tumors with increased RAD51 do not have a proliferative advantage over those with lower RAD51 expression [67]. There are two possible explanations for why increased RAD51 expression did not correlate with decreased survival. First, as mRNA was not extracted from either primary or recurrent tissue samples, there is no data to indicate if RAD51's sequence was mutated [67]. Interestingly, increased RAD51 expression was found in the cytoplasm of RAD51 high tumors, which is rather unusual as RAD51 functions as a nuclear protein [67]. Accumulation of nuclear proteins in the cytoplasm, such as P53, is usually indicative of mutations resulting in loss of function. However, although a few cases have indicated loss of heterozygosity and a miniscule number have

mutated RAD51, most GBMs are RAD51 wild type [61].The second explanation is that elevated RAD51 is not indicative of survival but rather of cells on the brink of mitotic catastrophe. The accumulation of DNA damage resulting from multiple rounds of radiation and chemotherapy as well as genomic instability caused by aneuploidy could account for increased RAD51 in a viable cell incapable of proliferating.

A second study in 2012 reported a contradictory finding in which increased RAD51 expression correlated with decreased survival, corroborating the hypothesis that was proposed but refuted in the above-mentioned study [67]. Until additional studies are published, the correlation between RAD51 expression and clinical survival remains to be determined. As noted above, these complications may relate to RAD51 post-translation modifications and subcellular localization. However, the fact that RAD51 mediates HR cannot be negated, suggesting it is a relevant factor be investigated and targeted.

RAD51 promotes P53 mutant glioma cell survival during radiation and temozolomide treatment

Radiation generates DSBs breaks through reactive oxygen species [68]. As RAD51 mediates the repair of DSBs, it is not surprising that GBM cell lines have increased expression of RAD51 versus normal human astrocytes and that increased expression enhances survival following response radiation treatment [62]. Conversely, knockdown of RAD51 decreases viability of irradiated glioma cells [17]. *In vivo* studies show that delivery of RAD51 anti-sense

oligonucleotides in mice with intracranial implanted glioma cells increases their overall survival [17]. Importantly, survival was further increased when RAD51 anti-sense delivery was combined with radiation [17]. This suggests interference of RAD51 sensitizes glioma cells to radiation *in vitro* and *in vivo*, making it an attractive therapeutic target.

Interestingly, irradiation of glioma cells lacking functional P53 produced a prolonged G2 arrest that correlated with increased duration of RAD51 foci compared to P53 wild type glioma cells or to NHAs [18]. Because P53-deficient glioma cells have decreased P21-mediated G1 arrest, they can enter the cell cycle with damaged DNA. To avoid apoptosis, they use the G2 delay to resolve lingering DNA damage [18]. For this to occur, P53-deficient glioma cells depend on ATM activation of CHK2 to initiate G2 arrest. Inhibition of ATM in P53-deficient cells results in decreased survival following radiation therapy, suggesting interference of DNA damage repair is detrimental to gliomas and a plausible therapeutic target [18].

TMZ alkylates DNA and generates single strand DNA breaks that are converted into DSBs during subsequent rounds of replication [29] [33]. RAD51 over-expression mitigates TMZ-induced damage in glioma cells by increasing HR [62]. For example, glioma cells with stable RAD51 knockdown show decreased clonogenic survival following TMZ treatment versus RAD51 empty vector transfected control cells [69]. RAD51 control TMZ-treated glioma cells repaired and resolved DNA DSBs within 48 hours after treatment. Conversely, treatment

of RAD51-suppressed cells with TMZ resulted in sustained DNA DSBs, lasting up to144 hours post treatment [70]. Inability to resolve DNA DSBs resulted in increased apoptosis, presumably due to decreased HR. To eliminate the possibility that RAD51-suppressed cells utilize NHEJ to repair DNA DSBs, the effects of a NHEJ inhibitor was explored in RAD51 suppressed TMZ treated cells. However, as no significant sensitization resulted from TMZ treatment of RAD51 knockdown cells with a NHEJ small molecule inhibitor, it is likely that glioma cells with suppressed HR do not use NHEJ to repair TMZ generated DNA damage [70]. This is especially important from a therapeutic perspective as GBMs become resistant to small molecule inhibitors by activating compensatory pathways, negating the inhibitors' effect. The suggestion that RAD51 suppressed cells do not use NEHJ to compensate for HR inhibition further corroborates why RAD51 inhibition would be an effective treatment in GBMs.

Treatment of glioma cells with TMZ results in significant G2 arrest, persisting up to 72 hours [62]. The combination of radiation with TMZ leads to increased RAD51 foci formation. Conversely, knockdown of RAD51 reduces glioma cells' ability to resolve DSBs accrued from either TMZ or RT, suggesting that DNA DSBs persist when RAD51 levels are decreased [62]. Furthermore, a significant increase in γH2A.X foci occurred in RAD51 knockdown glioma cells following treatment with both radiation and TMZ, supporting the hypothesis that increased RAD51 levels promote therapeutic resistance, and interference with

RAD51 sensitizes cells to DNA damage caused by radiation or chemotherapy [62].

RAD51 regulators are mutated or act as oncogenic transcription factors in glioma cells

Studies in the late 1990's and early 2000's suggested that P53 directly interacts with RAD51 to negatively regulate its HR function [60] [70]. Co-immunoprecipitation experiments indicate a direct P53-RAD51 protein-protein interaction [71]. Nuclease treatment did not disrupt this, validating that the interaction was not mediated by an intermediate nucleic acid [71]. It is thought that P53 binding inhibits RAD51's ATPase activity, preventing it from catalyzing strand exchange during HR [71]. This suggests P53 regulates if and when HR occurs. P53 inhibition of RAD51-mediated HR prevents repair of DNA DSBs during G2 arrest, resulting in cell death due to unresolved DNA damage. Supporting this negative regulation, P53 mutant proteins were unable to bind wild type RAD51 [71]. Further corroborating this, P53 mutant lines are unable to inhibit strand exchange, leading to aberrant and increased use of HR that contributes to genomic instability [71]. This is especially interesting in the context of cancer development. P53 is the most commonly mutated tumor suppressor gene, and loss or mutation of P53 results in genomic translocation, aneuploidy, deletions, and inversions [59, 60] [71]. As secondary and recurrent gliomas are associated with P53 mutations, it is plausible that glioma cells rely on P53 mutations to increase RAD51 repair of chemotherapy driven DNA DSBs, further

strengthening the reason for why RAD51 inhibition may be an effective treatment for GBMs [17, 18].

Recurrent tumors express higher levels of RAD51 than primary tumors and exhibit increased resistance to TMZ [68]. FOXM1, an oncogenic transcription factor commonly over-expressed in GBMs, is associated with increased resistance to DNA damaging agents such as cisplatin. Comparison of 38 recurrent versus primary tumor samples indicated increased FOXM1 levels [68]. Interestingly, increased FOXM1 expression correlated with increased DNA repair pathway mediators such as BRAC2, CHK2, and, of course, RAD51 [68]. This suggests that recurrent GBM tumor cells may use FOXM1 to sustain their growth and viability by increasing their capacity to resolve DNA damage by increasing expression of DDR factors. ChIP as well as luciferase assay reporter assays confirm that FOXM1 binds to and regulates the RAD51 promoter [68]. This suggests that disruption of FOXM1 may be an alternative means to prevent RAD51 expression. Indeed, knockdown of FOXM1 decreases RAD51 expression, sensitizing recurrent GBM tumor cells to TMZ treatment, while rescue of RAD51 in FOXM1 silenced cells rescues survival [68]. This validates the hypothesis that glioma cells rely on FOXM1 to increase RAD51 levels to promote increased DNA repair, developing chemotherapeutic resistance. As RAD51 inhibition leads to decreased viability and increased cell death in response to radiation or TMZ, exploring ways to interfere with its role in HR remain a viable and active area of interest and research.

Targeting the DDR: ATM, RAD51, and CHK2 inhibitors

Although RAD51 promotes cell survival by increasing the cell's capacity to resolve DNA damage by HR, it also induces genomic instability. Hence, increased RAD51 expression is a double-edged sword. On one hand, genomic rearrangements may benefit cancer cells by inactivating tumor suppressors or placing strong constitutively active promoters in front of oncogenes. Conversely, increased HR and genomic relocations may push the cell towards mitotic catastrophe. As RAD51 and other DNA repair factors are no longer able to mitigate accrued DNA damage, the cell is at risk of undergoing senescence or cell death. This weakness may be therapeutically exploited. Treating cells with chemotherapies that exacerbate DNA damage, such as TMZ, may overwhelm DNA repair mechanisms, pushing the cell towards apoptosis. It is also possible that treatment of cells with drugs that inhibit DNA repair sensitize cells to death. For example, pre-treatment of cells with an ATM inhibitor before irradiation, results in decreased γH2A.X , decreased RAD51 recruitment, and increased cell death in glioma cells [55].

To this end many drugs have been developed against the DDR pathway [50] [52]. There are at least six inhibitors of ATM. However, at this time, they are unsuitable for clinical use as they inhibit other targets, particularly ATM related kinase (ATR), and exhibit high levels of toxicity in patients [52]. At least five inhibitors of the CHK2 and RAD51 axis have also been synthesized and are currently being studied *in vitro*. The majority of CHK2 inhibitors function as ATP

competitors [52]. Although they sensitize glioma cells to radiation, there are no CHK2 inhibitors in the clinic for GBMs at this time due to lack of permeability, specificity, and synergy with DNA damaging agents [52]. Screens of over 200,000 compounds from the NIH repository as well as over 100,000 molecules from the DIVERSet Chembridge Corporation library identified several promising RAD51 candidates [52]. Although these candidates are in early stages of development, there is exciting data suggesting some specifically inhibit RAD51 HR by covalently binding to its cysteine residues, preventing DNA binding and nucleoprotein filament formation [52].

At this time, the best-case scenario for inhibiting DDR activity is the use of combination therapies that result in synthetic lethality. For example, Gleevec, an FDA approved drug that inhibits the Abl kinase, decreases RAD51 protein, radio-sensitizing glioma lines [72]. It is easy to envision how combining Gleevec, which indirectly inhibits HR, with either a PARP inhibitor, such as Olaparib, or an ATM inhibitor, would increase sensitivity of gliomas to RT or chemotherapies. This would prevent repair of and lead to accumulation of both single and double stranded DNA breaks. These exacerbations would push the already tumultuously unstable genomic background of the cell towards genetic collapse, resulting in death. This proof of principle concept was validated when PARP inhibition in either a RAD51 knockdown or HR deficient cellular background was lethal, demonstrating the potential of harnessing synthetic lethality [73].

Summary

These studies serve as models for why combination therapies are the best therapeutic approach to cancer. Although TMZ induces DNA damage that may push the cell towards apoptosis, simultaneously preventing repair of DNA damage and exacerbating a second reliant pathway increases the likelihood of lethality. To understand why the ER stress inducing JLK1486 agent results in a robust cell death response when combined with TMZ requires understanding of key players of the ER stress response and how the DDR and ER pathways crosstalk.

Introduction to the Endoplasmic Reticulum and Unfolded Protein Response

Rationale

Unresolved ER stress is detrimental as it triggers ER mediated death through three key players, PERK, ATF4, and CHOP [10] [39] [74]. The ER stress signaling axis and its players will be discussed in detail, as they are responsible for decreasing glioma cell viability in response to TMZ and JLK1486 treatment.

Overview of ER function, requirements, stress triggers, and response

The endoplasmic reticulum (ER), an evolutionary conserved organelle present in all eukaryotic cells, is required for the synthesis and folding of secreted and transmembrane proteins [10] [39] [75]. The ER must (1) maintain high luminal levels of ATP to sustain the energy demands of protein folding, (2) an oxidizing environment to facilitate the formation of disulphide bonds, and (3) increased calcium and molecular chaperone levels to guide and stabilize folding

proteins so that correct tertiary structures are achieved [39] [75]. This process is dependent on favorable cell conditions promoting ER homeostasis and is easily disrupted.

The ER is extremely sensitive to cellular perturbations such as hypoxia and decreased levels of nutrients, calcium, ATP, iron, amino acids, and molecular chaperones [39] [75]. These changes not only alert the ER to unfavorable cellular environments but also impair ER function, resulting in activation of the ER stress response [10] [39] [75]. Radiation, which generates reactive oxygen species, as well as infection, hyperplasia, and the accumulation of unfolded and misfolded proteins also activate the ER stress response [75].

The initial response to ER stress is twofold. The first is inhibition of protein translation [10] [39]. This not only alleviates the number of nascent proteins shuttled into the ER for folding but also reduces the cellular demand for ATP. This is of particular importance if ER stress is triggered by hypoxia as decreased oxygen forces the cell to shift from aerobic metabolism to anaerobic glycolysis. In addition, translational inhibition depletes cyclin D1 levels, resulting in a G1 arrest, preventing stressed cells from propagating [76] [77]. The second ER stress response is increased expression of genes that enhance amino acid metabolism, molecular chaperones, protein transportation, and formation of disulfide bonds [10] [39]. This allows the ER to fold or refold proteins already within its lumen. However, because folding proteins is a cost effective process, there is a finite time by which this must occur, or else the unfolded proteins are targeted for

proteasomal degradation, a process known as ER associated degradation (ERAD) [10] [39]. This prevents the ER from using more energy and reduces the number of unfolded proteins present in the ER. This initial pro-survival response is tightly and carefully regulated as it is only meant to resolve stress and promote survival in non-aberrant cells.

The ER pro-survival response is mediated by PERK, ATF6, and Ire1

The pro-survival response mediated by the ER is due to the coordinated activation and regulation of three transmembrane ER receptors, PERK, ATF6, and Ire1 [10] [39] [75]. Glucose regulated protein 78 (Grp78/BiP), a molecular chaperone and member of the heat shock protein 70 family, binds to the luminal domain of all three ER receptors, rendering them inactive during ER homeostasis [10] [39] [78, 79]. When ER stress occurs, BiP dissociates from the receptors, triggering their activation [10] [39] [80].

The first arm of the ER stress response is activated by PKR like kinase (PERK) homodimerization and autophosphorylation. PERK is a serine/threonine kinase that regulates eukaryotic initiation factor two alpha (eIF2α), a key member of the 43S initiation complex required for cap dependent mRNA translation [80, 81]. Activated PERK phosphorylates eIF2α on serine51 (P- eIF2α), preventing it from forming the 43S complex, resulting in inhibition of cap dependent translation [39] [81] [82]. Attenuation of protein translation serves two purposes. First, as earlier discussed, it reduces the demand of the ER to fold newly synthesized proteins, and, second, increases translation of cap independent transcripts, such

as activating transcription factor four (ATF4), which alleviate ER stress by increasing amino acid metabolism and molecular chaperone levels [10] [39] (Figure 2).

The second arm of the ER stress response is regulated by the transmembrane receptor activating transcription factor 6 (ATF6) [10] [39]. Dissociation of BiP from its luminal domain frees its Golgi localization sequence. Once localized to the Golgi, two site specific protease (Sp-1, Sp-2) cleave it, revealing a basic leucine zipper domain, inducing translocation to the nucleus to drive the expression of pro-survival factors such as BiP, X box binding protein 1 (XBP-1), and disulphide isomerase, which catalyzes the formation of disulphide bonds [10] [39] (Figure 2).

The third arm of the ER stress response is mediated by the transmembrane receptor Ire1, which functions as both a serine /threonine kinase and an endoribonuclease [10] [39]. After BiP dissociation, Ire1 dimerizes, autophosphorylates, and alternately splices XBP1 mRNA, resulting in XBP1 transcription factor activity [10] [39]. XBP drives the expression of molecular chaperones, increases phospholipid synthesis, as well as p58 that serves as a negative regulator of PERK, terminating the PERK – P- eIF2α mediated signaling cascade initiated by ER stress [10] [39] (Figure 2).

The activation of PERK, ATF6, and Ire1 in response to ER stress promotes cell survival by preventing cell cycle entry, stalling protein translation,

and up-regulating factors to alleviate stress, allowing the cell to re-establish homeostasis [10] [39] (Figure 2).

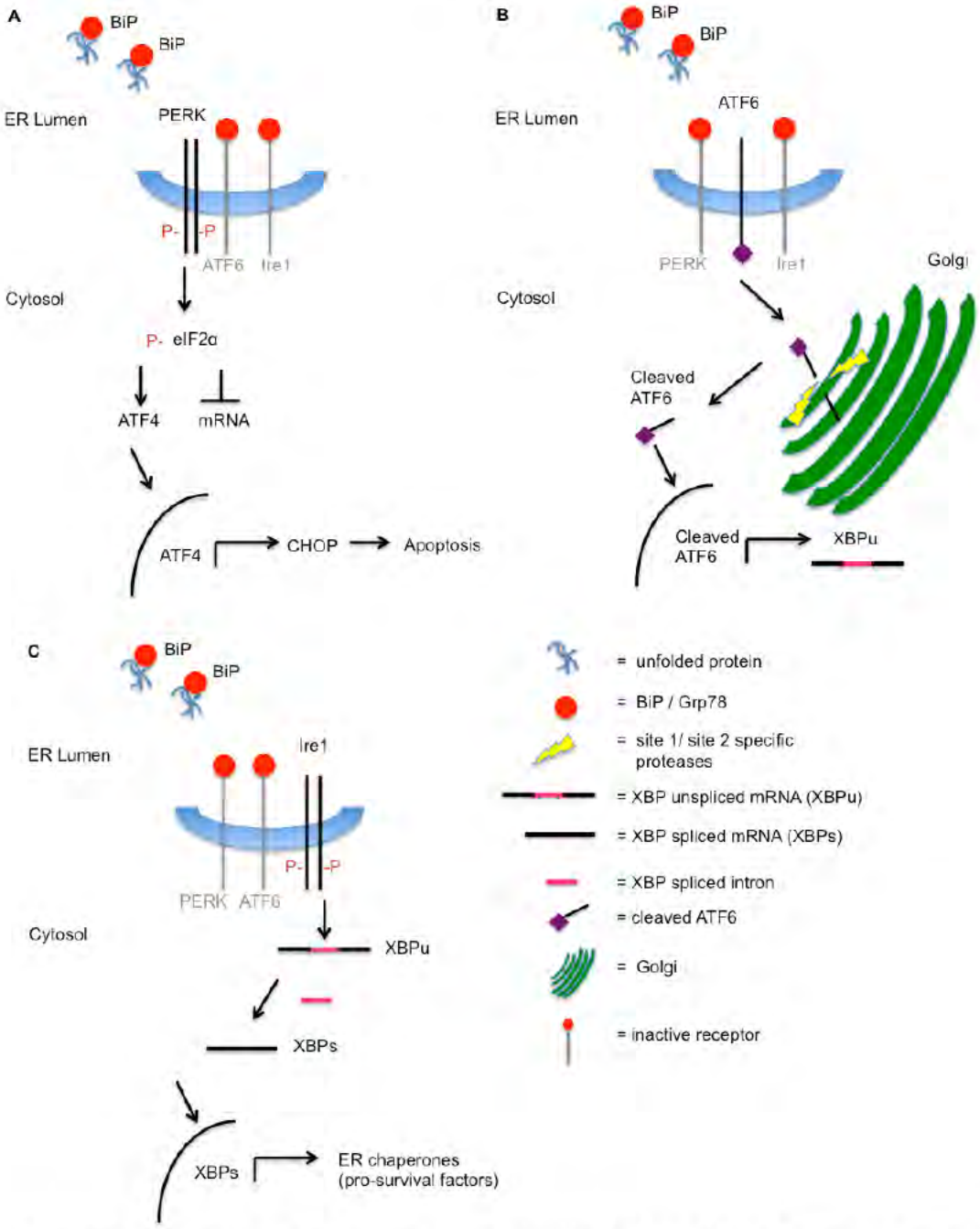

Figure 2: The endoplasmic reticulum stress response is regulated by the PERK (A), ATF6 (B), and Ire1 (C) receptors.

The ER pro-death response is mediated by CHOP

After ER stress is resolved, BiP re-associates with the luminal domains of PERK, ATF6, and Ire1, switching off the ER stress induced signaling cascade. However, if ER stress is irreversible or if the cell is in a chronic state of stress, PERK, ATF6, and Ire1 induce expression of the pro-apoptotic transcription factor C/EBP homologous protein (CHOP) to initiate a pro-death response [39] [75]. This response induces either extrinsic or intrinsic mediated apoptosis through release of mitochondrial cytochrome C activating the effector caspase 3 or by death receptor activation by TRAIL binding [83-87]. Induction of cell death in response to unresolved ER stress serves to protect the organism; however, cancer cells often bypass this and instead manipulate the ER response to promote survival and growth in unfavorable environments [10] [39].

The ER stress response promotes cancer cell survival

Overview

Solid tumors are characterized by rapidly proliferating cells that outstrip available blood vessels and deplete available nutrients to create regions of hypoxia [7] [41]. To alleviate this, GBMs promote blood vessel development, but these networks are leaky, inefficient, and often form dead-end junctions [4] [8] [14] [21]. This aberrant vasculature contributes to decreased nutrient delivery as well as a buildup of toxic metabolic wastes, leading to a state of chronic ER stress [8]. This state triggers the pro-death ER stress response through activation of the pro-apoptotic transcription factor CHOP. However, cancer cells

circumvent this by up regulating ER factors that promote survival such as BiP, XBP, PERK, and ATF4, preventing CHOP induction [14] [39] [88].

BiP, Ire1, and PERK promote cancer cell survival

BiP over-expression promotes cancer cell survival by holding the ER stress response in check, preventing sustained ER stress from initiating the pro-death response [39] [89, 90]. Evidence suggests that BiP binds to and blocks the cleavage of caspase 7 and 12 as well as to BIK/BAX, preventing the release of cytochrome C from mitochondria [91]. Additionally, because BiP serves as a molecular chaperone, elevated expression increases the folding capacity of the ER [92]. This helps to compensate for the increased number of mutated proteins in cancer cells that require multiple folding attempts. BiP up-regulation has been found in a myriad of cancers, including breast, stomach, gastric and brain [15, 93, 94]. BiP expression in GBM cells correlates with increased cell survival and proliferation while knockdown results in decreased survival and cell growth [13] [15]. A mouse mammary model showed BiP heterozygous mice have decreased tumor progression and increased cell death, resulting from activation of caspase 3 and 7, suggesting that BiP mitigates *in vitro* ER stress, supports survival and proliferation, and promotes tumorigenesis [39] [95].

The IRE1/XBP pathway has also been implicated in promoting cancer cell survival. XBP is often over-expressed in breast cancer cells and over-expression of spliced XBP contributes to the development of multiple myeloma in transgenic mice [96, 97]. Human fibrosarcoma cells deficient in XBP are unable to initiate

tumors in SCID mice, suggesting XBP adapts cells in response to ER stress [98]. Additionally, prolonged IRE1 signaling has been shown to promote cell proliferation without activating cell death [99].

We will focus on how the PERK-eIF2α-ATF4-CHOP pathway affects cancer development and progression as JLK1486 treatment exacerbates this axis.

PERK

PERK identification and function

Delineation of the ER stress response pathway resulting in eIF2α phosphorylation and translational inhibition was first characterized in yeast [100]. GCN2, which is conserved and expressed in all eukaryotic cells, was the first kinase identified to phosphorylate eIF2α in response to amino acid deprivation [101-103]. This led to the discovery of two uniquely expressed mammalian kinases, PKR (double-stranded RNA dependent kinase) and HRI (heme regulated inhibitor kinase), which phosphorylate eIF2α in response to viral infection and decreased heme concentrations [104, 105]. Both kinases, when activated, recapitulate stalled mRNA translation. However, as both PKR-/- and GCN2-/- deficient cells were able to attenuate mRNA translation in response to ER stress inducing agents (ERSAs), it suggested that a third kinase was responsible for eIF2α phosphorylation in response to ERSAs [102]. In the late 1990’s and early 2000’s, three separate groups identified a novel mammalian serine/ threonine kinase that phosphorylates eIF2α in response to ERSAs, such

as thapsigargin (THAP) which releases calcium from the ER, and tunicamycin (TUN) which blocks N-linked glycosylation [82] [102] [106]. As the kinase localized to the ER and had a similar, but not identical, luminal domain amino acid sequence as PKR, it was named PERK, for PKR-like kinase [102]. Its kinase activity was validated as both serine and threonine residues were found to be phosphorylated and, more importantly, could phosphorylate eIF2α [82] [102] [108]. Mutation of PERK's kinase domain results in a PERK that is unable to phosphorylate eIF2α and inhibit mRNA translation in response to ERSAs, validating its kinase role in ER stress [82] [102]. The identification of four eIF2α kinases, each one responding to a unique ER stress trigger, demonstrates how important eIF2α phosphorylation is to regulating the ER stress response and how tightly controlled the response is.

PERK expression patterns

PERK expression was detected in 50 different human tissues, including brain, with increased levels corresponding to tissues involved in secretion, such as the stomach, salivary gland, pituitary, and pancreas [82]. This corroborates PERK's role in ER function and protein folding. Although PERK is expressed in a variety of organs, PERK knockout is not embryonic lethal. Instead, mice develop early onset diabetes by 4 weeks, accompanied by increased activation of IRE1, suggesting prolonged ER stress [107]. These mice ultimately die by 8 weeks due to increased apoptosis in pancreatic islet cells [109].

PERK activation and pathway delineation

In the absence of ER stress, BiP binds to PERK's luminal domain, preventing dimerization and activation of the receptor [79]. Treatment of cells with ERSAs decreases BiP association, as suggested by reduced co-immunoprecipitation, promoting receptor oligomerization and autophosphorylation [80]. The precise mechanism leading to BiP dissociation has not been elucidated, but it is plausible that BiP, acting as a molecular chaperone, dissociates from the luminal domains of the receptors to bind unfolded or misfolded proteins in the ER. Alternatively, it is possible that PERK undergoes conformational changes in response to ER stress, resulting in BiP dissociation. Regardless of the mechanism, dissociation of BiP is required for the dimerization of all three ER receptors and their subsequent activation [80].

Activated PERK phosphorylates eIF2α on serine 51 [81] [83]. This particular site is important as eIF2α must bind GTP to form the 43S initiation complex, which is required for cap dependent mRNA translation [108]. Phosphorylation of eIF2α on serine 51 prevents the eIF2β guanine nucleotide exchange factor (GEF) from exchanging GDP for GTP [108]. Although eIF2α serine 51 phosphorylation blocks the eIF2β GDP-GTP exchange, the serine 51 phosphorylation increases eIF2α 's binding affinity for eIF2β, sequestering the GEF, reducing formation of other 43S complexes, resulting in decreased mRNA translation.

PERK promotes *in vitro* cancer cell survival

Phosphorylation of eIF2α by PERK is essential for promoting survival of cells experiencing ER stress [81] [83]. If PERK is unable to stall translation, protein folding demands overwhelm the ER as its calcium, ATP, molecular chaperones, and oxygen levels are unbalanced. Unfolded and misfolded proteins accumulate in the ER lumen, causing ER swelling and activation of the unfolded protein response (UPR). Cell death soon follows due to ER incapacitation.

PERK deficient mouse embryonic fibroblasts (MEFs) are incapable of attenuating protein translation in response to ER stress inducing agents, such as THAP or TUN [81] [83]. Instead of dissociating polyribosomes into monosomes, PERK deficient ERSA treated cells have increased polyribosomal formation and continue to synthesize proteins [81] [83]. To mitigate their stress, PERK deficient MEFs rely on prolonged activation of other arms of the ER stress pathway, in particular, Ire1. However, protracted Ire1 signaling is unable to robustly inhibit translation in response to ERSAs, and cells show decreased survival due to caspase 12 cleavage [81] [83]. PERK rescue reverses the phenotype, resulting in phosphorylation of eIF2α, stalled mRNA translation, and increased survival [81] [83]. This response highlights the important role PERK plays in inhibiting protein translation and promoting cell survival [108]. It also accounts for why cancer cells increase PERK expression to promote survival.

Although PERK mediated eIF2α phosphorylation inhibits translation of most mRNAs, a microarray study identified a subset of proteins with increased

translation in response to hypoxia activated PERK. Isolation of mRNAs from polysomes in PERK +/+ versus PERK -/- hypoxia treated MEFs revealed a four-fold increase in mRNAs associated with angiogenesis, cell adhesion, protein transportation and folding [109]. Interestingly, a ten-fold increase in VEGF and type I collagen inducible protein, key to blood vessel formation, was found in PERK +/+ hypoxic treated MEFs compared to PERK -/- MEFs [111]. Furthermore, PERK+/+ hypoxic treated MEFSs had increased expression of matrix metalloproteinase 13, a protease that cleaves the extracellular matrix in tissues, suggesting PERK promotes metastasis [111]. Mammary epithelial cells increase PERK activation in response to loss of attachment, supporting PERK mediated survival following loss of attachment [110]. Additionally, treatment of human fibrosarcoma cells undergoing EMT with the PERK inhibitor, GSK414, resulted in 70% cell death while non-treated cells had only 20% cell death during EMT [111]. Critical to PERK's role in supporting survival during EMT, attached fibrosarcoma cells did not undergo significant cell death in response to GSK414 [113]. Overall, this suggests PERK increases translation of mRNAs that promote blood vessel development in response to hypoxia while promoting survival during EMT, both processes critical to the survival of cancer cells in unfavorable environments [111-113].

PERK activation may protect cancer cells and promote their growth by creating a cytoprotective response to sublethal doses of ER stress. When MEF PERK+/+ cells were exposed to two hours of hypoxia, allowed to recover for four

hours, and then re-incubated for an additional 24 hours at low oxygen, they exhibited increased survival in comparison to cells not pre-exposed to hypoxia before the 24 hour incubation [11]. This also held true for ERSA treatment. MEF PERK+/+ treated with THAP prior to incubation for 24 hours at low oxygen survived at higher rates than cells not pre-treated with THAP before the 24 hours exposure to low oxygen levels [11]. This suggests that activation of PERK in response to low levels of ER stress may prime the pathway for increased survival in response to future stress [11]. This is critical as cancer cells, GBMs in particular, are resistant to chemotherapies. It is possible that drug treatments utilizing multiple low doses may trigger PERK mediated cytoprotection instead of inducing cell death. Furthermore, sub-lethal doses of radiation therapy (RT) may pre-condition cells to clear generation of reactive oxygen species (ROS), reducing RT efficacy. This is plausible as PERK activation results in phosphorylation of its downstream target Nrf2, which increases the expression of enzymes that clear harmful intracellular ROS [112]. This would protect cancer cells from RT-ROS-generated single and double strand breaks, maintaining DNA integrity.

Knockdown of PERK in human breast and esophageal carcinoma cells resulted in activation of DNA damage response and checkpoint proteins, inducing a G2/M arrest and decreased proliferation [42] [114]. Inhibition of cell cycle progression and activation of the DNA damage response was due to accumulation of ROS and a two-fold increase in DSBs [114]. This suggests that

PERK contributes to RT resistance by decreasing ROS that would normally result in single and double strand breaks [42] [114]. Cancer cells utilize PERK to circumvent chemotherapy and RT induced growth arrest and cell death and to protect their survival against current ER stress and, in some cases, future stress. This is of particular interest to our studies of TMZ+JLK1486 treatment as it suggests crosstalk between the ER stress response and DNA damage response pathways (DDR). JLK1486 may not only exacerbate ER stress but also increase DDR dependence, increasing cells sensitivity to TMZ.

PERK promotes *in vivo* cancer cell survival

PERK promotes the *in vitro* survival and proliferation of cancer cells and plays an integral role in promoting *in vivo* tumorigenesis. PERK deficient K-RAS transformed MEFs formed tumors at slower rates with decreased tumor volumes than PERK +/+ K-RAS transformed cells [110]. Sectioning of PERK deficient tumors indicated increased apoptosis in hypoxic regions [110,111]. Conversely, PERK wild type K-RAS cells in hypoxic regions exhibited decreased apoptosis, suggesting PERK was able to mitigate the effects of low oxygen [110,111]. PERK +/+ transformed MEFs had increased levels of P-eIF2α in cells in hypoxic regions while PERK deficient tumors did not [81[[83] [110]. Furthermore, expression of a non-phosphorylatable eIF2α in K RAS PERK +/+ transformed MEFs resulted in decreased survival and increased apoptosis due to caspase and PARP cleavage. Decreased tumor volume correlated with cells in hypoxic regions unable to phosphorylate eIF2α [110]. This suggests that tumors with PERK

expression have not only a survival but also a proliferative advantage over PERK deficient cells in response to hypoxia [11] [81] [83] [110,111]. The survival advantage mediated by PERK could be an attractive therapeutic target, however, long term knockdown of PERK led to increased genomic instability in normal cells, making PERK inhibition a double edged sword in that the initial knock down may increase RT and chemotherapy efficacy but long term knockdown may result in transformation of normal, bystander cells [114].

Additionally, PERK induction may increase angiogenesis, promoting tumor cell survival in hypoxic environments. Sectioning of PERK -/- K-RAS transformed tumor sections when compared to PERK +/+ tumors exhibited decreased blood vessel density, with the majority of blood vessels presenting as non-functional [111]. The aberrant vasculature, resulting from cuboidal instead of elongated endothelial cells, formed vessels densely filled with endothelial cells instead of hollow structures that allow blood flow [111]. The accumulated endothelial cells prevent blood flow and increase pressure within the vessel. This, along with the misshapen blood vessels and the lack of cell-to-cell adhesion along the vessel, likely contributes to the 22% of PERK -/- tumors that hemorrhage [111].

Although PERK may increase vasculature formation to alleviate hypoxia, it is detrimental for cells to remain in this chronic state. To alleviate this, cancer cells metastasize to new locations that are more favorable. PERK promotes the *in vitro* migration of breast and melanoma lines by increasing survival during EMT and by increasing enzymes that degrade ECM [42] [112]. This was

recapitulated *in vivo* as PERK promoted increased metastasis of breast cancer cells in a mouse mammary carcinoma model. Conversely, PERK deficiency resulted in decreased metastasis [114]. This suggests that PERK not only contributes to blood vessel development to promote tumorigenesis but also provides a mechanism for cancer cells to exit unfavorable conditions.

In addition to promoting blood vessel development and metastasis, PERK protects cancer cells from DNA damage. PERK-/- mammary carcinoma cells form tumors with decreased volume versus wild type mammary carcinoma cells [114]. This was due to increased levels of ROS that correlated with decreased expression of enzymes, such as Nrf2, that clear ROS from the cell [114]. Sectioning of PERK -/- tumors found that increased ROS correlated with increased DNA damage, specifically elevated levels of DNA DSBs [114]. This suggests that decreased tumor formation is the result of catastrophic DNA insults. PERK activation promotes survival in regions of hypoxia, maintains DNA stability by reducing DNA damage, and increases tumor cell proliferation and volume [81] [83] [110,111] [114]. As JLK1486 induces prolonged ER stress, it is easy to envision how the addition of further insults, such as the DNA alkylating agent TMZ, would be deleterious to cell survival.

PERK contributes to GBM development

Although the majority of PERK's *in vitro* and *in vivo* contributions to cancer cell survival and tumorigenesis has been studied in transformed MEFS and breast cancer lines, recent data suggests a role for PERK mediated GBM cell

survival. As the ER stress response is evolutionary conserved, it is reasonable to think PERK mediated mechanisms of protection plays a role, at least to some degree, in GBM tumorigenesis. Indeed, PERK expression increases with glioma tumor grade, with grade IV GBMs presenting with higher PERK expression than grade III which exhibit higher levels than grade II which are elevated in comparison to normal brain tissue [12]. This suggests that PERK is important for tumor progression and may be vital for GBM cell survival. Treatment of PERK-silenced GBM established lines with ERSAs, such as TUN or low glucose media, decreased viability and increased apoptosis [12]. This suggests PERK mediates a similar mechanism of cell protection as observed in breast and transformed MEFs. Knockdown of PERK in the U87MG GBM cell line resulted in decreased tumor formation, implying PERK promotes GBM tumorigenesis, as observed in breast cancer and transformed MEFs [12].

PERK summary

PERK is an evolutionarily conserved serine / threonine kinase ER receptor that promotes survival in unfavorable conditions, such as hypoxia, or in response to ERSAs [10] [39]. It enhances cancer cell survival and supports tumorigenesis by stalling mRNA translation, while activating pathways that eliminate ROS, decreasing DNA damage, increasing cell cycle progression, promoting blood vessel formation, improving survival after loss of cell-to-cell attachment, and mediating cytoprotection in response to sub lethal doses of RT and ERSAs [11] [42] [81] [83] [102] [108] [110,111] [114]. PERK inhibition sensitizes cancer cells

to ERSAs and RT, suggesting drugs that disrupt PERK activation may improve the efficacy of RT and chemotherapeutic agents [81] [83] [110,111] [114]. However, drugs that effectively target PERK remain elusive due to issues of specificity and achievable clinical concentrations [10] [39]. Perhaps the most feasible approach to disrupting PERK mediated survival is not the targeting of PERK itself but rather the ER stress response as a whole. Two ways to address this have been suggested. The first utilizes drugs to inhibit the ER pro-survival responses while the second uses drugs that further increase ER stress to overwhelm and incapacitate the ER [10] [39].

We utilized the second approach, combining the novel ER stress-inducing agent, JLK1486, with the standard chemotherapeutic agent, temozolomide (TMZ), to induce sustained ER stress while generating DNA DSBs [19]. To understand why TMZ+JLK1486 results in unresolved ER stress and apoptosis, we must understand two PERK-regulated proteins, activating transcription factor 4 (ATF4) and CAAT/enhanced binding homologous protein (CHOP). Persistent, irreversible ER stress activates ATF4 and CHOP, switching the PERK mediated pro-survival response to one of pro-death, as observed in TMZ+JLK1486 treated cells [19] [75].

ATF4

ATF4 identification and function

Eight activating transcription factors (ATFs) were identified in the late 1980's that recognized and bound the cAMP responsive element (CRE)

consensus sequence 5’ GTGACGT A/C A/G 3’ [113, 114]. Each ATF is expressed from a different gene locus, resulting in related but distinct family members [116]. Of the eight ATFs, six have basic leucine zipper motifs [116]. The basic domain recognizes and binds DNA consensus sequences while the unique leucine domain promotes either homo or heterodimerization [116]. This is essential to regulating gene expression as it creates a diverse pool of factors that can activate or repress a wide variety of genes with similar consensus sequences, resulting in specific cell, tissue, organ, and developmental expression.

In particular, activating transcription four (ATF4), can form cross family bZIP dimers, most notably with CAAT box/ enhancer binding proteins (C/EBP), which tend to regulate differentiation as well as inflammatory responses [116, [115, 116]. The crystal structure of ATF4 associated with C/EBP indicates that ATF4’s alpha helix is ordered [118]. This suggests that when ATF4 is bound to a C/EBP family member it can still recognize and bind its consensus sequence [118] . Therefore, depending on its binding partner, ATF4 can positively or negatively regulate gene expression [117]. For example, ATF4 can bind to the symmetric CRE sequence in the somatostatin gene [117]. However, when ATF4 dimerizes with the C/EBP β family member, the complex synergistically increases somatostatin expression [117]. Conversely, dimerization of ATF4 with C/EBP β prevents C/EBP β from binding to C/EBP sequences, repressing transcription of genes that would be increased in response to C/EBP β homodimers [117].

Therefore, expression patterning of genes depends on the increasing and decreasing ratios of ATFs to C/EBPs [115] [117]. This is of particular importance during ER stress as PERK activation results in increased ATF4 protein levels, making it easy to surmise how one TF could effect a multitude of genes.

ATF4 expression patterns

Identification of a CRE sequence in human T cell receptors led to the isolation of human ATF4 [117, 118]. The transcript was ubiquitously expressed in brain, kidney, liver, spleen as well as T and B cells [115] [119,120]. Although the transcript is quite stable, the protein has a very short half -life, less than 30 minutes [117]. This allows for tightly regulated gene expression in response to fluctuating environmental conditions.

For ATF4 knockouts, 70% of mice die between ED 17.5 and day 14 post natal, leaving only 30% of mice to survive to adulthood [115]. The surviving mice develop serve micropthalmia due to lack of eye lens development [115]. This is caused by p53-mediated apoptosis in secondary lens fiber cells during differentiation [119]. Loss of ATF4 is thought to promote apoptosis as it is not present to heterodimerize and sequester ZIP, a kinase that induces apoptosis when homodimerized [121]. This is another example of how ATF4 can act as a repressor and regulate different outcomes, such as cell survival or cell death, depending on its binding partner. It is rather surprising that ATF4 knockout only results in lack of lens development as its transcript is found in a variety of organs. However, because ATF4 belongs to such a large, diverse family, another ATF

member may compensate for its loss, but is unable to do so in the eye. This again highlights how specific ATF expression affects cell survival.

ATF4 pathway delineation

Where and how ATF4 fit into the mammalian ER stress response was unknown until the mechanism regulating GCN4, the yeast homolog of ATF4, was characterized. In response to amino acid deprivation, yeast phosphorylate eIF2α, triggering inhibition of mRNA translation [108]. However, GCN4 mRNA translation is up-regulated in response to eIF2α phosphorylation [81] [83] [108]. Sequence analysis of GCN4 revealed an upstream open reading frame (uORF) that inhibited translation when eIF2α was unphosphorylated but, conversely, facilitated it when it was [120, 121]. As mammalian cells also phosphorylate eIF2α in response to ER stress, it was suggested that mammalian ATF4 regulation might mimic GCN4s. A database of 7,000 mammalian transcription factors was compiled to specifically look for transcription factors that contain uORFs and whose translation is inhibited when eIF2α is not phosphorylated and is increased when it is [81] [83]. ATF4 was identified and found to contain two uORFs, both which are conserved from invertebrates to mammals [81] [83] [122]. Protein, not mRNA levels, increased within 24 hours in response to hypoxia and increased levels of Ca^{2+}, suggesting ATF4 is regulated post transcriptionally in response to ER stress [81] [83] [115]. To verify ATF4 translation was indeed regulated by its' uORF, the AUG start codon found in the second uORF was mutated to AUA and used to drive expression of luciferase. Mutation resulted in

luciferase expression with or without the ERSA THAP [83]. Conversely, the control non-mutated AUG luciferase reporter only exhibited luciferase expression in response to THAP treatment, suggesting ATF4 is regulated by its uORFs in response to ER stress [83].

If ATF4 is regulated by its uORF in response to phosphorylated eIF2α, ER stress induction should increase ATF4 protein levels. Indeed, when cells are treated with ERSAs such as THAP, DTT, or TUN, ATF4 protein increases [81] [83]. When ATF4 levels increase is cell and context dependent. For example, NIH 3T3 cells are able to increase ATF4 protein levels within four to eight hours after THAP treatment while wild type MEFs up-regulate ATF4 protein expression within two hours of THAP treatment [76, 123]. Regardless of the time of induction, ERSA-induced ATF4 protein expression is dependent on PERK. PERK deficient cells have constitutive high levels of ATF4 mRNA but are unable to translate it in response to ERSA treatments as they cannot phosphorylate eIF2α [81] [83]. In this case, increased ATF4 protein levels in response to ERSA treatment, is dependent on PERK mediated phosphorylation of eIF2α [81] [83]. This also suggests that treatment of glioma cells with JLK1486, which acts as an ERSA, will lead to PERK mediated ATF4 translation.

Further confirming that ATF4 protein increases in response to ER stresses, ATF4 mRNA was associated with polyribosomes during ERSA treatment, hypoxia, or amino acid deprivation [81] [83]. Conversely, in unstressed cells, ATF4 mRNA is mainly associated with monosomes, indicating lack of

translation [81] [83]. Additionally, cell stress induced a four-fold incorporation of labeled S35 methionine into ATF4 protein, verifying that ER stress induction regulates ATF4 by increasing its translation in a cap independent manner [81] [83].

The three arms of the ER stress response pathway carefully regulate ATF4 expression through phosphorylation of eIF2α [10] [39] [81] [83]. This maintains organism integrity by preventing stressed cells from entering the cell cycle, giving cells time to resolve stress and the chance to re-enter the cell cycle. If cells are unable to resolve the initial stress response or enter a state of prolonged or chronic stress, the pro-survival response switches to one of pro-death [75]. ATF4 regulates this switch by upregulating the expression of transcription factors that induce mitochondrial-mediated apoptosis [81] [83] [124, 125]. Cancer cells circumvent ER induced death by either suppressing or mutating pro-apoptotic factors or over expressing pro-survival factors in the mitochondrial pathway to promote viability [87] [123].

ATF4 promotes *in vitro* survival

Increased ATF4 expression promotes cell survival in disadvantageous environments. Its expression is elevated in several human cancers, including cervical, breast, skin, and GBMs [87] [110] [113] [120]. As previously addressed, ATF4 can act as either a repressor or an activator, depending on its binding partner, allowing it to regulate a multitude of pro-survival responses that cancer cells depend upon for survival [116, 117] [119].

In response to ER stress, ATF4 increases expression of the pro-survival molecular chaperone BiP, facilitating protein folding to promote cell survival. The finding that ATF4 increases BiP in response to ERSAs was extremely important because it was previously thought that only ATF6 could induce BiP expression [125]. Analysis of the BiP promoter showed the presence of three ER stress response elements (ERSE) that ATF6 recognizes, as well as an ATF-CRE like sequence [125] [126]. ATF4, when dimerized with CREB1, is able to recognize and bind the ATF-CRE like sequence, increasing BiP expression in response to ERSAs [125]. The presence of both sequences is vital for a prompt response to ER stress triggers. Cells lacking ERSEs have decreased BiP induction in response to THAP treatment and ATF4 mutant cells with ERSE and ATF-CRE sequences are unable to increase BiP to the same level as ATF4 wild type THAP treated cells [125]. This suggests that ATF4 and ATF6 synergistically increase BiP. That two arms of the ER stress pathway, ATF6 and ATF4, are both capable of increasing BiP expression speaks to the important role BiP plays in alleviating ER stress and how quickly survival factors can be activated in response to stress.

To alleviate ER stress and promote recovery, ATF4 contributes to the two to ten-fold increase observed in genes that regulate amino acid biosynthesis [127]. For example, ATF4 binds to the nutrient sensing response element in the promoter of asparagine synthetase, increasing expression of the enzyme that converts aspartic acid to asparagine [128]. This increase in amino acid

production facilitates the translation of mRNAs backlogged in the ER as well as increases the translation of proteins triggered by cap independent mechanisms in response to phosphorylated eIF2α.

In addition to increasing levels of molecular chaperones and amino acid production, ATF4 can also protect cells from hypoxia by inducing autophagy [113]. A microarray study in breast cancer cells indicates that ATF4 increases expression of MAPILC3B (LC3B), a key member of the autophagosomal membrane, in response to hypoxia [129]. Sequence analysis of LC3B promoter region indicated a 5' consensus sequence in the UTR that ATF4 can recognize and bind to [131]. Increased expression of LC3B, which occurs after 48 hours exposure to hypoxia, suggests it may not be induced until levels of ATF4 accumulate in response to eIF2α phosphorylation [131]. Knockdown of ATF4 results in a 65% decrease in LC3B mRNA, suggesting that it in part regulates its' transcription [131]. Increased LC3B and subsequent induction of autophagy correlates with increased cell survival and decreased cell death in breast cancer cells exposed to hypoxia, implying that ATF4 increases cancer cell survival in detrimental conditions.

ATF4 promotes *in vivo* survival of cancer cells

Solid tumors are dependent on PERK mediated phosphorylation of eIF2α to activate ATF4 to alleviate hypoxia *in vivo* [81] [83] [110, 111]. Transformed Kras MEFs expressing a mutant eIF2α variant give rise to tumors with high levels of cell death in hypoxic regions [110, 111]. In comparison, transformed wild type

MEFs give rise to larger tumors with less cell death in hypoxic tumor regions. Sectioning of wild type and mutant tumors correlated lack of ATF4 expression with increased sensitivity to hypoxia, accounting for the 80% of apoptotic cells found in hypoxic regions of eIF2α mutant cells versus only 17% in eIF2α wild type tumors [110]. This suggests that ATF4 promotes cell survival in hypoxic regions.

The ability of cancer cells to survive in regions of hypoxia leads to the selection of increasingly resistant cells. ATF4 further promotes chemotherapeutic drug resistance by binding to the ATF-CRE like sequence in SIRT1's promoter [130]. Increased SIRT1 expression leads to increased expression of ABC transporters that selectively pump chemotherapy drugs out of cells [131]. This reduces chemotherapy concentration inside the cell, decreasing drug efficacy [133].

ATF4 not only increases survival in hostile environments while increasing drug resistance, it also promotes survival during metastasis, allowing cells to leave unfavorable surroundings. Loss of attachment in non-transformed cells triggers anoikis, a mitochondrial mediated apoptotic response, and increases ROS [113]. Fibrosarcomal and colorectal adenocarcinoma cancer cells circumvent this by using PERK to increase ATF4 levels. ATF4 binds to the antioxidant response element in heme oxygenase 1 (HO-1), an antioxidant gene, driving a five-fold increase of HO-1, decreasing ROS mediated damage and death [113]. Conversely, knockdown of ATF4 decreases survival during loss of

attachment as cells are unable to induce expression of HO-1 [113]. This was substantiated in a lung cancer colonization mouse models in which ATF4 knockdown inhibited colonization and tumor formation in all mice tail vein injected with human fibrosarcoma cells [113]. Conversely, lung colonization and tumor formation resulted in 6 of 7 mice tail vein injected with ATF4 wild type human fibrosarcoma cells [113]. This suggests that ATF4 promotes survival of cells as they are transported in the vasculature, increasing naïve tissue colonization. Of utmost importance, Kaplan Meier curves generated via the Georgetown Database of Cancer correlated increased levels of HO-1 with decreased survival rates of GBM patients [113]. This same trend was also found in lung cancer patients, with increased HO-1 expression correlating with decreased survival [113]. As GBMs have increased ATF4 expression, it is very possible that ATF4 is a key factor in promoting tumor cell survival by increasing levels of amino acid synthesis, molecular chaperones, enzymes that degrade ROS, transporters resulting in drug efflux, as well as increased survival in response to hypoxia while mediating protective autophagy.

If the stress is resolved, then the ER stress-signaling cascade needs to be de-activated. ATF4 mediates this aspect of the ER stress response by increasing BiP and GADD34 levels [76] [125] [128]. As BiP accumulates in the ER, it binds to the luminal domain of PERK, turning the kinase off [39]. ATF4 reverses the PERK-induced translational block induced by eIF2α phosphorylation by binding to its consensus sequence in the GADD34 promoter. GADD34 activates PPI,

type 1 protein serine/threonine phosphatase, which de-phosphorylates eIF2α, reinstating mRNA translation [77]. Turning off the ER stress response signaling pathway is just as important as turning it on. Mutant ATF4 MEFs are unable to induce GADD34 expression, resulting in prolonged eIF2α phosphorylation and decreased recovery in response to ER stress [77].

ATF4 Summary

ATF4 promotes the survival of cancer cells in deleterious environments. However, its prolonged expression can lead to induction of the pro-apoptotic transcription factor CHOP. As cancer cells are dependent on ATF4 to mitigate ER stress, it is possible to exploit this weakness by forcing even more ATF4 expression in response to drug induced ER stress [10] [39]. This would tip the balance between the pro-survival and pro-death ER responses to favor one of pro-death. Exacerbating ER stress to induce death has been validated *in vitro* with the ER stress inducing agents THAP and TUN; however, these drugs cannot be used in the clinic because of high toxicity and off target effects [10] [81] [83]. We have found that the novel ER stress- inducing agent, JLK1486, when used in combination with TMZ, induces ER stress and sustains ATF4 expression over an extended time course, resulting in CHOP mediated apoptosis [19].

CHOP

CHOP identification and function

GADD153, growth arrest and DNA damage inducible protein 153, was one of twenty novel transcripts identified in the late 1980's to increase in response to

UV DNA damage [132]. As GADD153 was localized to the nucleus it suggested that it regulated transcription [124] [133]. Later studies confirmed that GADD153 encodes the CAAT/EBP homologous protein known as CHOP [127] [134].

CHOP is a bZIP transcription factor comprised of a basic DNA-binding domain and a leucine zipper motif that facilitates the formation of homo and heterodimers [127]. Similar to ATF4, CHOP can act as either a repressor or an activator depending on its binding partner. For example, CHOP dimerization with C/EBP transcription factors blocks binding to classical C/EBP consensus sequences, repressing transcription of genes normally activated by C/EBP homodimer formation [127]. Conversely, ATF3 and CHOP heterodimers prevent ATF3 from binding to c/AMP sites, resulting in activation of genes that ATF3 normally represses [127].

CHOP itself is regulated by cis-acting elements in its promoter. Its C/EBP binding site is recognized by C/EBP β, which induces CHOP [127]. As CHOP accumulates, it dimerizes with C/EBP β, preventing C/EBP β from binding to its own promoter, resulting in decreased transcription of itself [127].

CHOP induction is tightly regulated. There is low to undetectable mRNA levels in non-damaged cycling cells, suggesting CHOP expression inhibits proliferation [135]. Indeed, it was found that CHOP induces cell cycle arrest and apoptosis when ectopically expressed [137[136]. For instance, forced expression of CHOP in HeLa or 3T3 cells results in 90% reduction of BrdU incorporation,

suggesting that CHOP inhibits DNA synthesis during S phase [136]. This is advantageous as it ensures that only unstressed, undamaged cells propagate.

It was suggested that CHOP expression prevents damaged cells from entering the cell cycle, preserving genomic integrity. Supporting this, CHOP wild type versus mutant cells have a 60% decrease in BrdU incorporation in response to serum starvation [136]. When starved cells are stimulated with complete media, the cells undergo a G1/S arrest, confirming that CHOP blocks stressed and damaged cells from entering the cell cycle [136]. In order to do so, CHOP is expressed in early G1 [136]. A G1 arrest allows cells to repair DNA damage before entering the cell cycle, preventing the loss of genetic material during sister chromatid separation. Mutations in either the basic domain or leucine zipper of CHOP results in loss of G1/S arrest, suggesting that CHOP must recognize DNA and form functional dimers to prevent cell cycle progression [136]. The importance of CHOP preventing aberrant cells from cycling is evident in myxoid liposarcoma cancer cells. These cells express a fusion protein of CHOP with a RNA binding protein, rendering CHOP inactive [136]. As a result, myxoid liposarcoma cells are unable to initiate a G1/S arrest, facilitating the propagation of these cancer cells, highlighting the vital role CHOP mediates in protecting genomic integrity [136].

CHOP responds to ER stress triggers

Although initial work suggested CHOP solely responds to DNA damage, others found amino acid and glucose deprivation as well as ERSA treatment also

induced CHOP [127] [137]. More puzzling, UV irradiation of keratinocytes only resulted in a slight induction of CHOP, quite the opposite of the study that first identified CHOP as an important factor of DNA damage response in CHO cells [137]. Surprisingly, exposure of keratinocytes to metabolic insults significantly increased CHOP levels [137]. Taken together, the data suggests that CHOP induction occurs in response to alternative environmental cues not linked to DNA damage.

It was later found that the cells used in the initial report linking CHOP induction to DNA damage were cultured under nutrient deprived conditions [136, 137]. As nutrient deprivation induces ER stress, resulting in CHOP induction, it was suggested that its induction was the result of ER stress, not DNA damage. To verify this, the initial experiment was repeated with the same experimental conditions; however, protein was collected before and after UV exposure. CHOP was significantly elevated before UV exposure, but it was further increased in response to UV, suggesting that UV exposure exacerbated the response to the nutrient stressed environment [137]. This demonstrated that CHOP responds to both DNA damage and ER stress, preventing aberrant cells or those in unfavorable conditions from propagating.

CHOP expression is regulated by the ER stress response

CHOP is the ER stress effector that induces cell death [75]. How the ER stress response pathway regulated CHOP expression was unknown until sequence analysis revealed the presence of an ER stress response element

(ERSE) in its promoter [126]. This was important because many mammalian chaperone genes involved in the ER stress response have the 5' CCAAT-9bp-CCAGC3' sequence, with at least one GGC triplet in the 9 base pair region separating the 5' from 3' end [126]. Indeed, it was found that ATF6 bound to CHOP's ERSE in response to amino acid deprivation and induced its expression when TFII-1 was associated with CHOPs GGC triplet [126]. Validating this, mutations in CHOP's ERSE sequence in CHO cells reduced CHOP expression, suggesting that CHOP may be regulated in response to ER stress [126]. However, as CHOP induction was only reduced, not blocked, in response to ERSE mutation, it suggested other factors with non-ERSE dependent binding domains also regulated its expression [126].

Interestingly, increased CHOP expression did not occur in ERSA-treated cells until ATF4 protein levels accumulated [126, 127]. This suggested ATF4 may directly or indirectly regulate CHOP expression. To delineate a PERK-ATF4-CHOP pathway, PERK deficient MEFs were treated with THAP and assayed for ATF4 and CHOP induction. However, PERK deficient cells were unable to induce either factor [81] [83]. Transfection of ATF4 in PERK deficient THAP treated MEFs rescued CHOP expression, suggesting ATF4 acts as an upstream regulator of CHOP [81] [83]. Expression of a mutant ATF4 lacking its N terminal activation domain in PERK deficient MEFs was unable to induce CHOP, corroborating an ATF4 mediated CHOP regulation [81] [83]. The identification of a C/EBP-ATF composite site in CHOP's promoter validated the observed link

between ATF4 and expression and CHOP induction [126, 127]. Although CHOP is only observed after accumulation of ATF4 protein, ATF4 alone is unable to induce expression of CHOP. In order to increase CHOP expression in response ERSAs, ATF4 must form a heterodimer with C/EBP β [126, 127]. In fact, ATF4-C/EBP β complexes are only found at CHOP's promoter after treatment with THAP, and deletion of either the ATF site or the C/EBP consensus site inhibits ATF4 mediated CHOP expression [126]. This suggests that ATF4 increases CHOP expression, that it must be bound to C/EBP β to do so, and that both ATF-C/EBP consensus sites are required for CHOP induction. This again points to the tight regulation of genes through ATF4 heterodimerization and how induction of CHOP cannot occur until elevated levels of ATF4 accumulate, giving the cell time to recover from ER stress and hostile environments before initiating cell death.

CHOP induction promotes cell death

ERSA treatment of pancreatic and glioma cancer cell lines increases CHOP expression, resulting in caspase 3 activation and cell death [95] [137]. Cisplatin, a cross linking agent, induces apoptosis in HeLa cells due to increased calcium efflux from the ER [138]. Glioma cells treated with desipramine, a tricyclic antidepressant, have increased CHOP levels correlating with increased caspase 3 and 9 cleavage, resulting in apoptosis [139]. Treatment of glioma and breast cancer lines with TZD18, the ligand for the peroxisome proliferating receptor, induced ER stress, resulting in decreased cell growth and increased cell death [140]. Amiodarone, an antiarrythmic drug, increased ATF4 and CHOP

levels, resulting in apoptosis when combined with TRAIL in glioma cells [141]. Minocycline, a derivative of tetracycline that works as a bacteriostatic agent, induces ER stress, increasing P EIF2 alpha, CHOP, and spliced XBP in glioma cells, leading to apoptosis [142]. Although these, and a myriad of other drugs, effectively harness the ER stress response to induce cell death, it is important to understand how the ER pathway uses CHOP to initiate cell death.

Increased CHOP expression precedes ER stress induced cell death; however, the question remains whether CHOP itself induces cell death or CHOP is an ER stress marker prefacing cell death. To determine if CHOP mediates ER cell death, a CHOP deficient mouse model was generated. CHOP deficient mice are viable and fertile, demonstrating that CHOP is not required for development as no major abnormalities were detected [138]. Both CHOP wild type and deficient MEFs induced BiP in response to ER stress, demonstrating that CHOP is not required for the initial ER stress response [138]. However, CHOP deficient MEFs treated with ERSAs were resistant to cell death. Wild type MEFs balled up and detached from substratum in response to ERSAs, resulting in an almost 100% cell death after 48 hours of treatment [138]. Conversely, CHOP deficient MEFs remained attached to the plate and only exhibited a 50% reduction in cell viability at 48 hours post treatment [138]. This was validated as CHOP deficient TUN treated MEFs had a 3 to 5 fold increase in colony formation versus wild type MEF TUN treated cells, showing loss of CHOP correlates with increased viability [138]. Injection of sublethal doses of TUN in CHOP deficient mice resulted in

decreased cell death as well as reduced swelling of proximal tubular epithelium cells in the kidney compared to wild type mice, suggesting that CHOP knockout mice had decreased cell death [138] [143]. As CHOP was determined to play a vital role in ER stress death, the next question became how CHOP executed this.

CHOP activates the intrinsic cell death pathway

CHOP mediated ER cell death involves both intrinsic and extrinsic apoptotic pathways. The Bcl-2 family has 20 plus members and controls the intrinsic apoptosis pathway [84]. The Bcl-2 family includes three subsets: anti-apoptotic, pro-apoptotic, and BH3 only. The anti-apoptotic members, including Bcl-2 itself, Bcl-xl, Bcl-w, and A1, inhibit the activity of pro-apoptotic members BAX, BAK, and BOK, as well as BAD, BID, BIK, BIM, PUMA, and NOXA, which belong to the BH3 only pro-apoptotic subdivision. Both pro and anti apoptotic Bcl-2 family members localize to the ER membrane where they either directly or indirectly interact with two pumps that regulate calcium efflux and influx [84].

The sarco/ER calcium ATPase pump, SERCA, imports calcium from the cytosol into the ER while the inositol triphosphate receptor, IP3R, releases calcium from the ER into the cytosol [84]. Regulating calcium efflux and influx is essential for maintaining ER homeostasis and mitochondrial function. If a flood of calcium is released from the ER, it is absorbed by nearby mitochondria. Calcium absorption inhibits the mitochondrial respiration chain, ultimately triggering release of cytochrome C from the mitochondrial outer membrane, and activating the caspase apoptosis pathway [84]. Although some evidence

suggests that Bcl-2 regulates SERCA, more convincing data suggest it interacts with IP3R, inhibiting release of calcium from the ER, reducing activation of mitochondrial mediated apoptosis [84]. Increased expression of the pro-apoptotic member BAK inhibits Bcl-2 and Bcl-xl from localizing to the ER membrane, preventing their interaction with SERCA or IP3R, resulting in calcium efflux from the ER [84]. BAX exacerbates BAK calcium efflux by forming homo oligomer pores in the outer membrane of the mitochondria, stimulating cytochrome C release [84] [86]. As calcium efflux and influx is regulated by both Bcl-2 pro and anti-apoptotic family members, it is easy to envision how changes in pro to anti-apoptotic ratios would either inhibit or promote ER stress induced death [84].

Analysis of CHOP over-expressing cell lines show that increased CHOP expression results in decreased mRNA and protein levels of Bcl-2 [84] [144]. This inverse relationship was corroborated as CHOP deficient MEFS were unable to decrease Bcl-2 levels when treated with ERSAs [145]. CHOP rescue in MEF deficient lines restored the inverse relationship in response to ERSAs, with increased CHOP levels resulting in decreased Bcl-2 levels. Further substantiating this, use of a Bcl-2 CAT reporter showed increased CHOP levels correlated with decreased reporter levels, indicating CHOP repression of Bcl-2 transcription during ER stress [145]. Mutation of CHOP's leucine zipper domain resulted in loss of transcriptional repression of the Bcl-2 CAT reporter, showing that CHOP regulates Bcl-2 expression and must form a functional dimer to do so [145]. Additional experiments suggest CHOP represses Bcl-2's promoter,

shifting the anti-apoptotic ratio to favor pro-apoptotic factors [86]. Shifting expression would promote cell death as Bcl-2 levels would be too low to inhibit pro-apoptotic factors. If this is indeed the mechanism, then over expression of Bcl-2 in CHOP over expressing lines would prevent ER stress induced death. Over expression of Bcl-2 in CHOP over expressing lines led to a four-fold decrease in cell death in response to THAP or TUN treatments, suggesting that CHOP decreases Bcl-2 levels in response to prolonged ER stress [145].

When Bcl-2 levels decrease, pro-apoptotic factors initiate cell death as Bcl-2 anti-apoptotic members no longer inhibit them [84] [86]. To this extent, CHOP may promote cell death by both transcriptionally repressing Bcl-2 and increasing Bcl-2 pro-apoptotic family members. TUN treatment increases CHOP levels, leading to increased expression of pro-apoptotic BH3 members, PUMA and BIM [135]. In response to ER stress, PUMA and BIM bind to Bcl-2, neutralizing it, resulting in release of cytochrome C from the mitochondria due to permeabilization of the outer membrane mediated by pro-apoptotic members BAX and BAK [135]. Data suggests CHOP increases BIM transcription and binds to PUMA's promoter during ER stress; however, the factors that promote this binding and subsequent up-regulation remain to be identified. A potential candidate is FOXO3a, a member of the forkhead transcription factor family regulated by the PI3K/AKT survival signaling cascade [135]. When AKT is active, FOXO3a is phosphorylated, preventing it from translocating to the nucleus to increase expression of genes associated with apoptosis and cell cycle arrest [4].

As FOXO3a has been implicated in regulating PUMA transcription, it was asked if CHOP and FOXO3a interact. CHOP and FOXO3a interaction, as shown by co-immunoprecipitation, was only detected in nuclear lysates of TUN treated cells, demomstrating that the two factors do interact [135]. Interestingly, TUN treatment of CHOP knockdown cells decreases PUMA expression with little to no BIM induction and cell death, and results in sustained PI3/AKT mediated FOXO3a phosphorylation and sequestration [135]. Although the model is speculative, it is tempting to suggest that CHOP may negatively regulate the PI3K/AKT axis in response to ER stress, resulting in FOXO3a translocation and association with CHOP to drive PUMA expression and promote cell death. This is an attractive model as it suggests CHOP mediates ER stress and PI3K/AKT survival pathway crosstalk, allowing cells to properly respond to unfavorable environmental cues.

CHOP activates the extrinsic cell death pathway

Although the intrinsic pathway is primarily used to mediate and initiate ER stress induced cell death, the extrinsic pathway also contributes through activation of the death receptor pathway. When the tumor necrosis factor-related apoptosis inducing ligand, TRAIL, binds to death receptor 4 (DR4) or death receptor 5 (DR5), FASS-associated protein with death domain (FADD), is recruited to the receptors, serving as a platform for pro-caspase 8 and 10 binding [85] [87]. Pro-caspase 8 is cleaved, cleaving pro-caspase 10, which, in turn, activates the caspase signaling cascade, ending with cleavage of the effector caspase 3 [95]. Although TRAIL is expressed in many cancer cells lines, it is

unable to induce apoptosis as cancer cells amplify death decoy receptors and decrease DR5 [87]. Drugs that upregulate DR5 might re-sensitize cancer cells to TRAIL mediated death. Treatment of glioma cells with ER stress agents such as MG132, a proteasome inhibitor, or arsenic trioxide, which induces apoptosis in leukemia cells, increases expression of CHOP and DR5 [88] [145]. Importantly, increased expression of CHOP preceded enhanced DR5 expression. Both mutant and CHOP knockdown lines are unable to increase DR5 in response to arsenic trioxide, suggesting CHOP regulates DR5's increase in response to ER stress [146]. CHOP transcriptional regulation of DR5 was validated through DR5 reporter assays in which mutation of CHOP's DNA binding site led to a more than 3 fold decrease in DR5 driven luciferase [87] [146]. A variety of other ER stress inducing agents, such as caspaicin, amiodarone (anti-arrythmia drug), nelfinavir (FDA approved HIV protease inhibitor), MK886 (lipooxygenase inhibitor), confirmed the CHOP mediated upregulation of DR5. This led to the combination of ER drugs with TRAIL to significantly increase cell death [87] [143] [147,[147]. For example, glioma cells treated with amiodarone and TRAIL results in only 30% viability post treatment, suggesting TRAIL and ER stress inducing drugs are an advantageous means to increase death [143].

CHOP interferes with wnt, IL-6, and increases ROS to promote cell death

The majority of studies emphasize CHOP mediated cell death through activation of extrinsic and intrinsic apoptotic pathways; however, it is important to

note that CHOP also induces cell death by blocking pro-survival signals and exacerbating the response to ER stress conditions.

Recent data suggests that CHOP contributes to cell death by decreasing activation of the wnt pathway, resulting in decreased translocation of beta catenin [148]. Although the mechanism remains to be elucidated, there is precedent for CHOP mediated down regulation of wnt, the ligand responsible for frizzled receptor activation, in xenopus laevis embryos [149].

In addition to blocking survival signals transmitted by wnt, increased CHOP expression represses expression and secretion of interleukin 6 (Il-6) [26]. This may have therapeutic application as GBM cells, specifically EGFR VIII cells, increase IL-6 signaling to stimulate nearby endothelial cells, leading to the formation of larger, faster growing tumors [26]. Treatment of GBM cells with genistein increases expression of CHOP mRNA and protein, leading to the formation of CHOP-C/EBP β heterodimers [26]. This is problematic as CHOP-C/EBP β heterodimers prevent C-EBP β from binding to IL-6, resulting in decreased IL-6 expression and secretion. This would decrease stimulation of endothelial cells and result in smaller tumors, as seen in VIII genistein treated mice [26].

Lastly, CHOP exacerbates ER stress by increasing the translation of mRNAs in an already stressed and overwhelmed ER [144] [149]. CHOP wild type MEFs versus mutant CHOP MEFs increase GADD34 expression, which leads to the de-phosphorylation of eIF2A, alleviating the repression of mRNA

translation, while increasing oxidative stress [144] [150]. Reversing translational repression benefits cells recovered from ER stress and ready to resume cell processes. It is detrimental to cells that have not yet re-established ER homeostasis, thereby tipping the scale towards cell death.

GBM cells evade CHOP mediated cell death

GBMs evade CHOP mediated cell death by interfering with the activation of the extrinsic and intrinsic apoptotic pathways. To prevent pro-apoptotic Bcl-2 family members from initiating apoptosis, GBM cells increase expression of pro-survival Bcl-2 factors, including Bcl-2 itself and Bcl-xl [87]. Moreover GBM cells repress expression of pro-apoptotic Bcl-2 members, ensuring that the ratio of pro-survival to pro-apoptotic factors is always in favor of survival, decreasing the ability of pro-apoptotic member from initiating mitochondrial mediated apoptosis [3]. Furthermore, GBM cells have constitutively active PI3K/AKT signaling due to mutation of the tumor suppressor gene, PTEN, which negatively regulates the axis [1] [20] [22]. As previously addressed, AKT signaling inhibits translocation of FOXO3a, leading to decreased CHOP-FOXO3a heterodimer formation, resulting in decreased transcription of the pro-apoptotic member, PUMA [135]. GBM cells further avoid CHOP induced cell death by increasing expression of death decoy receptors on their surface [87]. This reduces TRAIL mediated activation of DR5, resulting in decreased induction of the extrinsic cell death pathway.

Summary

The ER stress pathway initially promotes a pro-survival response by stalling mRNA translation, and increasing the synthesis of amino acids, molecular chaperones, and enzymes to facilitate protein folding [10] [39]. However, if stress cannot be resolved, the pro-survival response switches to pro-death [75]. This is due to sustained ATF4 expression inducing transcription of the pro-apoptotic ER transcription factor, CHOP [95] [138] [145]. It is possible to force the pro-survival to pro-apoptotic switch by exacerbating ER stress with the use of drugs, such as JLK1486 [35] [39]. This is an attractive approach as GBMs rely on the ER to mitigate their unfavorable environment. Following this strategy, we found that addition of JLK1486 to TMZ not only forced this switch, but also impaired cells ability to resolve DNA DSBs, leading to increased cell death [19]. Our data suggests the use of ER stress inducing agents may provide an added benefit when combined with TMZ and should be further explored.

CHAPTER II

Rationale of drug combination

We tested if the addition of JLK1486, a novel ER stress- inducing agent, to TMZ, a DNA alkylating agent, increased the efficaciousness of therapy. We reasoned that formation of DNA DSBs occurring in the presence of an overwhelming ER stress response would be catastrophic to cell survival.

Results

JLK1486 is active as a single agent

To determine the efficacy of JLK1486 as a single agent, we utilized a panel of GBM adherent, non-adherent, and primary lines. For the majority of our established adherent GBM lines, a low concentration of JLK1486 inhibited proliferation (Figure 3A-E; U87MG IC50= 0.6 µM; A172 IC50 = 0.26 µM; U118MG IC50 = 0.87µM; LN18 IC50 = 0.27 µM); however, one line, T98G, was relatively resistant to JLK1486 (Figure 3D; T98G IC50 = 7.6 µM). To assess the efficacy of JLK1486 in both converted non-adherent and primary lines, we employed neurosphere assays in which spheres are dissociated, single cells are plated at clonal density, drug treated, and allowed to grow. On either the seventh (converted non-adherent cell lines) or tenth day (primary cell lines), neurospheres, defined as a single sphere containing ten or more cells, were counted to measure the effects increasing concentrations of JLK1486 had on growth. We found our two converted non-adherent cell lines, U87NS and U118NS, were sensitive to JLK1486 (Figure 3F-G; U87NS IC50 = 1.6 µM;

U118NS IC50 = 0.13 µM). Our primary lines, GS8-26 and 5075, were also sensitive to JLK1486, with an IC50 of 0.08 µM in both lines (Figure 3 H-I).

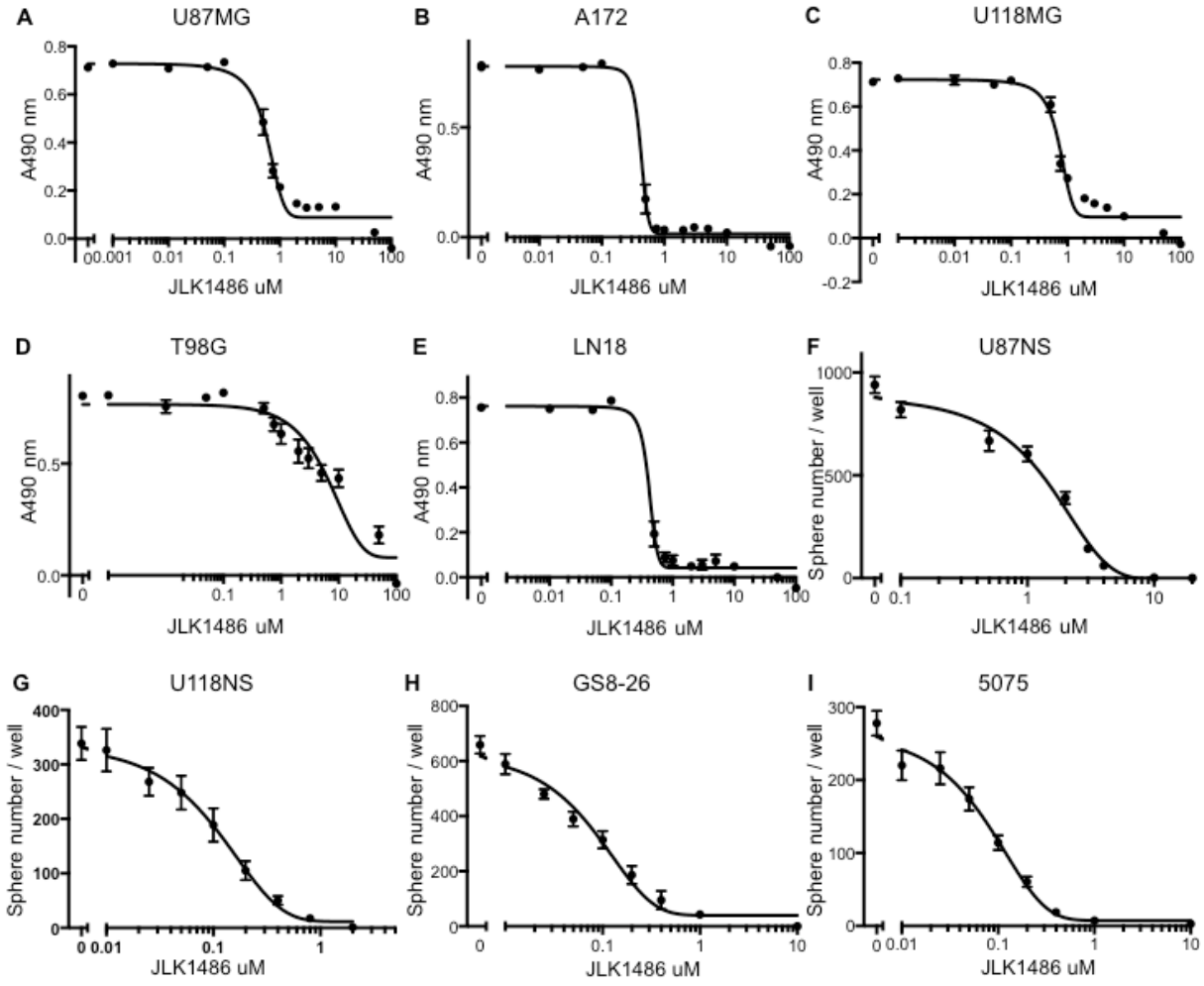

Figure 3: JLK1486 has activity as a single agent. (A-E) Determination of JLK1486 IC50s in adherent lines via MTS assay. Relative absorbance at 490 nm is shown. **(F-I)** Determination of JLK1486 single agent IC50s in non-adherent and primary lines generated by day 7 neurosphere formation counts. N=3, all error bars are SEM.

JLK1486 combined with TMZ reduces secondary sphere formation more effectively than JLK1486 or TMZ as single agents

Secondary sphere formation assays are an *in vitro* tool to mimic the clinical recurrence universally exhibited in GBM patients, allowing one to monitor self-renewal and durability of treatment. Additionally, non-adherent cells form more infiltrative tumors than established, adherent cell lines, such as U87MG cells, and are therefore a better representation of clinical GBMs [93]. Non-adherent cell lines are dissociated, plated at clonal densities, drug treated and allowed to grow for seven or ten days. Fresh medium is added on day seven (U87NS, U118NS) or ten (GS8-26, 5075), and cells are allowed to grow an additional seven (U87NS, U118NS) or ten (GS8-26, 5075) days, and then counted, allowing cell and sphere recovery to be assessed. On day fourteen (U87NS, U118NS) or day twenty (GS8-26, 5075), spheres are dissociated to single cells, re-plated, allowed to grow for an additional seven (U87NS, U118NS) or ten days (GS8-26, 5075), and then counted to assess secondary sphere formation (Figure 4; Figure 5 A-B).

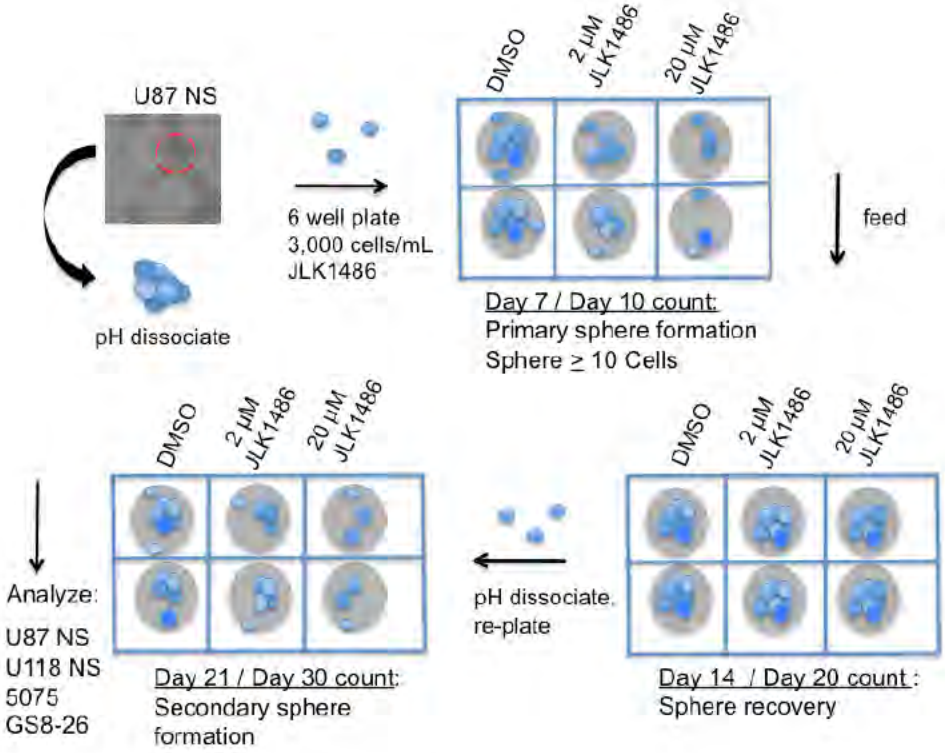

Figure 4: Graphical depiction of U87NS neurosphere assay. Cells are plated at single cell clonal density and treated in duplicate with either DMSO or increasing concentrations of JLK1486 (0μM – 20μM). Primary spheres are counted on either day 7 or day 10 and cells are fed after counting. Sphere recovery is counted on either day 14 or day 20, after which cells are pH dissociated and re-plated at single cell suspension. Secondary sphere formation is determined by either day 21 or day 30 counts. U87NS and U118NS lines follow the day 7, day 14, and day 21 counts while primary lines, 5075 and GS8-26, follow the day 10, day 20, and day 30 counts.

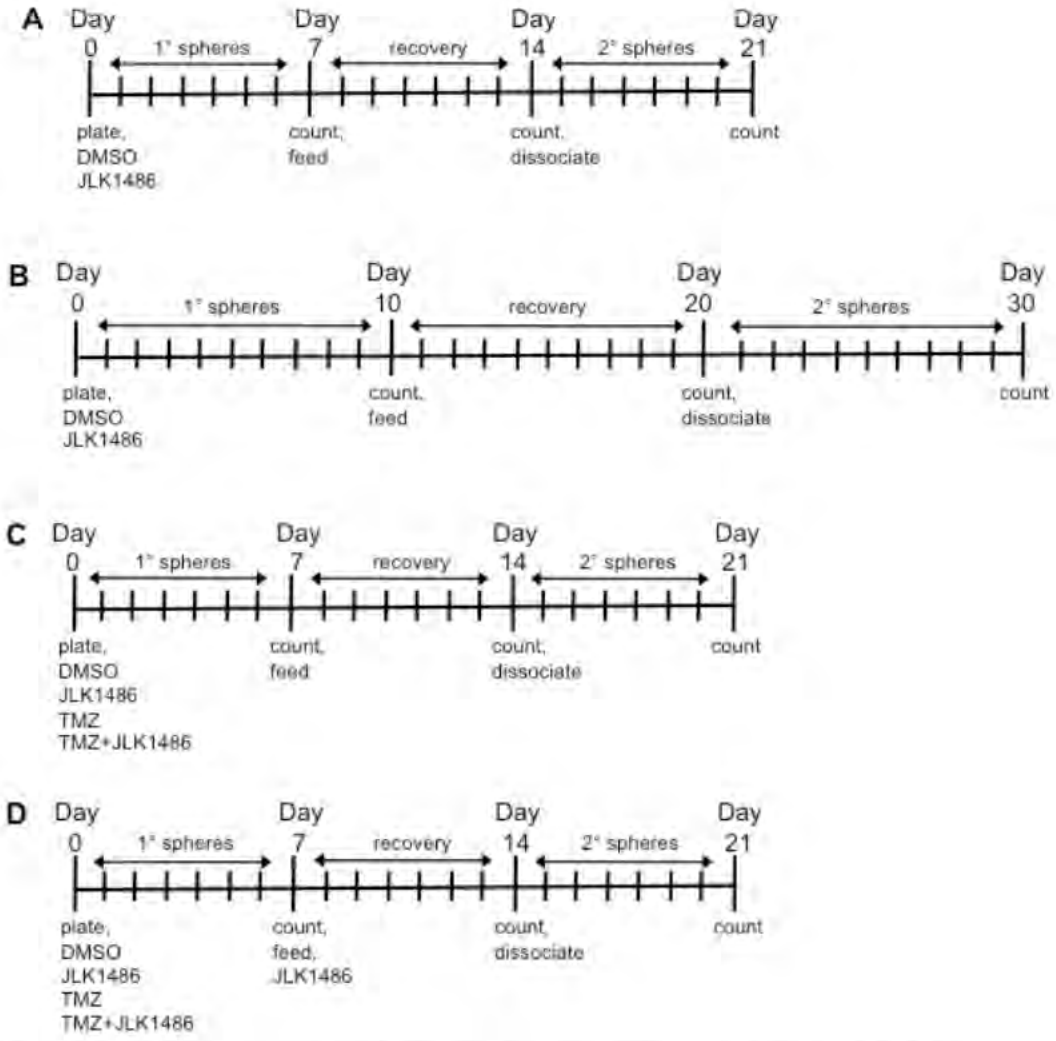

Figure 5: Secondary sphere formation timeline for JLK1486 and TMZ +JLK1486 dosing, dissociation, and counting of non-adherent and primary lines. (A) Scheme of secondary sphere formation assay depicting timeline of when U87NS and U118NS cell lines were treated with JLK1486 alone, counted, dissociated, and re-counted. **(B)** Scheme of secondary sphere formation assay depicting timeline of when GS8-26 and 5075 primary cell lines were treated with JLK1486 alone, counted, dissociated, and re-counted. **(C)** Scheme of secondary sphere formation assay depicting timeline of when U87NS and U118NS cell lines were treated with both JLK1486 and TMZ. GS8-26 and 5075 primary lines followed scheme shown in panel (B). **(D)** Scheme of secondary sphere formation assay depicting timeline of when U87NS and U118NS cell lines were treated once (1X) with TMZ and twice (2X) with JLK1486. GS8-26 and 5075 primary lines followed scheme shown in panel (B).

To determine if JLK1486 as a single agent blocked secondary sphere formation, we carried out a neurosphere formation assay with U87NS cells using a range of JLK1486 doses from 0μM to 20μM. Although JLK1486 alone at the IC50 for U87NS (2μM) (Figure 6A) did not completely block secondary sphere formation, there was a statistically significant reduction of day 21 secondary spheres compared to the DMSO control sample. A higher dose of JLK1486 (20μM, ten times higher than the IC50) completely blocked secondary sphere formation (Figure 6A). Reduced sphere formation suggests that JLK1486 may be a novel chemotherapeutic for delaying recurrence.

This led us to ask if the efficacy of TMZ, the chemotherapeutic agent currently used in the clinic, could be improved if used in combination with JLK1486. We performed secondary sphere formation assays using TMZ alone (the relevant dose of TMZ in our converted non-adherent lines has been previously described [150]) and in combination with a sub-IC50 dose of JLK1486 (1μM) as well as the IC50 dose (2μM) in U87NS cells (Figure 5C). We did not find a statistically significant reduction of secondary spheres for the sub-optimal dose of TMZ+ 1μM JLK1486 when compared to TMZ alone (Figure 6B). We did find significant reduction of secondary sphere formation in TMZ+ 2μM JLK1486 versus TMZ or JLK1486 alone (Figure 6B). However, there was not a complete block in secondary sphere formation in the TMZ+2μM JLK1486 dose, indicated

by the statistically significant increase in sphere formation in day 14 versus day 21 samples (Figure 6B).

In the clinic GBM patients receive multiple doses of chemotherapeutics [5] [34]. We asked if two doses of JLK1486 would increase the efficaciousness of the TMZ+JLK1486 combination treatment. We carried out secondary sphere formation assays in which cells were dosed with TMZ+JLK1486 on day 0 and then treated a second time with JLK1486 alone on day 7 (Figure 5D). Because the pharmacokinetics, mechanism, and durability of TMZ treatment have been established and shown to occur up to 120 hours, we reasoned that substantial TMZ induced DNA damage would have occurred by day 7 and that a second dose of JLK1486 on day 7 may exacerbate the TMZ induced damage [29] [33]. We found significant secondary sphere reduction in the sub-optimal dose combination of TMZ+ 1µM JLK1486 2X versus TMZ+ 1µM JLK1486 1X (Figure 6C versus Figure 6B) as well as inhibition of secondary sphere formation in TMZ+ 2µM JLK1486 2X versus TMZ+ 2µM JLK1486 1X (Figure 6C versus Figure 6B). Additionally, we found significantly decreased secondary sphere formation in our converted non-adherent U118NS line as well as our primary lines GS8-26 and 5075 when cells were treated on day 0 with TMZ+ JLK1486 and a second time with JLK1486 on day 7 (Figure 6D-F). This demonstrates that the TMZ+ JLK1486 is an effective combination therapy to decrease secondary sphere formation and may be a schedule-dependent process . All further

experiments were conducted using TMZ+JLK1486 2X (JLK1486 on day 0 and on day 7; figure 5D).

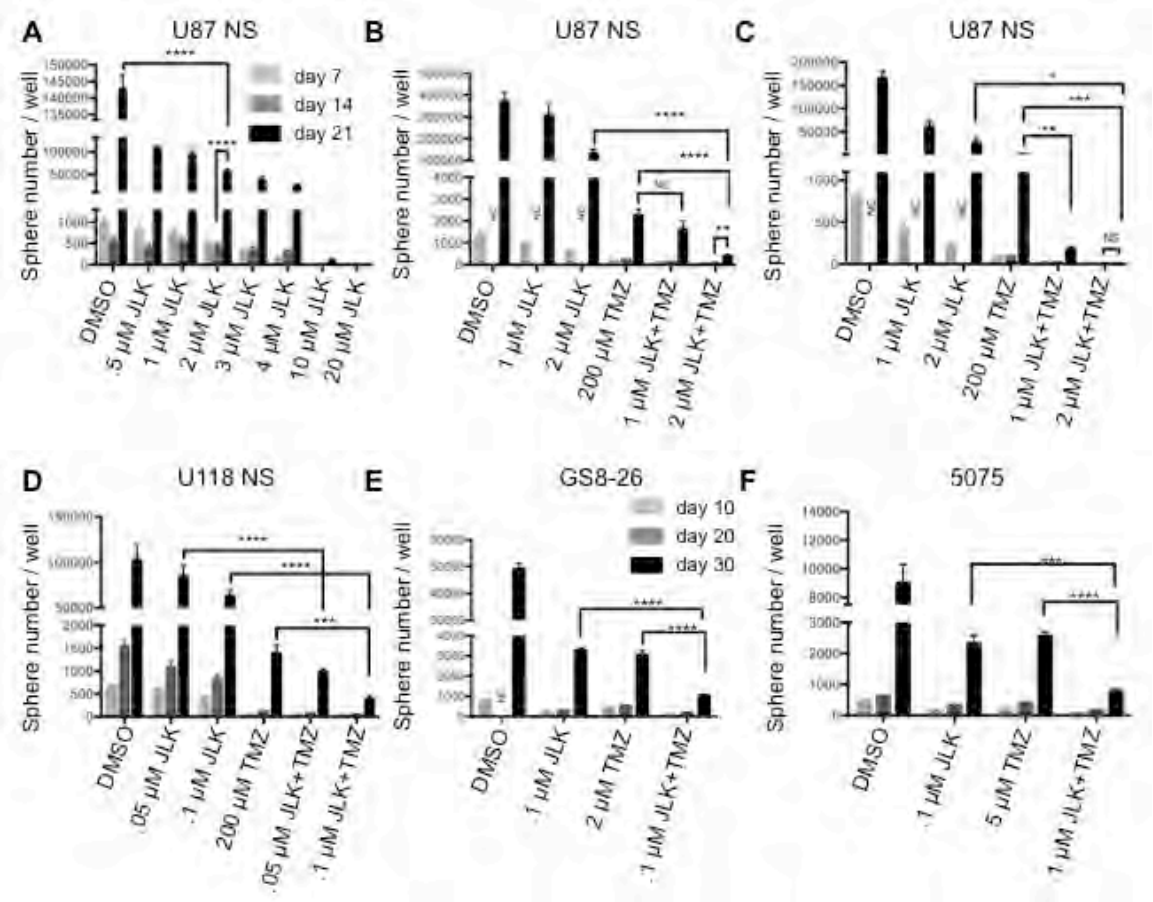

Figure 6: JLK1486 alone does not block secondary sphere formation but when combined with TMZ, secondary sphere formation in decreased. (**A**) Secondary sphere formation assay of U87NS cells treated with JLK1486 alone, one time on day 0 (n=3). (**B**) Secondary sphere formation assay of U87NS cells treated with TMZ+JLK1486. Cells were dosed one time on day 0 with both agents (n=4). (**C**) Secondary sphere formation assay of U87NS cells treated with TMZ+JLK1486. Cells were dosed on day 0 with both TMZ+JLK1486 and a second time with JLK1486 on day 7 (n=6). (**D**) Secondary sphere formation of U118NS cells treated with TMZ+JLK1486 on day 0 and a second time with JLK1486 on day 7 (n=3). (**E**) Secondary sphere formation of primary line GS8-26 cells treated with both TMZ+JLK1486 on day 0 and with JLK1486 on day 7 (n=3). (**F**) Secondary sphere formation of primary line 5075 cells treated with both TMZ+JLK1486 on day 0 and JLK1486 on day 7 (n=3). NC = not counted because neurospheres were too numerous. All error bars are SEM, two-tailed t-test, *P=0.01, **P=0.001-0.007,***P=0.0002-0.0005,****P <0.0001

TMZ+JLK1486 treatment results in decreased cell growth and increased cell death in U87NS

To determine how TMZ+2μM JLK1486 treatment reduced secondary sphere formation in U87NS cells, we carried out a time course ranging from 24 hours to 23 days to evaluate the number of trypan blue positive and negative cells. Control cells treated with DMSO had the highest rate of proliferation from day 0 to day 14 (Figure 7A). Cells treated with either 1μM or 2μM JLK1486 increased in number from day 0 to day 14, however, there were significantly fewer JLK1486-treated cells versus the DMSO control (Figure 7A). Cells treated with either TMZ alone or TMZ in combination with 1μM or 2μM JLK1486 did not undergo significant proliferation from day 0 to day 14 (Figure 7A). This was expected as it has been well established in the literature that TMZ induces DNA double strand breaks that result in G2/M arrest. After day 14 dissociation and re-plating, DMSO, 1μM and 2μM JLK1486-treated cells, as well as TMZ alone treated cells underwent significant proliferation from day 16 to day 23 (Figure 7A-B). Although the number of TMZ+1μM JLK1486- treated cells was less than TMZ alone treated cells on day 23, this was not statistically significant (Figure 7B). However, cells treated with TMZ+2μM JLK1486 were incapable of repopulating their cultures and maintained a statistically significant reduction in cell number versus JLK1486 alone as well as TMZ alone (Figure 7B). This suggests that

inhibition of secondary sphere formation in TMZ+2μM JLK1486-treated cells is at least partly the result of treated cells' inability to proliferate.

We simultaneously collected trypan-blue-positive counts to detect cell death in U87NS control, single agent, and TMZ+JLK1486-treated cells. We observed significant increases in cell death in TMZ alone as well as TMZ+1μM JLK1486 and TMZ+2μM JLK1486-treated cells versus DMSO and 1μM and 2μM JLK1486 single-treated cells in the first half of our time course (Figure 7C; days 0-14). However, post day 14, we observed a significant decrease in the percentage of trypan blue positive cells from day 16 to day 23 in TMZ alone treated cells (Figure 7C). Although the percentage of trypan-blue-positive TMZ+1μM JLK1486 cells also decreased for samples post day 14, the percent remained significantly higher than TMZ or 1μM JLK1486 alone (Figure 7C). Conversely, the percent of trypan-blue-positive cells in TMZ+2μM JLK1486-treated cells continued to increase post day 14 (Figure 7C). This resulted in a 70.0% (+/- 5.0) trypan-blue-positive population in TMZ+ 2μM JLK1486-treated cells versus 14.3% (+/- 3.2) in TMZ-treated cells and 10.3% (+/- 3.9) in 2μM JLK1486-treated cells (Figure 7D).

To test if the observed increase in cell death was due to apoptosis, we performed FACS analysis with annexin V and propidium iodide (PI) staining of 23-day samples. The annexin V and PI staining corroborated our trypan blue counts as we observed 70.6% double positive cells in TMZ+2μM JLK1486-

treated cells versus 3.9% in DMSO, 2.6% in 2μM JLK1486 alone, and 2.3% in TMZ alone treated cells (Figure 7 E-H;I-J).

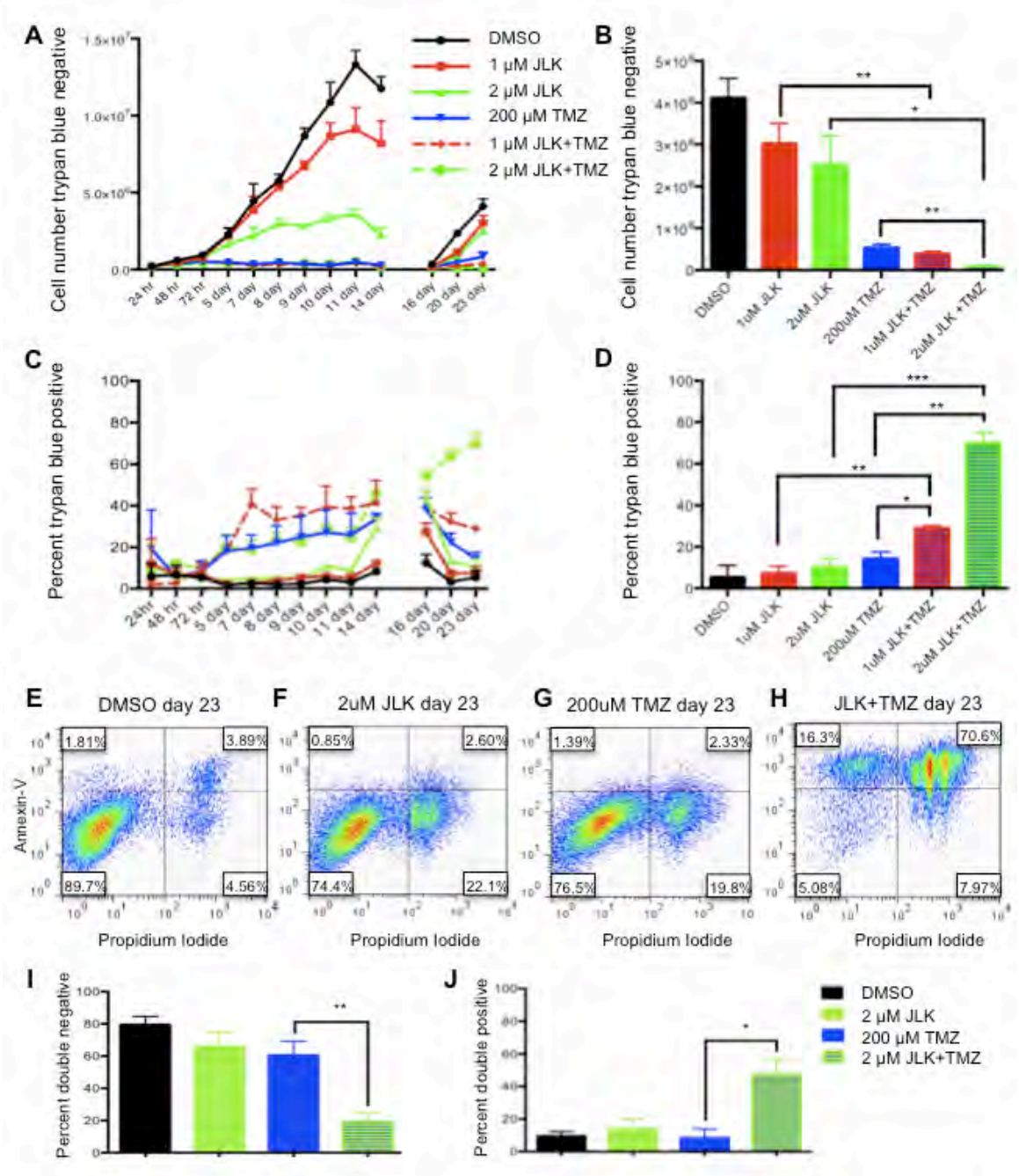

Figure 7: TMZ+JLK1486 double treatment results in decreased cell growth and apoptosis in U87NS cells. **(A)** The number of trypan blue negative cells in U87NS cells treated with DMSO, 1μM JLK1486, 2μm JLK1486, 200μM TMZ, TMZ+1μM JLK1486, and TMZ+2μm JLK1486 collected over 24 hours to 23 days (n=3). **(B)** Quantification of the number of trypan blue negative U87NS cells in DMSO, 1μM JLK1486, 2μm JLK1486, 200μM TMZ, TMZ+1μM JLK1486, and TMZ+2μm JLK1486 conditions at day 23 (n=3). **(C)** The percent of trypan blue positive cells in U87NS cells treated with DMSO, 1μM JLK1486, 2μm JLK1486, 200μM TMZ, TMZ+1μM JLK1486, and TMZ+2μm JLK1486 collected over a 24 hour to 23 day time course (n=3). **(D)** Quantification of the percent of trypan blue positive U87NS cells in DMSO, 1μM JLK1486, 2μm JLK1486, 200μM TMZ, TMZ+1μM JLK1486, and TMZ+2μm JLK1486 conditions at day 23 (n=3). **(E-H)** Representative FACs analysis comparing propidium versus annexin V staining of day 23 U87NS cells treated with DMSO, 2μm JLK1486, 200μM TMZ, and TMZ+2μm JLK1486 (n=4). **(I)** Percent of PI and Annexin V double negative cells in day 23 U87NS cells treated with DMSO, 2μm JLK1486, 200μM TMZ, and TMZ+2μm JLK1486 (n=4). **(J)** Percent of PI and Annexin V double positive cells in day 23 U87NS cells treated with DMSO, 2μm JLK1486, 200μM TMZ, and TMZ+2μm JLK1486 (n=4). All error bars are SEM, two-tailed t-test, *P=0.01-0.02,**P=0.001-0.008,***P=0.0007

This demonstrates that TMZ+ 2μM JLK1486 treatment in U87NS cells results in reduced cell growth due to the induction of apoptosis.

TMZ+JLK1486 treatment induces prolonged endoplasmic reticulum stress that results in induction of CHOP, a pro-apoptotic transcription factor

It is well established that prolonged, unresolved ER stress triggers apoptosis [151-153]. To determine if TMZ+2μM JLK1486 treatment results in prolonged ER stress induction, we collected a series of protein lysates over a 24-hour to 23-day time course. We probed protein lysates for levels of BiP, a key heat shock molecular chaperone indicative of ER stress, as well as ATF4, a transcription factor that initially serves as a pro-survival signal but switches to pro-apoptotic when ER stress is unresolved. ATF4 drives increased expression of the pro-apoptotic transcription factor CHOP. We therefore analyzed protein lysates for ATF4 and CHOP to detect this switch.

In 2μM JLK1486 and TMZ+2μM JLK1486-treated cells we observed increased expression of BiP that was maintained 14 days post treatment suggesting that JLK1486 induces prolonged ER stress (Figure 8). For post

treatment day 14, BiP levels were highly elevated in all conditions (Figure 8). Increased expression of ATF4 was observed only in JLK1486 and TMZ+2μM JLK1486-treated cells (Figure 8). Induction began three days post treatment and was maintained 21 days post treatment, suggesting generation of long-term ER stress (Figure 8). We did find strong expression of ATF4 in day 14 DMSO-treated cells (Figure 8). We suggest this induction is due to nutritional deprivation resulting from these rapidly proliferating cells becoming overgrown. This is substantiated by a slight decrease in day 14 trypan blue negative cell number (Figure 7A) as well as the lack of increased and sustained CHOP induction of day 14, 19, and 21 DMSO versus 2μM JLK1486 alone or TMZ+2μM JLK1486-treated samples (Figure 8). Induction of CHOP was not observed until 9 days post 2μM JLK1486 and TMZ+2μM JLK1486 treatment (Figure 8). CHOP levels were maintained until day 14 in 2μM JLK1486 alone and TMZ+ 2μM JLK1486-treated cells. Increased CHOP expression was detected in TMZ+ 2μM JLK1486-treated cells in day 19 and day 21 lysates (Figure 8). ATF4 and CHOP were undetectable in all day 23 protein lysates (Figure 8). Induction of BiP and ATF4 in 2μM JLK1486 and TMZ+ 2μM JLK1486-treated cells suggests that JLK1486 is an effective ER stress-inducing agent and may promote cell death via prolonged ATF4 expression driving CHOP in TMZ+ 2μM JLK1486-treated cells.

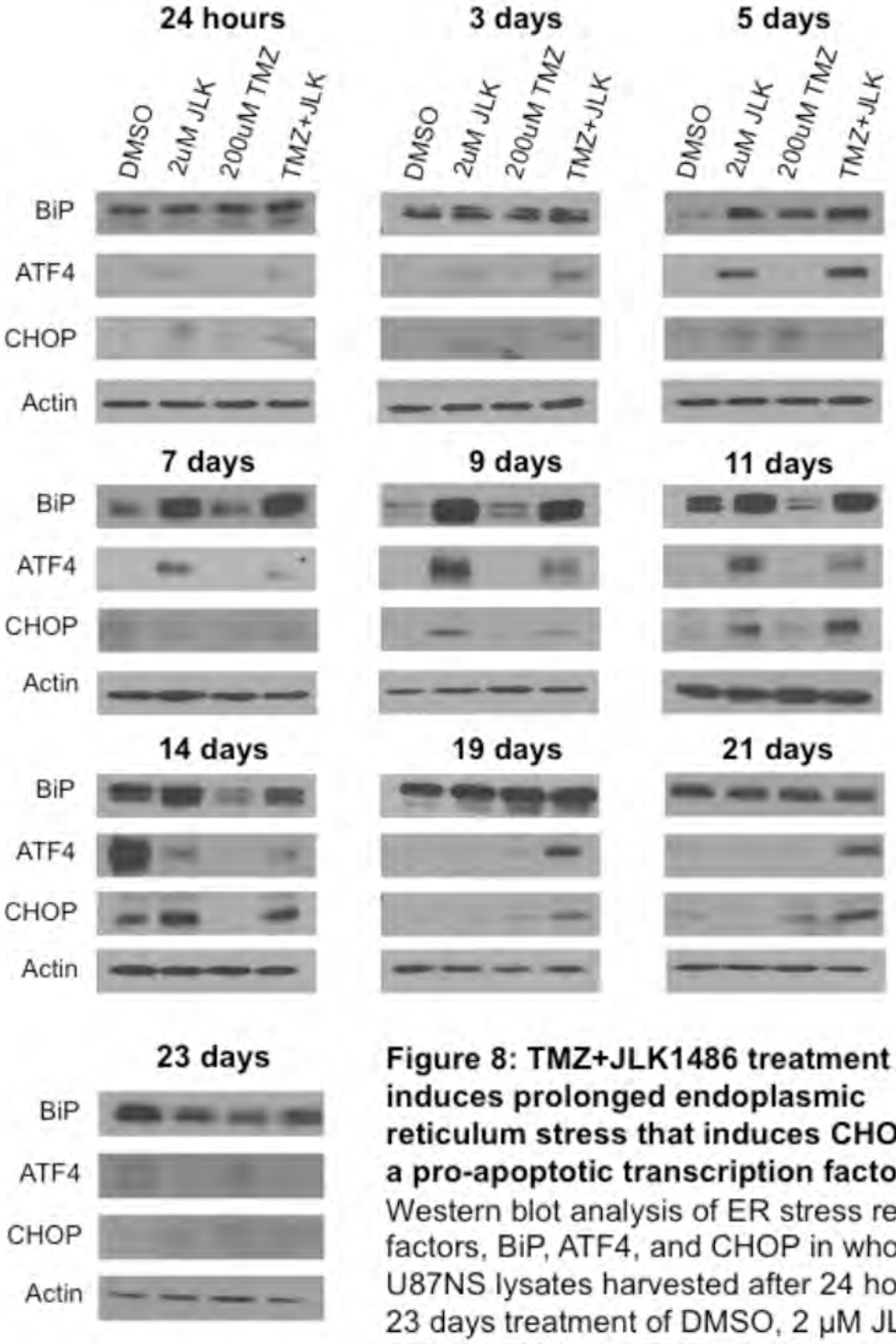

Figure 8: TMZ+JLK1486 treatment induces prolonged endoplasmic reticulum stress that induces CHOP, a pro-apoptotic transcription factor. Western blot analysis of ER stress response factors, BiP, ATF4, and CHOP in whole cell U87NS lysates harvested after 24 hours to 23 days treatment of DMSO, 2 μM JLK1486, 200 μM TMZ, and TMZ+ 2 μMJLK1486. Blots are representative of n=3.

TMZ+JLK1486 treatment triggers prolonged activation of DNA damage response pathway and promotes unresolved DNA double stand breaks

TMZ induces the formation of DNA DSBs. This results in phosphorylation of DNA damage transducers, ATM and CHK2, which in turn induces phosphorylation of H2A.X, a key marker for DSBs, and recruitment of RAD51 to DSBs to initiate homologous recombination [154-156]. To determine if the combination of TMZ+2μM JLK1486 increases and/or prolongs DNA damage, we analyzed a series of protein lysates collected from 24 hours to 23 days post treatment for P ATM, ATM, P CHK2, CHK2, RAD51, and γH2A.X.

We observed phosphorylation of ATM and CHK2 24 hours post treatment in TMZ and TMZ+2μM JLK1486-treated cells (Figure 9). Increased levels of P ATM and P CHK2 were maintained in TMZ and TMZ+2μM JLK1486-treated cells throughout the time-course, however, we noted higher levels of P ATM and P CHK2 in post day 14 combination lysates, suggesting TMZ+2μM JLK1486 treatment results in a sustained DNA damage response (Figure 9). Additionally, we detected extended phosphorylation of H2A.X in TMZ+2μM JLK1486-treated cells, suggesting substantially more unresolved DNA DSBs in combination versus TMZ single treated cells (Figure 9; Figure 10). Although high levels of RAD51 were initially observed in all conditions, we found RAD51 levels decreased 5 days post treatment in 2μM JLK1486 alone and TMZ+2μM JLK1486-treated cells and were continually lower than TMZ alone treated cells until 21 days post treatment (Figure 9). Increased expression of RAD51 was not

detected until 23 days post treatment. Detection of increased P ATM, P CHK2, and prolonged γH2A.X in TMZ+2μM JLK1486 cells suggests that combination treatment not only prolongs the DNA damage response, but also promotes unresolved DNA DSBs over an extended time course through reduction of RAD51.

Knockdown of ATF4 does not rescue secondary sphere formation but does decrease cell death in TMZ+JLK1486 treated cells

Because we observed inhibition of secondary sphere formation (Figure 6), increased cell death (Figure 7) and prolonged expression of ATF4 in TMZ+2μM JLK1486- treated cells (Figure 8), we asked if knockdown of ATF4 would rescue secondary sphere formation and decrease cell death. To determine this, we generated three stable U87NS lines, one expressing an shRNA control, and two lines expressing shRNAs against ATF4, shATF4 C1 and shATF4 E7. The U87NS sh control, shATF4 C1, and shATF4 E7 lines were treated with DMSO, 2μM JLK1486, 200μM TMZ, and TMZ+2μM JLK1486, protein lysates were collected at 24 hours and five days post treatment, and ATF4 levels were examined via western. Because neurosphere and trypan blue assays were carried out with cells plated at passage four and assays completed by passage six, we analyzed ATF4 expression levels in our knockdown lines at passage number six to verify that knockdown was maintained throughout the experimental time-course. We observed robust induction of ATF4 in 2μM JLK1486 and TMZ+2μM JLK1486 sh control treated U87NS cells, slight induction of ATF4 in 2μM JLK1486 and

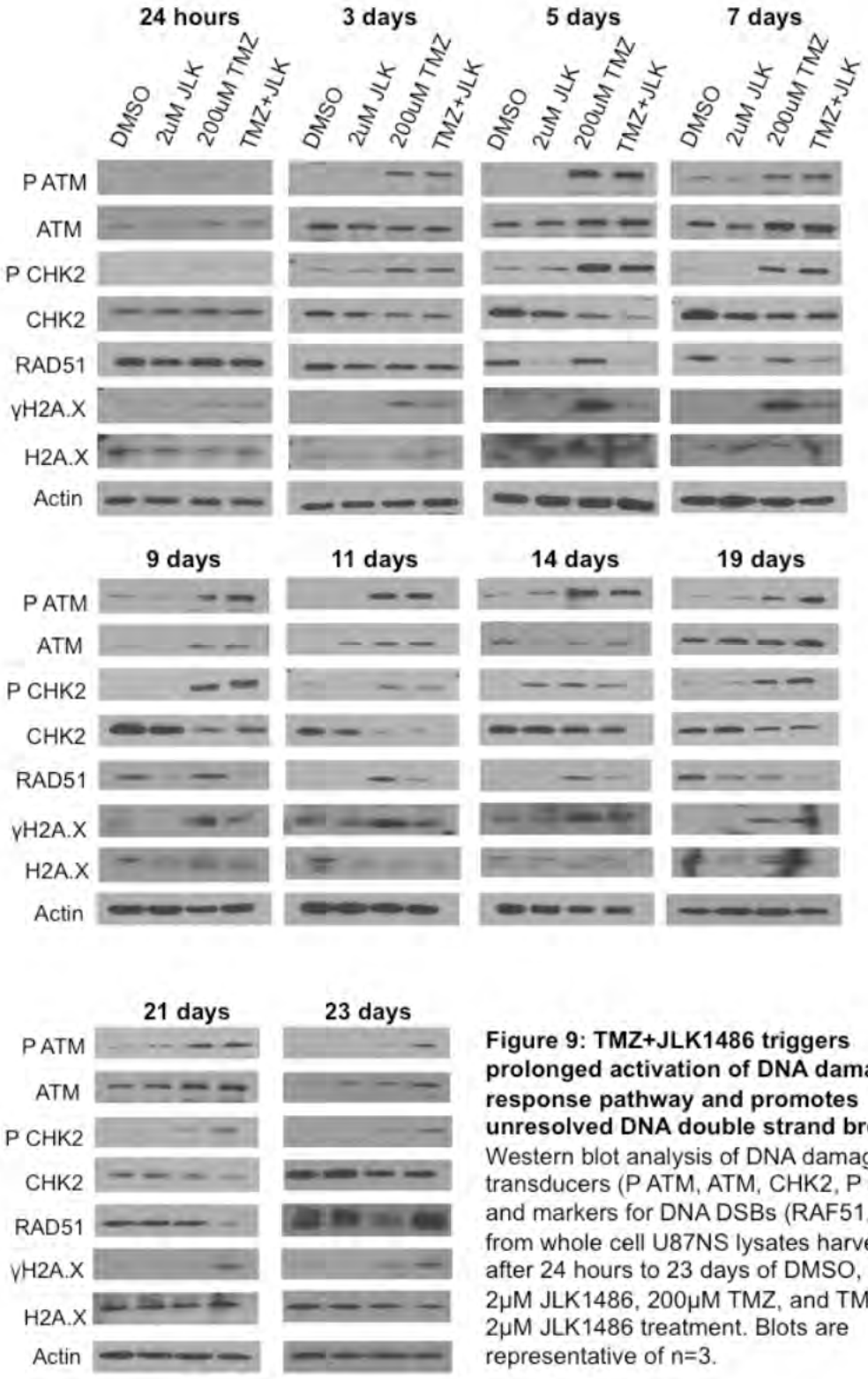

Figure 9: TMZ+JLK1486 triggers prolonged activation of DNA damage response pathway and promotes unresolved DNA double strand breaks. Western blot analysis of DNA damage transducers (P ATM, ATM, CHK2, P CHK2) and markers for DNA DSBs (RAF51, γH2A.X) from whole cell U87NS lysates harvested after 24 hours to 23 days of DMSO, 2μM JLK1486, 200μM TMZ, and TMZ+ 2μM JLK1486 treatment. Blots are representative of n=3.

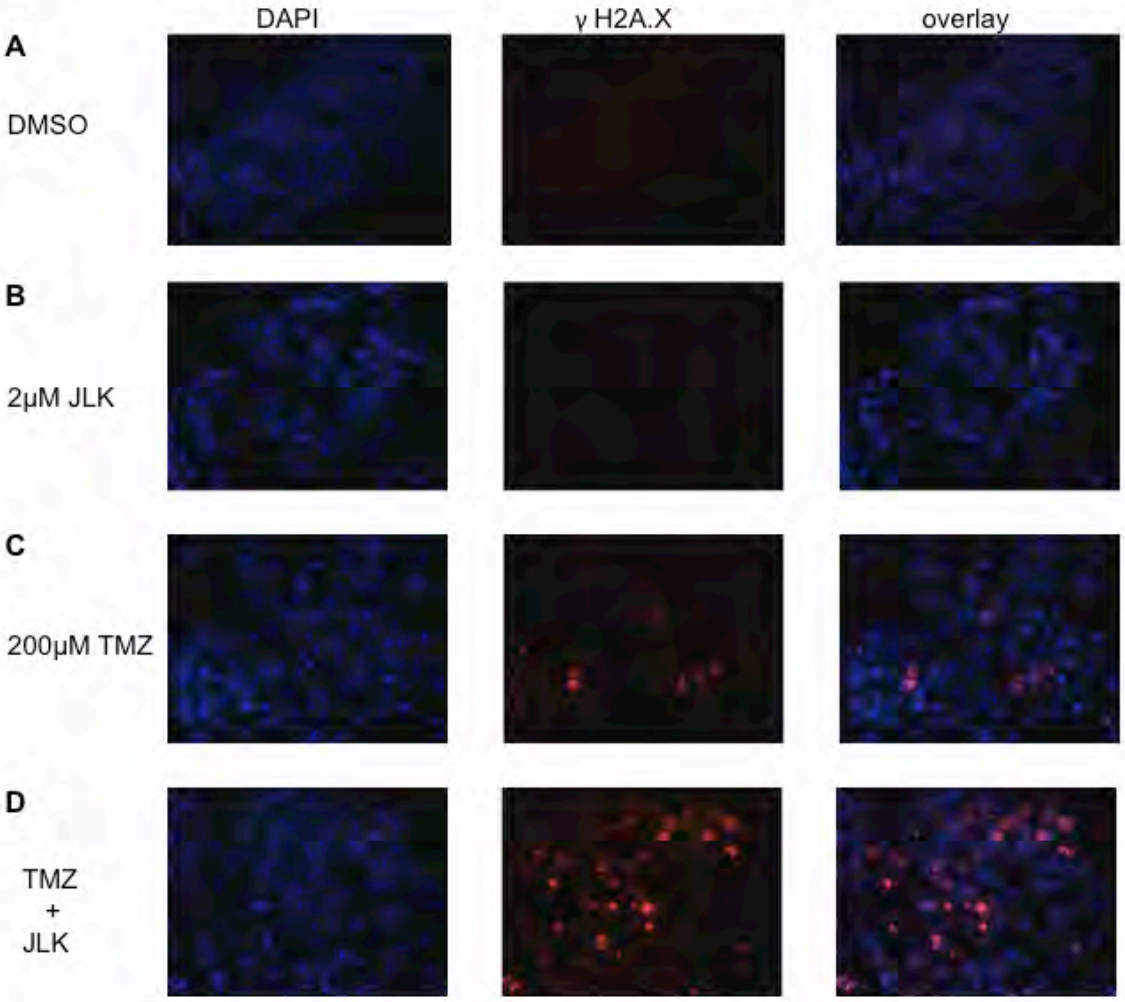

Figure 10: Prolonged γH2A.X at day 21 in U87NS TMZ+JLK1486 drug treated cells. (A) Day 21 γH2A.X immunofluoresence of DMSO treated U87NS cells. **(B)** Day 21 γH2A.X immunofluoresence of 2μM JLK1486 treated U87NS cells. **(C)** Day 21 γH2A.X immunofluoresence of 200μM TMZ treated U87NS cells. **(D)** Day 21 γH2A.X immunofluoresence of TMZ+ 2μM JLK1486 treated U87NS cells (N=3).

TMZ+2μM JLK1486 shATF4 C1 treated U87NS cells, and no expression of ATF4 in 2μM JLK1486 and TMZ+2μM JLK1486 shATF4 E7 treated U87NS cells (Figure 11F).

To determine if knockdown of ATF4 rescues secondary sphere formation, we treated our sh control, shATF4 C1, and shATF4 E7 U87NS lines with DMSO, 2μM JLK1486, 200μM TMZ, and TMZ+2μM JLK1486 and carried out neurosphere assays. On day 21, we did not observe formation of secondary spheres in the U78NS sh control or in either of our U87NS shATF4 lines, C1 or E7, demonstrating that knockdown of ATF4 does not rescue secondary sphere formation in TMZ+2μM JLK1486-treated cells (Figure 11 A-C).

As neurosphere assays may not evaluate the effect drug treatment has on viability, we determined if ATF4 knockdown decreased cell death in our U87NS sh control and shATF4 C1 and E7 lines by carrying out a time course of trypan blue counts. As increased cell death in U87NS TMZ+2μM JLK1486-treated cells was most significant at later time points (Figure 7), we focused on analyzing the number of trypan-blue-positive cells in our control and ATF4 knockdown lines at day 16, 19, and 21 time points. Furthermore, because U87NS cells treated with TMZ alone had significant reduction in cell growth, but were able to repopulate the culture versus TMZ+ 2μM JLK1486-treated cells (Figure 7B), we were most interested in comparing the effects of ATF4 knock down in TMZ versus TMZ+2μM JLK1486-treated cells (all conditions shown in Figure 12).

We observed a statistically significant decrease in the number of trypan-blue-positive cells in ATF4 knockdown versus sh control TMZ+2μM JLK1486-treated cells at day 19 and day 21 (Figure 11D-E; Day 19: C1= 31%; E7= 24%; control= 53%) (Figure 11D-E; Day 21: C1= 32%; E7= 18%; control = 56%). Reduction of cell death in ATF4 U87NS knockdown cells treated with TMZ+2μM JLK1486 suggests ATF4 may play a role in promoting cell death in TMZ+2μM JLK1486-treated cells.

To explore why ATF4 knockdown results in decreased cell death in TMZ+2μM JLK1486-treated cells, we analyzed levels of RAD51 in sh control versus shATF4 U87NS treated with DMSO, 2μM JLK1486, 200μM TMZ, and TMZ+2μM JLK1486. We analyzed lysates collected 24 hours and 5 days post treatment as we saw decreased expression of RAD51 in 2μM JLK1486 and TMZ+2μM JLK1486 U87NS treated cells at day 5 (Figure 9). Interestingly, we observed increased RAD51 levels in shATF4 knockdown lines versus sh control U87NS cells after 5 days of TMZ+2μM JLK1486 treatment (Figure 11F). This suggests a potential inverse relationship between ER stress induction of ATF4 and RAD51 protein levels.

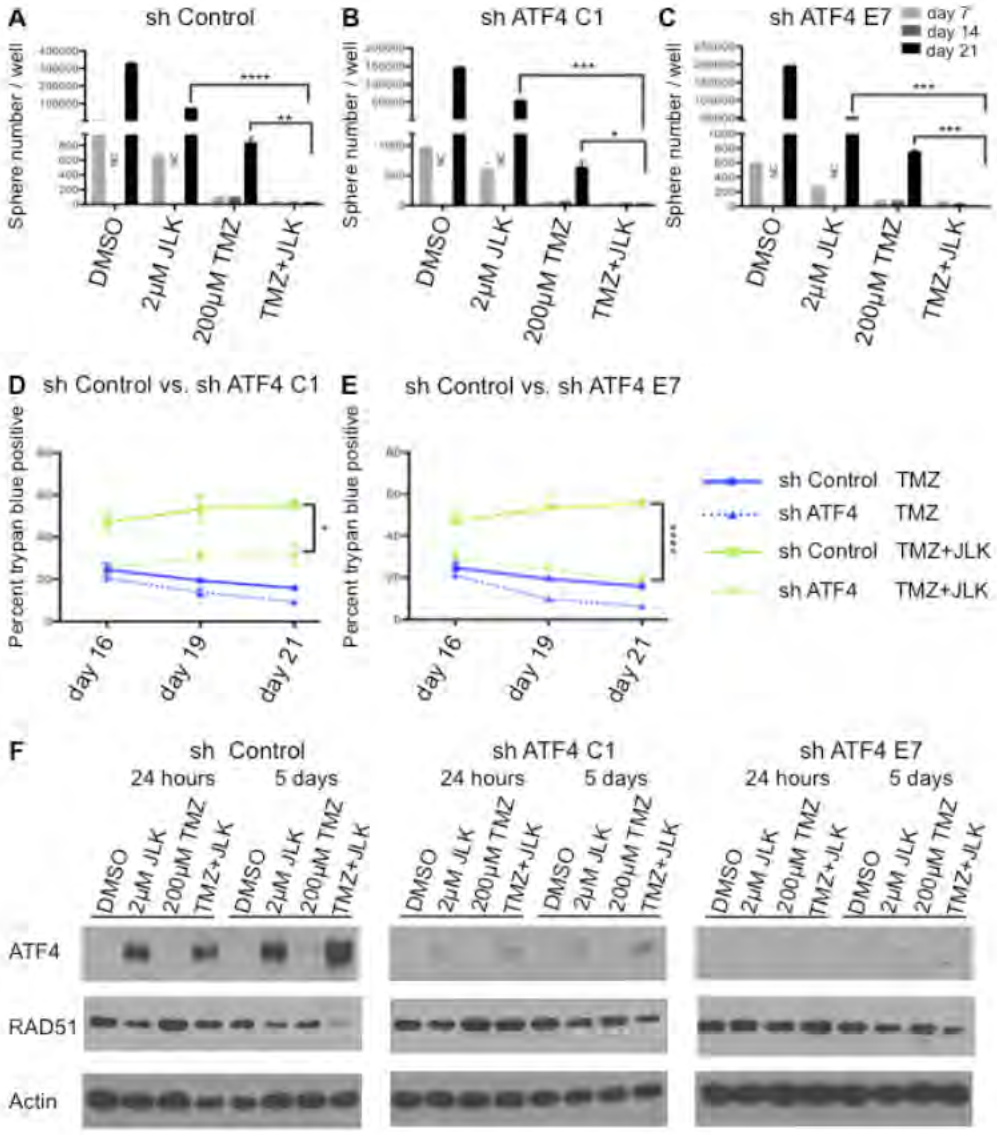

Figure 11: Knockdown of ATF4 does not rescue secondary sphere formation but does decrease cell death in TMZ+JLK1486 treated cells. **(A)** Secondary sphere formation of U87NS sh control treated cells (n=3). **(B)** Secondary sphere formation of U87NS shATF4 C1 treated cells (n=3). **(C)** Secondary sphere formation of U87NS shATF4 E7 treated cells (n=3). **(D)** Percent of trypan blue positive cells in U87NS sh control versus shATF4 C1 after 16, 19, and 21 days of 200μM TMZ versus TMZ+2μM JLK1486 treatment (n=3). **(E)** Percent of trypan blue positive cells in U87NS sh control versus shATF4 E7 after 16, 19, and 21 days of 200μM TMZ versus TMZ+2μM JLK1486 treatment (n=3). **(F)** Western blot analysis of RAD51 and ATF4 protein extracted from whole cell U87NS sh control, U87NS shATF4 C1, and U87NS shATF4 E7 cells treated with DMSO, 2μM JLK1486, 200μM TMZ, TMZ +2μM JLK1486 for either 24 hours or 5 days. NC= not counted because neurospheres too numerous. Representative blot shown (n=3). All error bars are SEM, two-tailed t-test, *P=0.03,**P=0.008, ***P=0.001-0.003,****P=0.0001-0.0007.

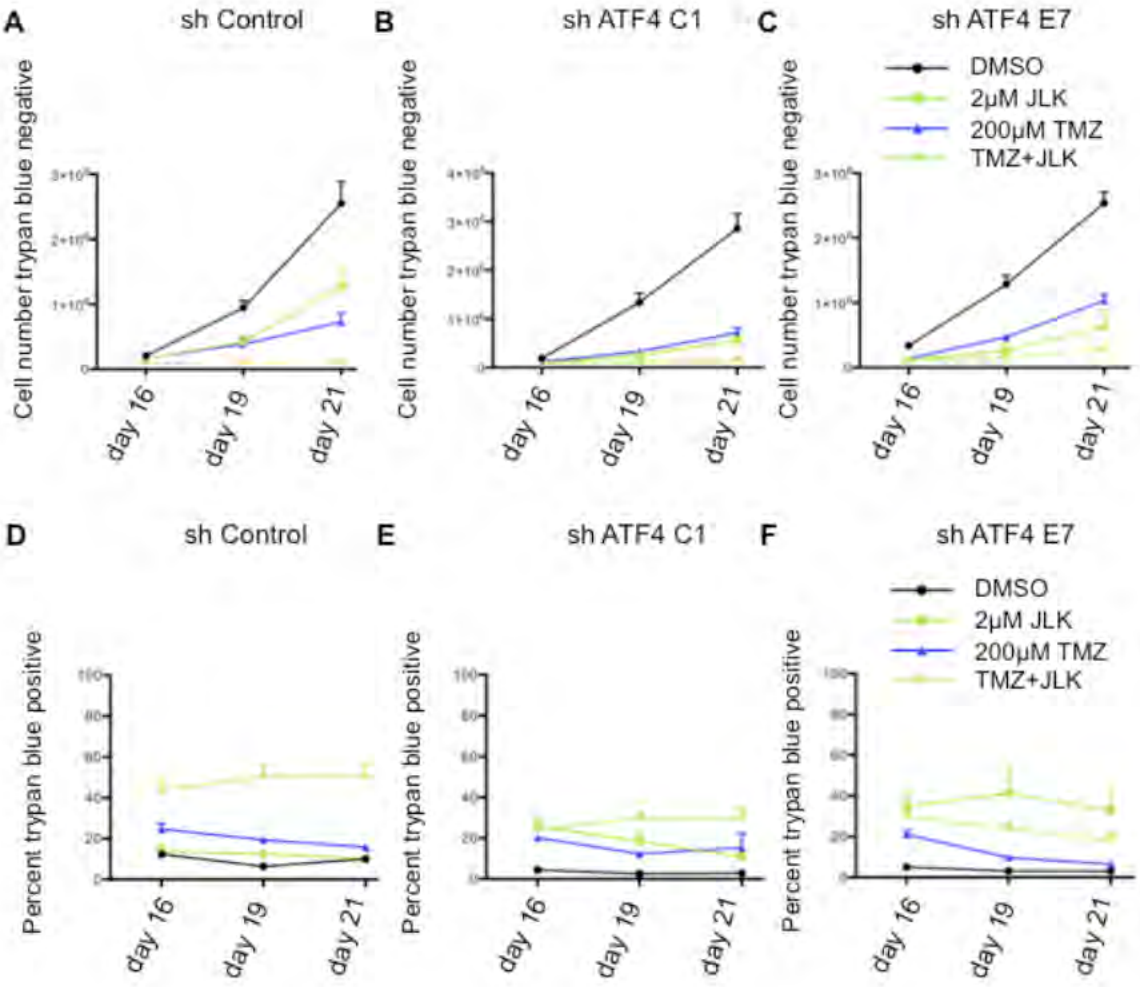

Figure 12: Knockdown of ATF4 does not rescue cell growth but does decrease cell death in TMZ+JLK1486 treated U87NS cells (all conditions shown). (A-C) Trypan blue negative counts at day 16,19, and 21 of U87NS sh Control (A), shATF4 C1 (B), shATF4 E7 (C) cells treated with DMSO, 2μM JLK1486, 200μM TMZ, or TMZ+ 2μM JLK1486. **(D-F)** Percent of trypan blue positive cells at day 16, 19, and 21 of U87NS sh Control (D), shATF4 C1 (E), shATF4 E7 (F) cells treated with DMSO, 2μM JLK1486, 200μM TMZ, or TMZ+ 2μM JLK1486 (N=3), SEM.

TMZ+JLK1486 treatment delays tumor doubling *in vivo*

To determine if the combination of TMZ+JLK1486 is effective *in vivo*, we subcutaneously injected nude mice with U87NS cells, allowed tumors to form, and treated with DMSO, JLK1486 15mg/kg, TMZ 5mg/kg, or TMZ with JLK1486 (Figure 13A). We used time to tumor volume doubling as our readout to compare control, single agent, and double agent treated mice.

We found significant delay in tumor doubling in JLK1486 versus DMSO ($p = 0.0002$), TMZ versus DMSO ($p = 0.0005$), TMZ versus JLK1486 ($p = 0.0007$), TMZ+JLK1486 versus JLK1486 ($p = 0.0003$), and TMZ+JLK1486 versus TMZ alone ($p = 0.04$) treated mice (Figure 13B). This significant delay in tumor volume doubling for TMZ+JLK1486-treated mice suggests the combination should be further studied as it may have clinical applications.

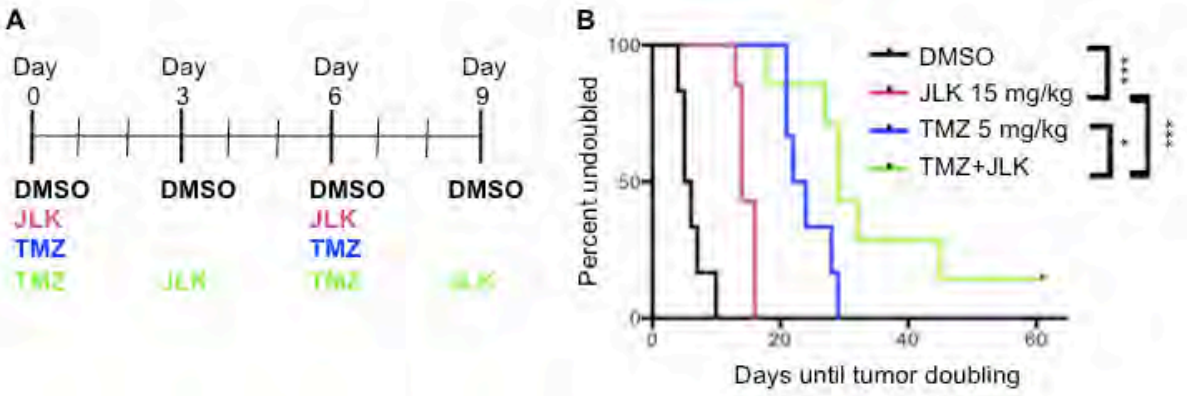

Figure 13: TMZ+JLK1486 treatment delays tumor doubling *in vivo*. **(A)** Dosing schedule implemented for NU/NU mice intraperitoneal (IP) injected with DMSO vehicle, JLK1486 15mg/kg, TMZ 5mg/kg or both drugs. **(B)** Kaplein-Meier curve comparing time to tumor doubling in DMSO, JLK1486 15mg/kg, TMZ 5mg/kg, and combination treated NU/NU mice. JLK1486 vs. DMSO ***p=0.0002; TMZ vs. DMSO p=0.0005; TMZ+JLK1486 vs. DMSO p=0.0002; TMZ vs. JLK1486 p=0.0007; TMZ+JLK1486 vs. JLK1486 ***p=0.0003; TMZ+JLK1486 vs. TMZ *p=0.04. Statistics generated via a log-rank test.

Conclusion

We found that JLK1486 induces ER stress in GBM cells and when combined with TMZ, reduces proliferation. Decreased proliferation correlated with increased apoptosis. Interestingly, in combination treated cells, we observed decreased RAD51 expression, a key protein for repair of DNA DSBs. We propose reduction of RAD51 levels as the mechanism that accounts for prolonged and unresolved DNA DSBs and increased apoptosis. Combination of JLK1486 with TMZ may provide a potential new chemotherapeutic regimen and, more intriguingly, may link unresolved ER stress with interference of DNA damage repair (Figure 14).

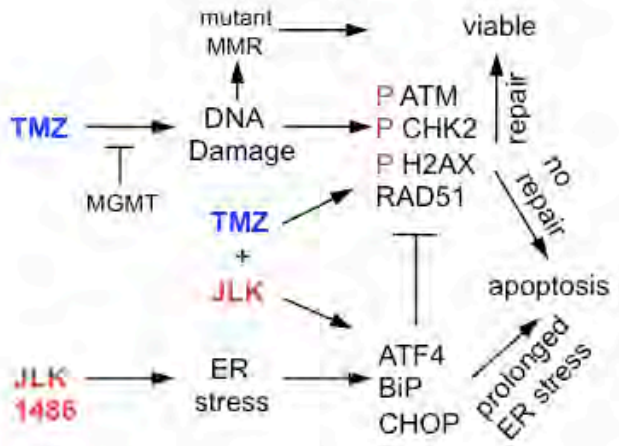

Figure 14: TMZ+JLK1486 treatment induces prolonged ER stress and unresolved DNA damage that results in increased cell death. TMZ activates the DNA damage response pathway due to the generation of DNA double strand breaks. If the breaks are repaired, the cells survive; if not, cells undergo apoptosis. JLK1486 induces ER stress. If ER stress is resolved, cells survive; if not, cells undergo apoptosis through ATF4 mediated up-regulation of CHOP. TMZ+2μM JLK1486 treatment prolongs ER stress, activates the DNA damage response, and causes unresolved DNA DSBs that result in apoptosis due to decreased RAD51 levels, possibly mediated by ER stress induced ATF4 expression. GBM cells generate resistance to TMZ through several mechanisms, including increased expression of methyl guanine methyl transferase (MGMT), which removes alkyl groups from O6 guanine residues, and mutations of the mismatch repair (MMR) system, allowing aberrant cells to enter and complete the cell cycle.

Materials and Methods

Cell lines and cell culture reagents

U87MG, A172, T98G, and LN18 cell lines were purchased from American Type Culture Collection (ATCC). U118MG cells were a kind gift from the laboratory of Dr. Larry Recht (Stanford University, Stanford, CA, 2003). Cell lines were verified via the Radil Idexx Cell Check (9 short tandem repeats) and maintained as monolayers in 10% FBS / DMEM (GIBCO; #11965-092) at 5% C02. 5075 and GS8-26 primary GBM lines were acquired from the UMASS tissue bank and maintained in defined medium DMEM/F12 1:1, 15mM/L HEPES, 1X B27 without

vitamin A, and supplemented with 20ng/mL bFGF and EGF [150]. The establishment of the primary line GS8-26 has been presented [150]. The 5075 primary line was prepared in a similar procedure except Liberase instead of trypsin was used to digest the tumor [157]. U87NS and U118NS neurosphere lines were generated from adherent lines, maintained, and passaged as previous described [150].

Reagents

Temozolomide (T2577) was purchased from Sigma-Aldrich, re-suspended at 10mg/mL in 100% DMSO, aliquoted, and stored at -20°C. The synthesis and structure of JLK1486 synthesis was previously described [158, 159]. JLK1486 was re-suspended at 10mM in 100% DMSO, aliquoted, and stored at -20°C.

MTS assay

The IC50s' of adherent lines was determined by plating $1X10^3$ cells/100µL in 96 well plates and after 24 hours treating the adherent cells with increasing concentrations of JLK1486 (0µM – 100µM). Media was aspirated five days later and replaced with CellTiter 96 Aqueous One Solution Cell Proliferation Assay (MTS; Promega G35A) for ~3 hours. Plates were read at A490 nm.

Primary and secondary neurosphere assays

Neurosphere assays were carried out as previously described [160]. Briefly, U87NS, U118NS, GS8-26, and 5075 lines were pH dissociated, filtered (40 µm), plated at 6,000 cells /2mL in 6 well plates, and treated with DMSO, JLK1486, TMZ, or TMZ+JLK1486. Primary spheres were counted, fed, and dosed with

JLK1486 a second time on day 7 for U87 and U118 and on day 10 for primary lines GS8-26 and 5075. Sphere recovery was determined by counting spheres 7 or 10 days later, day 14 for U87NS and U118NS and day 20 for primary lines. Spheres were then pH dissociated, diluted (U87NS, U118NS: DMSO=1:100; JLK1486= 1:50; TMZ= 1:1; TMZ+JLK1486=1:1; 5075, GS8-26: DMSO= 1:25; JLK1486= 1:2; TMZ= 1:2; TMZ+JLK1486= 1:1), re-plated, and counted 7 or 10 days later, day 21 for U87NS and U118NS and day 30 for 5075 and GS8-26 lines , to determine secondary sphere formation capability.

Western blotting

Cells were lysed in RIPA Buffer (Boston BioProducts #BP-115), supplemented with protease inhibitor cocktail tablets (Roche, complete mini, #11 836 153 001), and 5mM NaF. Protein was quantified via Bio-RAD Protein Assay Dye Reagent Concentrate (BIO-RAD, #500-0006) on the Beckman Coulter DU640 Spectrophotometer. Proteins were separated by PAGE and electo-transferred to PVDF membranes (Pall Corporation, BioTrace PVDF 0.45um, P/N 66543). Membranes were blocked in 5% milk tris-buffered saline with tween 20 (0.1%; TBS-T). Primary antibodies were incubated overnight on a rocker in 5% bovine serum albumin in TBS-T at 1:1000 at 4°C. Membranes were washed the following day 3x, 5', TBS-T, and incubated with either mouse or rabbit horseradish peroxidase secondary (Cell Signaling #7076S and #7074) for 2 hours room temperature. Proteins were detected via film following the Thermo Scientific's SuperSignal West Pico Chemiluminescent Substrate (Thermo Fisher

Scientific, #34087) or Thermo Scientific's SuperSignal West Femto Maximum Sensitivity Substrate (#34095) protocol. The following antibodies were purchased from Cell Signaling Technology: B-Actin (#3700), BiP (#3177), CHOP (#2895), ATF-4 (#11815), Rad51 (#8875), Phospho-Histone H2A.X (#2577), H2A.X (#2595), ATM (#2873), Phospho-ATM (#13050), CHK2 (#6334), Phospho-Chk2 (#2661).

Trypan blue positive and negative counts

U87NS cells were pH dissociated, filtered, and plated at 250,000/10mL in T75 flasks. Cells were treated with DMSO, JLK1486, TMZ, or TMZ+JLK1486. On day 7 cells were given fresh media and dosed a second time with JLK1486. On day 14 cells were pH dissociated and re-plated at 172,000/10mL in T75 flasks. Cells were pH dissociated and positive and negative trypan blue cells (GIBCO, Trypan Blue Stain 0.4%, #15250) were counted.

FACS analysis

Drug treated U87NS were pH dissociated, filtered, washed 3X in PBS, and fixed in 95% ethanol overnight at 4°C. Propidium iodide versus Annexin V staining was performed by the UMASS FACS Core, and samples were run on the Calibur FACS machine. Analysis was completed using Flow Jo 7.6.

shRNA ATF4

pGIPZ shATF4 C1 (OligoID: V2LHS_132755), shATF4 E7 (OilgoID: VDLHS_132757), and sh Control were purchased from the UMASS RNAi Core Facility. U87MG cells were infected according to the UMASS RNAi Core Facility

Protocol. Briefly, $1x10^5$ cells/well were plated, infected 24 hours later with viral supernatant and 1 µg/µl polybrene (Millipore, TR-1003-G), media changed 24 hours post infection and cells were selected for seven days in 2 µg/mL puromycin (GIBCO, #A11138-03). Infected U87MG cells were then converted to U87NS cells as described above.

Ethics Statement

Investigation has been conducted in accordance with the ethical standards and according to the Declaration of Helsinki and according to national and international guidelines and has been approved by the author's institutional review board.

Mouse xenograft models

Six-week old male NU/NU mice were purchased from Charles River Laboratories and injected with $1x10^6$ U87NS cells in 100uL PBS/ right flank. When tumor volumes reached $150mm^3$ mice were dosed intraperitoneal (IP) with either DMSO (day 0, day3, day 6, day 9), JLK1486 15mg/kg (day 0, day 7), TMZ 5mg/kg (day 0, day 7) or with the following dosing regimen: TMZ 5mg/kg (day 0), JLK 1486 15mg/kg (day 3), TMZ 5mg/kg (day 6), JLK1486 15mg/kg (day 9). Mice were sacrificed when tumors reached $1200mm^3$.

H2A.X Immunofluoresence Staining

U87NS cells were adhered to slides using Double Cytofunnel Disposable Chambers (Thermo Scientific, #5991039), fixed in 4% PFA/PBS (10 minutes), permeabilized in 0.5% TRITON X/ PBS (5 minutes), blocked in normal goat

serum (1 hour), stained overnight with either phospho-histone H2A.X (Ser139) (Cell Signaling, #2577) or rabbit (DA1E) mAb IgG XP isotype control (Cell Signaling, #3900), washed in 1X PBS, incubated with goat anti-rabbit IgG (H+L) secondary antibody, Alexa Fluor 568 (Life Technologies, #A-11011), and mounted via ProLong Gold Antifade Mountant with DAPI (Molecular Probes by Life Technologies, #P36941). Images were acquired with a Leica wide field scope microscope.

Statistical analysis *in vitro*

The t-test analysis was performed using GraphPad Prism version 6.00 for Mac, GraphPad Software, La Jolla California, USA, www.graphpad.com

Statistical analysis *in vivo*

Kaplan-Meier time to tumor volume doubling curves were analyzed via the log-rank test.

CHAPTER III

Discussion overview

Glioblastoma multiforme tumors are comprised of genetically heterogeneous cells [1-3] [4]. This results in highly proliferative, therapy-resistant, and infiltrative tumors with limited treatment options [1]. The current standard of care, which has not changed in over a decade, is comprised of surgical resection followed by radiation with concomitant and adjuvant temozolomide [1] [5]. Despite treatment, patients relapse within 6.9 months of completing therapy and have an overall survival of only 12-14 months [5]. This leaves much room to improve the standard of care and tackle unanswered questions regarding resistance, recurrence, and the cell of origin. Answering these difficult questions may facilitate the development of better-targeted therapies.

Triad failure: caveats of surgical resection, radiation, and temozolomide

Caveats of surgical resection

Surgical resection is limited by two factors. First, tumor location determines whether or not resection is feasible [161]. Second, because GBMs are highly infiltrative, complete surgical resection is nearly impossible [1] [23]. This leaves a population of glioma cells at or near the primary tumor bed that contribute to nearly 90% tumor recurrence at the initial site [1] [21]. Although residual tumorigenic cells are a likely source of recurrence, it does not explain how they remain viable and re-populate the tumor bed following multiple rounds of radiation and chemotherapy.

Caveats of radiation: tolerance, increased DNA repair, proliferation

Although the addition of radiation to surgical debulking increased overall survival from 3-4 months to 7-12.1 months, radiation is limited by neurological toxicity to normal brain tissue [5] [47, 162]. Patients receive focal fractionated doses over a 6-week time course, 2 Gy per day for five days, resulting in a total of 60 Gy [5]. As radiation does not prevent tumor recurrence, it is important to understand how cells remain viable despite multiple insults.

In order for radiation to be effective, it must create DNA lesions either through direct ionization or through the formation of free radicals [69]. These lesions include base damage, single strand breaks, and double strand breaks. Mammalian cells dosed with 1-2 Gy have over 1,000 damaged bases, 1,000 single strand breaks (SSBs), and 40 double strand breaks (DSBs) [69]. Damaged bases accounting for the highest number of lesions generated by radiation are easily repaired by either nucleotide excision repair (NER) or base excision repair (BER) [69]. Similarly, SSBs are not lethal if they are repaired by the BER enzyme, poly(ADP) ribose polymerase (PARP) [69]. However, if SSBs are not repaired, they generate DSBs during a second round of replication, resulting in a G2/M arrest [69]. If DSBs are not repaired by either homologous recombination (HR) or non-homologous end joining (NHEJ) during the arrest, the cell undergoes apoptosis. Damaged bases and SSBs DNA lesions occur at a 25:1 ratio in comparison to DSBs [69] [74]. As the majority of accrued lesions from RT result in repairable SSBs and damaged bases, it becomes clear how

cells can survive multiple rounds of therapy. If SSBs are converted into DSBs, or DSBs arise from RT, gliomas circumvent their lethality by increasing expression of DNA DSB repair factors, in particular RAD51 [16] [59]. This limits the formation of catastrophic DNA DSBs, reducing cell death. The types of DNA damage coupled with increased DNA repair explains, in part, how cells remain viable following RT.

Two additional factors must also be considered when assessing glioma cells response to RT. In order for RT to be effective, cells must be replicating. As previously discussed, GBMs are highly proliferative due to mutations in receptor tyrosine kinase pathways resulting in loss of cell cycle control [1] [4] [25]. This should increase GBM tumor cells' sensitivity to radiation; however, isolation of slow-cycling cells with cancer stem cell like properties and increased resistance to RT have been isolated [163, 164]. These cells likely contribute to recurrence. Lastly, the formation of ROS are dependent on the presence of oxygen. As GBMs are solid tumors with an aberrant vasculature causing moderate to severe levels of hypoxia, this may limit ROS formation, increasing glioma cell viability [9] [46,47] [69]. Although the addition of RT to surgery significantly increased patient survival, its limitations eventually result in resistance and recurrence, through increased expression of DNA repair factors, slow cycling cells, and hypoxia.

Caveats of temozolomide: MGMT, MMR, P53, proliferation

In 2005 Stupp et al published their landmark study showing that addition of the DNA alkylating drug, temozolomide (TMZ) to RT significantly increased

survival from 7-12.1 months to 14.6 months [5]. Although this combination significantly improves overall survival, it is unable to prevent tumor recurrence [34] [162]. As TMZ's mechanism has been delineated, caveats leading to its resistance have been identified.

TMZ, a pro-drug stable at acidic pH, crosses the blood brain barrier, is hydrolyzed to form the reactive intermediate MTIC, which breaks down to a DNA-alkylating methyldiazonium ion [29, 30]. This results in alkylation of guanine N7 (70%), adenine N3 (9.2%), and guanine O6 residues (5%) [29] . Because DNA glycosylases and BER recognize and remove the alkyl groups on guanine N7 and adenine N3 residues, these adducts are not considered deleterious [29] [165]. However, neither DNA glycosylases nor BER are capable of removing guanine O6 adducts, resulting in stable adduct formation [29]. During replication, the alkylated guanine is paired with a thymine. This activates the mismatch repair pathway (MMR) [29] [31]. However, due to changes in its shape, the only base that can pair with an alkylated guanine is thymine, causing repeated insertion and excision of the thymine. This results in futile rounds of MMR and generates a single strand break as the polymerase skips over the alkylated base. The single strand break, if not repaired, is converted to a catastrophic double strand break during a second round of replication, eventually triggering apoptosis [32, 33].

The first caveat to TMZ treatment is expression of methyl guanine methyl transferase (MGMT) [1]. MGMT recognizes O6 alkylated guanine residues and catalyzes the transfer of the alkyl from the guanine to its internal cysteine residue

[32]. This restores DNA base integrity, preventing formation of SSB and DSBs [166]. Forty five percent of GBM patients present with methylated MGMT promoters, leading to a two-year survival rate of 46% compared to a dismal 13.8% two-year survival of patients with non-methylated MGMT promoter [1]. A similar trend is observed in vitro. Over-expression of MGMT in MGMT negative lines reduces cell death by 90% in response to TMZ, highlighting how vital this enzyme is in promoting TMZ resistance [33]. Accordingly, only 5.4% of recurrent GBM patients respond to TMZ [1]. This leads one to think that MGMT positive cells serve as a reservoir of resistant cells during TMZ treatment and lead to tumor repopulation when treatment is completed. This also raises the possibility that radiation and chemotherapy leads to the selection of a population of resistant cells, resulting in a cohort of highly malignant cells upon treatment completion.

TMZ's efficacy is dependent on MMR detection of alkylated guanines paired with thymines. If MMR proteins are mutated, the cell is unable to recognize the guanine-thymine pairing and does not undergo futile rounds of MMR resulting in SSBs and DSBs [62] [167]. Instead of initiating apoptosis, inactivated MMR leads to A:T transitions [32]. Depending on where the point mutations occurs, this may promote tumorigenicity by inactivating tumor suppressor genes. Several studies have implicated loss of MMR factors, MSH6 and MSH2, with increased resistance to TMZ [32] [168-170]. This is especially true of recurrent GBM tumors in which MSH6 deficiency correlates with

increased growth during treatment [169] [171]. This highlights the second caveat in which TMZ treatment eradicates MGMT negative and MMR intact cells, leaving resistant MGMT positive and/or MMR negative cells to repopulate the tumor bed.

In addition to MGMT and MSH6 status, efficacy is dependent on three additional factors: RAD51, P53, and proliferation. Even if GBM cells have an intact MMR system that generates DSBs, glioma cells evade death by increasing expression of RAD51, a DNA repair factor that facilitates homologous recombination [62]. Increased RAD51 expression decreases catastrophic DNA DSBs, promoting viability and resistance to TMZ.

P53 mutant glioma cells are significantly more viable and undergo less death than P53 wild type cells in response to TMZ treatment [33] [171]. TMZ induces DNA DSBs, activating the DNA damage response kinase ATM [172]. ATM activates P53, increasing transcription and activation of FAS receptor mediated apoptosis [33] [50] [173]. P53 mutant cells do not increase FAS transcription in response to TMZ, accounting for the observed decrease in cell death. However, decreased levels of the anti-apoptotic Bcl-2 protein and activation of mitochondrial caspases (Csp9, Csp3) are detected in TMZ treated P53 mutant cells [33]. Although mitochondrial apoptosis does result in a small percent of cell death, it is significantly less than P53 wild type cells, suggesting TMZ induced apoptosis is dependent on P53 [33]. As the majority of de novo GBMs are P53 wild type, the cells should be sensitive to TMZ treatment [173].

Conversely, 65% of secondary GBMs present with P53 mutations [20] [33]. This severely limits TMZ efficacy, resulting in maintenance of a viable population of P53 mutant cells. As radiation also relies on P53 induced apoptosis, these cells may exhibit dual resistance.

Lastly, TMZ is only efficacious in proliferating cells [29] [32]. If a cell is in G0 or has already exited M phase when a guanine residue undergoes O6 alkylation, generation of deleterious DNA DSBs do not occur. If cancer stem-like cells have a slower propagation cycle , this would also prevent them from undergoing cell death in response to TMZ. Therefore, non-proliferating cells may lead to recurrence.

Radiation and temozolomide efficacy is limited by delivery, tolerance, the type of DNA damage, as well as MGMT expression, MMR and P53 status, and proliferation. Although these factors contribute to the development of a population of resistant cells capable of re-populating the tumor bed, leading to the inevitable tumor recurrence, recent data suggests cancer stem like cells also contribute to resistance and tumor recurrence.

The cell of origin: glioma cancer stem cells versus astrocyte de-differentiation

Glioma cancer stem cells

A small percentage of cells from acute myeloid leukemia patients can recapitulate the parental disease when transplanted into immunodeficient mice [174, 175]. This finding led to the cancer stem cell (CSC) hypothesis that a sub-

population of cells within tumors mimics normal stem cell properties of self-renewal and differentiation, but acquire mutations that lead to the development and maintenance of heterogeneous tumors [176, 177]. The identification of a population of neural stem cells (NSCs) in the subventricular zone (SVZ) of adult brains capable of differentiating into astrocytes, oligodendrocytes, and neurons, while maintaining properties of self-renewal, gave basis for the glioma cancer stem cell hypothesis [178-181]. In 2003, Singh et al isolated a population of $CD133^+$ cells from brain tumors with self-renewal and proliferating properties that could differentiate into tumor cells that phenotypically mimicked the patient's tumor [164]. Further study showed intracranial implantation of $CD133^+$ cells gave rise to tumors that can be serially transplanted while maintaining the parental phenotype [164, 165]. As $CD133^-$ cells did not maintain stem cell properties and were unable to form tumors when implanted, it was suggested that $CD133^+$ cells were a population of cancer stem cells capable of initiating brain tumors [164, 165]. Characterization of these cells showed increased resistance to both radiation and temozolomide in comparison to $CD133^-$ due to activation of CHK1 and CHK2 DNA damage pathways and expression of ABCG2 transports, which export chemotherapies from the cell [24] [182, 183]. A population of therapeutic resistant brain CSCs capable of maintaining their oncogenic potential due to self-renewal properties provides an attractive alternative source accounting for GBM recurrence.

Although evidence suggests $CD133^+$ brain tumor CSCs contribute to GBM development, much controversy and skepticism surrounds this theory. Later studies suggested that $CD133^-$ cells can also be maintained in an undifferentiated state *in vitro*, are capable of self-renewal, and when implanted can give rise to tumors [24] [184-187]. This clearly calls to question the use of CD133 as a marker for identifying brain cancer stem cells. Indeed, this marker has been shown to be quite promiscuous, as it also labels epithelial cells in the liver, kidney, and pancreas, suggesting CD133 expression is not specifically limited to neural stem cell populations [188, 189]. Further complicating the matter, different dissociation methods result in different percentages of CSCs from tissue, and different CD133 antibodies detect alternative glycosylation patterns, resulting in different isolation efficiencies [190]. Currently, several new markers, such as CD44, CD15, and integrin 2 and 6, are being explored as potential candidates for brain CSCs [24]. However, until a specific marker validated for brain tumor cancer stem cells is identified, it is doubtful this debate will be resolved.

Two points should be kept in mind before dismissing the brain cancer stem cell hypothesis. First, the identification of cancer stem cells from several other solid tumors, including breast, colon, pancreas, lung, and skin, provides a foundation for cancer stem cells in solid tumors [24] [190]. Second, orthotopically transplanted $P16^{INK4a}$ $P19^{ARF}$ deficient neural stem cells transduced with EGFR gave rise to high grade gliomas, showing that loss of tumor suppressor genes

(TSGs) and activation of receptor kinases are capable of transforming NSCs [191, 192]. Similarly, ablation of PTEN, P53 and RB TSGs in stem cells isolated from the SVZ gave rise to gliomas [193]. This suggests it is possible for stem cells within the SVZ to lose TSGs, resulting in tumorigenic cells that give rise to GBMs. How CSCs gain these mutations is under investigation. As stem cells are closely associated with endothelial cells, their interactions with the vasculature may prevent differentiation and maintain the capacity for self-renewal while releasing cytokine that increase their proliferation [184]. Recent studies suggest aberrancies within this delicately balanced NSC niche may contribute to CSC development, but until further studies are completed, this remains to be seen [184] [194].

The proposed brain cancer stem cell suggests why these tumors are so difficult to treat and impossible to eradicate. A population of cancer cells with stem like properties would create a pool of cells with unlimited ability to re-populate the tumor. This would contribute not only to initial tumor development but also to tumor recurrence. It would then be critical to develop therapies that not only target the bulk of tumor cells, but also cancer stem cells. If specific markers for brain cancer stem cell can be identified, perhaps these can be manipulated and exploited by nano particle or viral mediated delivery of chemotherapies.

Astrocyte de-differentiation

Excluding astrocytes, the adult brain is mainly comprised of non-proliferating cells [24]. Because of this, it was suggested that GBMs result from loss of tumor suppressors and activation of oncogenes in astrocytes [24]. This traditional view suggests that these mutations trigger de-differentiation, increase proliferation, and generate tumorgenic astrocyte like cells. This would account for GBMs genetic and morphological heterogeneity.

The finding that adult fibroblasts can de-differentiate into induced pluripotent stem cell (iPSC) state by re-expression of stem cell transcription factors (OCT3/4, SOX2) gave merit to this argument [195, 196]. Further substantiating this, c-myc transformed iPSCs gave rise to subcutaneous tumors in mice, suggesting that de-differentiated cells are tumorigenic [196]. Building on this premise, astrocytes de-differentiate in response to loss of $P16^{INK4a}$ and $P19^{ARF}$ plus EGFR activation [192, 193]. This produced a transformed population of cells that gave rise to tumors that phenotypically matched high-grade gliomas.

Although this data suggests transformed astrocytes give rise to GBMs, whether or not a transformed astrocyte is the cell of origin has not been conclusively resolved in the field for two reasons. First, studies show that knockouts of PTEN, P53, and RB TSGs are unable to transform normal human astrocytes [194] [197]. This is surprising as P53 mutations occur in almost 65% of progressive GBMs and PTEN mutations have been reported as high as 63% in

de novo GBMs [20] [32]. One would expect that loss of these TSGs would result in transformation if astrocytes are indeed the cell of origin However, it is possible that lack of EGFR amplification or expression of the VIII variant, hallmarks of GBMs, could account for this non-transformed state [4] [21]. Experiments in which EGFR amplification/VIII expression in combination with loss of TSGs in astrocytes would help to resolve this question. Second, the marker used by many to isolate and identify astrocytes, GFAP, is also expressed on neural stem cells [24]. It is possible that astrocyte cultures were cross-contaminated with NSCs and resulting tumor formation was due to transformed NSCs, not transformed astrocytes.

The GBM cell of origin remains a contested subject. As attractive as brain cancer stem cells are to promoting GBM development, resistance, and recurrence, the use of controversial markers makes it difficult to isolate these cells and validate their roles. De-differentiation of astrocytes would account for the typical astrocytic phenotype and genetic heterogeneity of GBMs, but there is a debate whether these cells are maintained within the tumor and generate recurrences. As GBMs are comprised of heterogeneous populations of cells that are genetically aberrant, it is impossible to exclude one cell of origin from another. It is plausible that GBMs result from both de-differentiated astrocytes and cancer neural stem cells. Studies seeking to resolve this debate are complicated as many do not differentiate between de novo and progressive GBMs, while the dissociation protocol and culture condition vary, and the lack of

markers make it difficult for experiments to be reproduced. What does remain is that GBMs are aggressive grade IV brain tumors with limited treatment options that have not substantially changed in over a decade. Understanding the limitations of combination therapies and why they have not improved patient survival may lead to the design and development of smarter drug combinations.

Combination therapies: harnessing failures to improve drug combinations

MGMT inhibition

As MGMT expression promotes TMZ resistance, it was reasoned that its depletion could re-sensitive TMZ resistant lines. This was shown to be quite effective *in vitro* as treatment of MGMT positive cells with O6 benzylguanine (O6-BG) successfully inactivated MGMT due to transfer of a benzyl group to the cysteine residue essential for removal of alkyl groups [198-200]. This resulted in increased sensitivity to TMZ. This finding led to a phase I trial that explored the addition of O6-BG to TMZ treatment [201]. Although O6-BG effectively inhibited MGMT expression in patients' tumors, the combination induced severe myelosuppresion, limiting its clinical use [202]. Currently, the infusion of hematopoietic progenitor cells (HPCs) modified to express high levels of MGMT via retroviral vectors is being explored in animal models [168]. However, this has yet to be implemented in a clinical setting for GBM patients.

A second approach is to deplete MGMT levels with higher doses of TMZ over a longer time period. Because MGMT is a suicide enzyme, TMZ eventually depletes it [168]. This means that the cell must re-synthesize MGMT to replenish

its reservoir during and following TMZ treatment. A phase II study implementing a 21 days on, 7 days off, TMZ treatment at 75-100mg/m^2/day found the increased dose and duration to be safe, but only resulted in a 6 month progression free survival in 11% of patients, suggesting little advantage [168]. This could be due to cancer cells expressing increased DNA repair factors or mutations in MMR factors MSH2 or MSH6.

An alternative approach is to use viral vectors to delivers siRNAs against MGMT. Initial *in vitro* and murine *in vivo* studies are promising [168]. This has not yet been pursued in the clinic as vector toxicity, specificity, and duration must first be analyzed in higher primates.

Although MGMT inhibition resulting in re-sensitization to TMZ treatment has been achieved *in vitro*, this has not translated into clinical applications, leaving clinicians with the triad of resection, RT, and TMZ.

BCNU wafers

As GBMs are infiltrative and complete surgical resection is nearly impossible, it was thought that implantation of biodegradable chemotherapeutic wafers at the surgical site would target remaining glioma cells, preventing or at least delaying recurrence. In 2002, the FDA approved the use of Gliadel wafers containing the nitrosourea drug carmustine [168]. Over a course of several weeks, the drug is slowly released from the wafers, promoting deleterious DNA interstrand crosslinks. Despite direct wafer implantation, a phase III trial only increased median survival from 11.6 to 13.9 months [1]. Furthermore, addition of

Gliadel to TMZ and RT did not result in a statistically significant increase in overall survival in comparison to TMZ and RT [168]. This lackluster response was accompanied by edema and cerebrospinal fluid leakage. It is probable that glioma cells resolved Gliadel-induced crosslinks by NER and increased HR. The inability of BCNU wafers implanted at the primary tumor site to prevent recurrences highlights how difficult and challenging it is to find effective therapies for this cancer.

Angiogenic inhibition: Bevacizumab

GBMs are highly vascularized solid tumors. However, the vasculature network in GBMs is often aberrant due to hyperplastic endothelial cells forming twisted vessels that are leaky, lack pericyte coverage and cell-cell adhesion, and form dead-end junctions instead of interconnecting loops [202]. In 2009, the FDA approved bevacizumab (BEV), a monoclonal antibody against vascular endothelial growth factor A (VEGFA), for use in recurrent GBM patients [168] [203]. It was suggested that inhibition of VEGFA would decrease activation of the VEGF receptor on hyperplastic endothelial cells, resulting in vessel trimming and normalization, increasing blood flow and delivery of chemotherapeutics [168] [204]. Combination studies of BEV with irinotecan were explored in GBM patients. Irinotecan, a topoisomerase I inhibitor, was chosen for two reasons. One because it had been previously shown to cross the BBB and two, 15% of recurrent GBM patients showed partial response to Irinotecan as a single agent [204]. Although combination therapy did increase the 6 month progression free

survival, the treatment increased tumor infiltration [1] [4] [168]. Analysis of tumor sections indicated larger areas of hypoxia leading to increased expression of matrix metalloprotease 2 and insulin binding protein 2 [168]. The same phenotype resulted when intracranial injection of non-invasive GBM cell line into mice treated with BEV for 4-6 weeks gave to rise to invasive tumors expressing increased hypoxia as well as up-regulated glycolysis genes and targets of HIF1 alpha [168]. This suggests that BEV treatment is a double-edge sword in that it normalizes vasculature, increasing delivery of chemotherapies, but also increases invasion and metastasis. It is possible that combination of BEV with an agent other than irinotecan may prevent this phenotype; however, finding drugs capable of crossing the BBB greatly limits this. An alternative option would be the use of an EGFR inhibitor, such as erlotinib or gefitinib, with BEV, as EGFR contributes to angiogenesis, proliferation and survival. This combination coupled with RT may increase efficacy. Bevacizumab treatment is further limited as it only targets one of the five VEGF family members [204]. This allows other members to compensate for its depletion, maintaining the hyperproliferative state of endothelial cells within the vascular tumor niche, contributing to its decreased efficacy [168] [204].

Receptor tyrosine kinase inhibitors: erlotinib and gefitinib

The epidermal growth factor receptor is an attractive target to inhibit as it is amplified in 50-63% of primary GBMs, promoting glioma cell proliferation and apoptotic resistance [1] [4] [20]. It was thought that the use of erlotinib or gefitinib,

two small molecule inhibitors against EGFR, would decrease proliferation and sensitize cells to radiation and chemotherapy [4]. However, clinical use of the compounds resulted in little to modest advantage. Two factors contributed to this. First, 50% of patients with EGFR amplification express the VIII variant, resulting in loss of the extracellular domain due to deletions of exons 2-7 [1]. Erlotinib competes with the ATP catalytic site found in EGFR's intracellular domain [205]. Loss of the extracellular domain results in constitutive activation of the receptor, preventing the drugs from accessing EGFR's ATP catalytic site. Second, GBM patients develop erlotinib resistance by increasing expression of the RAC1 GTPase [206]. Increased RAC1 expression activates the MAPK and JNK pathways by an alternative mechanism, circumventing EGFR inhibition. *In vitro* studies show that combination of erlotinib with a RAC1 inhibitor decreases glioma cells viability and self-renewal [206]. *In vivo* studies show the combination decreases tumor volume and invasiveness, suggesting this combination may have clinical application and should be further explored [206]. This also suggests the best approach to glioma therapy is not single agents, but rather combination therapies targeting different biochemical pathways.

Although inhibition of MGMT, implantation of BCNU wafers, and anti-angiogenic and small molecules targeting EGFR are unable to prevent or increase time of tumor relapse, they do provide insight into how resistance is generated and mechanisms of treatment failure. Understanding these caveats may lead to smarter drug combinations, as illustrated by RAC1 and erlotinib.

Towards this goal, the use of drugs that interfere with endoplasmic reticulum (ER) associated degradation and function are further explored in this discussion.

Application and implementation of clinically approved drugs that disrupt ER function

Overview

GBMs are solid tumors with moderate to severe levels of hypoxia [7] [9] [46, 47]. Their aberrant vasculature results in decreased delivery of nutrients, glucose, and removal of toxic metabolites [4]. As protein synthesis and folding is dependent on ER homeostasis, its disruption triggers the endoplasmic reticulum stress response, resulting in decreased mRNA translation and expression of factors to alleviate ER stress [10] [39]. If the stress is resolved, normal ER functioning resumes. However, if the cell is unable to do so, it undergoes ER mediated apoptosis [75]. As GBMs are in a chronic state of ER stress, they should be at high risk of this. To avoid this, GBMs increase expression of pro-survival ER factors [11-15]. This is advantageous for two reasons. First, it decreases ER mediated apoptosis and, second, allows the synthesis of DNA repair and cell cycle proteins that glioma cells require for survival and proliferation. Two means of targeting this pathway have been suggested [10] [39]. First, it may be possible to push the ER past its capacity to function by treating cells with an ER stress-inducing drug. The second approach is to block ER associated degradation (ERAD) of proteins, preventing cells from clearing unfolded or misfolded proteins.

Bortezomib (Velcade)

Bortezomib prevents 26S proteosomal mediated degradation of unfolded or misfolded proteins by inhibiting its chymotrypsin property [206, 207]. In 2003, the FDA approved it for clinical use for multiple myeloma and mantle cell lymphoma [208]. As promising results ensued, trials in solid tumors followed [207]. This was based on *in vitro* studies suggesting bortezomib sensitizes non small cell lung cancer to radiation, increases apoptosis in glioma cell lines when combined with a histone deacetylase (HDAC) inhibitor or TMZ, and increases pancreatic and ovarian cancer cells sensitivity to the DNA crosslinking agent cisplatin [39] [45] [208] [209]. Additionally, the combination of bortezomib with RT or HDAC inhibitors decreases expression of DNA repair factors such as RAD51, BRAC1, and FANCD2 [44, 45] [210, 211]. This leads to decreased HR, making it an attractive drug candidate for GBM patients. A phase I trial analyzing bortezomib efficacy in recurrent gliomas has been completed, but study results have yet to be posted (completed April 2016; NCT01435395). There is a trial currently underway studying the combination of TMZ and radiation with bortezomib in GBM patients (NCT0099801). As the study has not been completed, no results are available. However, recent *in vitro* data of solid tumors responding to bortezomib suggest several limitations. First, solid tumor xenografts only had modest inhibitory growth effects with bortezomib due to delivery and penetration issues [207-209]. Second generation drugs are currently being developed using liposomal encapsulation to increase delivery; however,

this does not solve penetration issues [45]. An *in vivo* lung cancer model correlated decreased bortezomib response to decreased perfusion [209]. This is especially problematic in GBMs as the aberrant vasculature impedes drug penetration.

In addition to inhibiting proteasomal degradation, bortezomib also changes mitochondrial potential, triggering release of cytochrome C and activation of mitochondria mediated apoptosis [45]. It also inhibits the degradation of the NFkB inhibitor, decreasing transcription of downstream targets [45] [207, 208]. Although these additional mechanisms promote cell death, they may also increase the toxicity of the drug *in vivo*. Perhaps the most concerning side effect of bortezomib is data suggesting it induces proliferation of endothelial cells [208]. Taken together, it is understandable why many are skeptical and have concerns for the use of bortezomib in solid tumors. However, until the trial exploring bortezomib in combination with TMZ and radiation is completed, these concerns remain just that, concerns.

Celecoxib

Celecoxib, a COX2 inhibitor, is a non-steroid anti-inflammatory drug (NSAID) originally developed for pain management [10]. It was approved for clinical use in 1998 but in 2002 was suggested to have potential anti-tumor properties as it has the unintended side effect of sarco endoplasmic reticulum ATPase (SERCA) pump inhibition [212, 213]. SERCA is one of two pumps in the ER that regulate calcium influx and efflux [84]. Disrupted calcium homeostasis,

results in ER calcium leakage triggering release of cytochrome C from mitochondria [84]. This was attractive as, one, this drug has FDA approval and, two, induction of cell death through perturbed ER function has been validated by extensive in vitro studies using tunicamycin and thapsigargin [10]. Additionally, celecoxib increases the pro-death ER stress transcription factor, CHOP [214]. Although celecoxib was suggested to increase cell death in tumor cells due to ER disruption, clinical trials have generated unimpressive responses [10]. Because SERCA inhibition is not celecoxib's main function, development of celecoxib derivatives with increased SERCA inhibition is currently under investigation [10] [213] [215]. This may not only increase celecoxib's SERCA inhibition but also leads to increased CHOP expression. A phase II study using celecoxib in combination with TMZ has been completed in GBM patients (NCT00112502). Although study results have not yet been published, it does add conceptual merit to the argument of why ER stress manipulation may be a relevant therapy in GBMs.

Nelfinavir

The FDA approved nelfinavir, a HIV protease inhibitor, in 1997 for clinical use [10]. In addition to functioning as a protease inhibitor, it induces ER stress and activates the unfolded protein response (UPR) as well as induces autophagy and apoptosis [87]. The mechanism accounting for these multiple results is uncertain, but AKT inhibition has been suggested [216]. Nelfinavir treatment of *in vivo* GBM tumors leads to decreased tumor volume due to accumulation of

polyubiquinated proteins triggering ER stress and CHOP induction [214]. CHOP expression increased the transcription of death receptor 5 leading to TRAIL mediated apoptosis [87] [147] [214] . Because of these promising i*n vitro* results and the FDA approval of nelfinavir, a phase I clinical trial was established to study the combination of nelfinavir with radiation and TMZ in GBMs (NCT01020292). As this study is currently ongoing, no data is available.

The use of ER stress inducing drugs in combination with TMZ and/or radiation in GBM patients sets the precedent for the use of combination therapy. The aforementioned kinase, anti-angiogenic, MGMT, and proteasome / ER stress inhibitors show little efficacy as single agents [44,45] [207] [211]. It is not until they are used in combination with either TMZ or radiation that a robust effect is observed. Targeting two different pathways that gliomas rely on is more effective than targeting a single amplified or over-expressed signaling cascade. Although proteasome / ER stress inducing agents such as bortezomib, celecoxib, and nelfinavir are under clinical investigation, none of these agents specifically interferes with protein folding, directly inducing ER stress. Rather, their effects are either through proteasome inhibition or unintentional ER side effects. JLK1486 is mechanistically unique as it induces ER stress by alkylating thiol residues, preventing the formation of disulfide bonds, resulting in the accumulation of unfolded proteins [35, 36]. We reasoned that the inability to resolve ER stress would increase cell death caused by TMZ-induced DNA

damage. To explore this, we studied the *in vitro* and *in vivo* effects of TMZ+JLK1486 combination therapy.

TMZ+JLK1486 combination therapy

Overview

Treatment of GBM non-adherent and primary lines cells with TMZ+JLK1486 reduced secondary sphere formation and in the case of U87NS cells, completely blocked secondary sphere formation, suggesting this combination effectively inhibits tumor cells from re-populating their culture. This is an important finding as GBM therapies fail due to prevent tumor recurrence. The mechanism of secondary sphere inhibition in U87NS cells is increased cell death. Interestingly, this effect was maintained over an extended time course, suggesting that this combination provides a durable effect. Furthermore, we found that treatment of subcutaneous tumors in mice with TMZ+JLK1486 significantly delayed tumor doubling, suggesting the potential use of this combination in a clinical setting. We propose two interconnected models by which TMZ+JLK1486 promotes cell death. First, we suggest that prolonged, unresolved ER stress drives apoptosis through CHOP, and, second, the accumulation of unrepaired, deleterious DNA double strand breaks triggers apoptosis due decreased expression of the DNA DSB repair factor, RAD51.

TMZ+JLK1486 induces prolonged, unresolved ER stress

To understand the mechanism driving the enhanced efficacy observed with TMZ+JLK1486, we delineated the effects that this combination exerted on

the ER stress response pathway, with particular attention to levels of ATF4 and CHOP induction. It is well established that GBM cells are reliant upon the ER stress pathway and that overwhelming the ER stress pathway switches the initial pro-survival response to pro-death. JLK1486 is a viable candidate for this as it suppresses the formation of disulfide bonds that are essential for protein folding and functionality. Indeed, when U87NS cells are treated with JLK1486 we see induction of ATF4 and its downstream target, CHOP, in JLK1486-treated cells, not TMZ- treated cells. This validates our hypothesis that JLK1486 and TMZ target different pathways and provides an explanation for why this dual treatment provides a robust response.

We found our initial drug regimen, (Figure 5C) utilizing only one dose (1X) of JLK1486 at day 0 in combination with TMZ did not result in U87NS secondary sphere inhibition (Figure 6B). However, when we added a second dose (2X) of JLK1486 at day 7, we observed complete inhibition of U87NS secondary sphere formation (Figure 5D; Figure 6C). It is plausible the second dose of JLK1486 at day 7 enhances inhibition of sphere formation by maintaining increased ATF4 levels that contribute to a sustained and unresolved ER stress response. The expression levels of ATF4 correlate with increased expression of its downstream target, CHOP, consistent with this model. Increased levels of CHOP, a driver of apoptosis, are not observed until after the second dose of JLK1486 on day 7, again suggesting the second dose of JLK1486 prolongs ER stress levels and forces the pro-survival to pro-apoptotic switch that enhances cell death and

reduces secondary sphere formation (Figure 6C; Figure 7; Figure 8). Sustained ATF4 and CHOP expression in TMZ+JLK1486-treated cells correlates with our trypan blue positive time course, which shows increased cell death post day 14 (Figure 7C-D). This suggests a model in which TMZ+JLK1486 treatment initiates, maintains, and promotes unresolved ER stress that drives apoptosis.

TMZ+JLK1486 treatment generates and sustains DNA DSBs

TMZ treatment results in the formation of DNA DSBs. If these breaks are not repaired, cells undergo apoptosis. Both TMZ alone and TMZ+JLK1486-treated samples show DNA damage at early and late time-points; however, TMZ+JLK1486-treated samples exhibit stronger activation at later time points (Figure 9), suggesting prolonged DNA damage. Although both TMZ alone and TMZ+JLK1486 samples exhibit markers for unresolved DNA DSBs, only TMZ-treated cells have increased expression of RAD51, a key protein required for repair of DSBs. RAD51-mediated repair of DSBs would lead to cell survival and proliferation. We find this to be true in our TMZ alone treated cells where trypan blue positive counts decrease and trypan blue negative counts increase over time (Figure 7). Conversely, the decreased levels of RAD51 observed in TMZ+JLK1486-treated cells would lead to accumulation of unresolved DNA DSBs, prolonged γH2A.X induction and increased cell death. This pattern is exhibited in TMZ+JLK1486-treated samples where RAD51 levels are substantially lower than TMZ alone treated samples, correlating with increased DNA DSBs (Figure 9; Figure 10). Accumulation of unresolved DSBs due to

decreased RAD51 levels is a plausible second mechanism for why TMZ+JLK1486-treated cells are unable to re-populate and instead initiate apoptosis (Figure 7H; Figure 9; Figure 14).

Summary and Future Direction

As we suggest two possible mechanisms for induction of cell death in TMZ+JLK1486-treated cells, one due to prolonged ER stress and the second due to unresolved DNA DSBs, we asked if a link between ER stress induction and RAD51 protein reduction could be found. When ATF4 is strongly expressed in JLK1486 and TMZ+JLK1486-treated samples, we observe reduction of RAD51 protein (Figure 8; Figure 9; Figure 11F). Conversely, when ATF4 levels decrease over time, as in day 23 samples (Figure 8) or are reduced via shRNA (Figure 11), RAD51 increases (Figure 8; Figure 9; Figure 11F). As ATF4 knockdown increases RAD51 protein, it suggests that repression of RAD51 is dependent on ATF4 itself or an ATF4-regulated downstream pathway. This is intriguing as induction of ATF4 seems to greatly reduce RAD51 expression, but not other DNA repair factors, such as ATM and CHK2, to the same extent. This suggests a potential novel inverse relationship where ER stress leads to ATF4 induction, resulting in decreased RAD51 protein (Figure 14).

One can envision several possibilities for ATF4 regulation of RAD51 expression. As ATF4 is a transcription factor, it is possible that it directly binds to the RAD51 promoter and represses RAD51 transcription through recognition of CRE-like sequences. This is quite plausible as, addressed in the Introduction,

ATF4 can act as either an activator or repressor depending on its binding partners. ATF4 may block enhancers' access to or prevent scaffolding at CREB-like sequences promoting transcription. Alternatively, ATF4 may either decrease the expression of RAD51 enhancers or increase expression of repressors. This would provide ATF4 with a repressor-binding partner. Both of these would account for decreased RAD51 transcription resulting in decreased protein observed in TMZ+JLK1486 treated cells. Additionally, ATF4 may not effect RAD51 transcription but rather its translation. Perhaps ATF4 induction results in expression of a miRNA that increases RAD51 transcript degradation or prevents translation. This would also account for ATF4 induction leading to decreased RAD51 protein.

ATF4 may indirectly negatively regulate RAD51 expression through increased CHOP expression. CHOP, a member of the C/EBP family, may bind to and repress RAD51 expression in response to sustained ATF4 protein levels. It may also bind to and sequester RAD51 activating or enhancer factors, preventing them from interacting with RAD51's promoter. Either way, decreased RAD51 transcription leading to decreased protein levels would result.

Alternatively, decreased RAD51 protein may occur due to decreased protein translation. ER stress leads to phosphorylation of eIF2 alpha, decreasing translation of cap dependent mRNAs. If RAD51 is a cap dependent mRNA, then this could account for its decreased protein during sustained ER stress. This would also be an alternative way to decrease MGMT levels in MGMT positive

cells. As U87 cells are MGMT negative this could not be analyzed. However, a recent paper published by Xipell et al does show that ER stress induction correlates with not only decreased RAD51 protein levels but also MGMT levels [217]. As the effects of TMZ+JLK1486 treatment, ATF4 induction and decreased RAD51 protein, is sustained over a periods of 21 days, it suggests that this combination may be a durable means of decreasing MGMT *in vivo*.

Although TMZ+JLK1486 prolongs ER stress resulting in unresolved DNA DSBs and apoptosis, it is unknown if this is indeed the result of decreased RAD51 protein levels. Over-expression of RAD51 in TMZ+JLK1486 treated cells may rescue the phenotype, validating the hypothesis that reduction of RAD51 is the mechanism of cell death in TMZ+JLK1486 treated cells. It would also be interesting to explore this combination utilizing an intracranial mouse model in combination with radiation. This would give relevance to the potential clinical use of the treatment.

Although the combination of TMZ+JLK1486 resulted in robust *in vitro* growth suppression and increased cell death, the *in vivo* use of the drug was limited by solubility and toxicity. We were able to circumvent solubility by administering the drug in low volumes (<50µL) of dimethyl sulfoxide; however, we were unable to dose above 15mg/kg 2X because of substantial body weight loss (Figure 13). The Kraus Laboratory has synthesized new analogues of the JLK1486 drug and suggests these analogues are as potent *in vitro* but have reduced toxicity. Due to time restraints, we were unable to test these new

analogues in either of our *in vitro* or *in vivo* models; however, if these analogues do have decreased toxicity, then clinical application is much more feasible. Additionally, the Kraus Laboratory has recently encapsulated JLK1486 in nanoparticles, providing an alternative form of the drug that may lessen the drugs toxic side-effects. This may allow for increased dosing of the drug at higher concentrations and, when combined with TMZ, may provide a more durable and efficacious response *in vivo*.

At this time, the best available therapy for GBM patients is comprised of surgical resection, radiation, and temozolomide [1] [5]. Clinical trials exploring the standard of care in combination with small molecular inhibitors will, hopefully, lead to an improved standard of care. Perhaps this improvement will not come from small molecules but rather gene therapy. A phase III study exploring the effects of an adenoviral vector expressing the herpes simplex virus type 1 thymidine kinase (AdvHSV-tk) in combination with the standard of care found that addition of AdHSV-tk increased overall survival by 45 days [218]. As the 45 days was not found to be significant, the trial did not translate into clinical use [218]. However, this trial was conducted in 2005, the same year Stupp et al published their groundbreaking TMZ study. Due to approval and accessibility issues, not all patients across the 38 different European clinics received the same treatment or regimen [218, [219]. This discrepancy clearly influences overall survival and as a result has led to the preparation of a glioma based AdvHSV-tk phase III in the United States [219].

Until gene therapy and personalized medicine become achievable clinical therapy options for GBM patients, the best approach is the exploration, use, and implementation of combination therapies. To this end, we suggest that TMZ+JLK1486 is an effective novel drug combination that results in cell death of U87NS cells due to the combination of prolonged ER stress induction and unresolved DNA damage through reduced RAD51.

References

1. Wen PY, Kesari S Malignant Gliomas in Adults. *The New England Journal of Medicine*. **2008**, *359*, 492-507.
2. Mao X, Hamoudi RA Molecular and cytogenetic analysis of glioblastoma multiforme. *Cancer Genetics and Cytogentics*. **2000**, *122*, 87-92.
3. Bredel M, Bredel C, Juric D, Harsh GR, Vogel H, Recht LD, et al. High-Resolution Genome-Wide Mapping of Genetic Alterations in Human Glial Brain Tumors. *Cancer Research*. **2005**, *65*.
4. Furnari FB, Fenton T, Bachoo RM, Mukasa A, Stommel JM, Stegh A, et al. Malignant astrocytic glioma: genetics, biology, and paths to treatment. *Genes & Development*. **2007**, *21*, 2683-710.

5. Stupp R, Mason W Radiotherapy plus Concomitant and Adjuvant Temozolomide for Glioblastoma. *The New England Journal of Medicine*. **2005**, 987-96.
6. Pistollato F, Abbadi S, Rampazzo E, Persano L, Puppa AD, Frasson C, et al. Intratumoral Hypoxic Gradient Drives Stem Cells Distribution and MGMT Expression in Glioblastoma. *Stem Cells*. **2010**, N/A-N/A.
7. Marotta D, Karar J, Jenkins WT, Kumanova M, Jenkins KW, Tobias JW, et al. In Vivo Profiling of Hypoxic Gene Expression in Gliomas Using the Hypoxia Marker EF5 and Laser-capture Microdissection. *Cancer Research*. **2011**, *71*, 779-89.
8. Murat A, Migliavacca E, Hussain SF, Heimberger AB, Desbaillets I, Hamou M-F, et al. Modulation of Angiogenic and Inflammatory Response in Glioblastoma by Hypoxia. *PLOS one*. **2009**, *4*.
9. Bar EE, Lin A, Mahairaki V, Matsui W, Eberhart CG Hypoxia Increases the Expression of Stem-Cell Markers and Promotes Clonogenicity in Glioblastoma Neurospheres. *The American Journal of Pathology*. **2010**, *177*, 1491-502.
10. Schönthal AH Pharmacological targeting of endoplasmic reticulum stress signaling in cancer. *Biochemical Pharmacology*. **2013**, *85*, 653-66.
11. Blais J, Bell JC Novel Therapeutic Targets: The PERKs of Inhibiting the Integrated Stress Response. *Cell Cycle*. **2014**, *5*, 2874-7.
12. Hou X, Liu Y, Liu H, Chen X, Liu M, Che H, et al. PERK silence inhibits glioma cell growth under low glucose stress by blockage of p-AKT and subsequent HK2's mitochondria translocation. *Scientific Reports*. **2015**, *5*, 9065.
13. Pyrko P, Schonthal AH, Hofman FM, Chen TC, Lee AS The Unfolded Protein Response Regulator GRP78/BiP as a Novel Target for Increasing Chemosensitivity in Malignant Gliomas. *Cancer Research*. **2007**, *67*, 9809-16.
14. Virrey JJ, Dong D, Stiles C, Patterson JB, Pen L, Ni M, et al. Stress Chaperone GRP78/BiP Confers Chemoresistance to Tumor-Associated Endothelial Cells. *Molecular Cancer Research*. **2008**, *6*, 1268-75.
15. Lee HK, Xiang C, Cazacu S, Finniss S, Kazimirsky G, Lemke N, et al. GRP78 is overexpressed in glioblastomas and regulates glioma cell growth and apoptosis. *Neuro-Oncology*. **2008**, *10*, 236-43.
16. Raderschall E, Stout K, Freier S, Suckow V, Schweiger S, Haaf T Elevated Levels of RAD51 Recombinaton Protein in Tumor Cells. *Cancer Research*. **2002**, *62*, 219-25.
17. Ohnishi T, Taki T, Hiraga S, Arita N, Morita T In Vitro and in Vivo Potentiation of Radiosensitivity of Malignant Gliomas by Antisense Inhibition of the RAD51 Gene. *Biochemical and Biophysical Research Communications*. **1998**, *245*, 319-24.
18. Short SC, Martindale C, Bourne S, Brand G, Woodcock M, Johnston P DNA repair after irradiation in glioma cells and normal human astrocytes. *Neuro-Oncology*. **2007**, *9*, 404-11.

19. Weatherbee JL, Kraus J-L, Ross AH ER stress in temozolomide-treated glioblastomas interferes with DNA repair and induces apoptosis. *Oncotarget*. **2016**.
20. Watanabe K, Tachibana O, Sato K, Yonekawa Y, Kleihues P, Ohgaki H Overexpression of the EGF Receptor and p53 Mutations are Mutually Exclusive in the Evolution of Primary and Secondary Glioblastomas. *Brain Pathology*. **1996**, *6*, 217-24.
21. Louis David N A Molecular Genetic Model of Astrocytoma Histopathology. *Brain Pathology*. **1997**, *7*, 755-64.
22. Lang FF, Miller DC, Koslow M, Newcomb EW Pathways leading to glioblastoma multiforme: a molecular analysis of genetic alterations in 65 astrocytic tumors. *J Neurosurg*. **1994**, *81*, 427-36.
23. Taylor LP Diagnosis, treatment, and prognosis of glioma. *Neurology*. **2010**, *75*, S28-S32.
24. Chen J, McKay Renée M, Parada Luis F Malignant Glioma: Lessons from Genomics, Mouse Models, and Stem Cells. *Cell*. **2012**, *149*, 36-47.
25. Golding SE, Morgan RN, Adams BR, Hawkins AJ, Povirk LF, Valerie K Pro-survival AKT and ERK signaling from EGFR and mutant EGFRIII enhances DNA double-strand break repair in human glioma cells. *Cancer Biology & Therapy*. **2009**, *8*, 730-8.
26. Liu X, Liu K, Qin J, Hao L, Li X, Liu Y, et al. C/EBPβ promotes angiogenesis through secretion of IL-6, which is inhibited by genistein, in EGFRvIII-positive glioblastoma. *International Journal of Cancer*. **2015**, *136*, 2524-34.
27. Wang M, Wang T, Liu S, Yoshida D, Teramoto A The expression of matrix mealloproteinase-2 and -9 in human gliomas of different patholgoical grades. *Brain Tumor Pathology*. **2003**, *20*, 65-72.
28. McCormick DL Seceretion of cathepsin B by human gliomas in vitro. *Neuropathology and Applied Neurobiology*. **1993**, *19*, 146-51.
29. Newlands ES, Stevens MFG, Wedge SR, Wheelhouse RT, Brock C Temozolomide: a review of its discovery, chemical properties, pre-clincal development and clinical trials. *Cancer Treatment Reviews*. **1997**, 35-61.
30. Saleem A Metabolic Activation of Temozolomide Measured in Vivo Using Positron Emission Tomography. *Cancer Research*. **2003**, *263*, 2409-15.
31. Wedge SR, Porteous J, Newlands ES 3-Aminobenzamine and/or O6-benzylguanine evaluated as an adjuvant to temozolomide or BCNU treatment in cell lines or variable mismtach repair status and O6-alkylguanine-DNA alkyltransferase activity. *British Journal of Cancer*. **1996**.
32. Kaina B, Ziouta A, Ochs K, Coquerelle T Chromosomal instability, reproductive cell death and apoptosis induced by O6-methylguanine in Mex-, Mex+ and methylation-tolerant mismatch repair compromised cells: facts and models. **1997**.

33. Roos WP, Batista LFZ, Naumann SC, Wick W, Weller M, Menck CFM, et al. Apoptosis in malignant glioma cells triggered by the temozolomide-induced DNA lesion O6-methylguanine. *Oncogene*. **2006**, *26*, 186-97.
34. Stupp R, Hegi ME, Mason WP, van den Bent MJ, Taphoorn MJ, Janzer RC, et al. Effects of radiotherapy with concomitant and adjuvant temozolomide versus radiotherapy alone on survival in glioblastoma in a randomised phase III study: 5-year analysis of the EORTC-NCIC trial. *Lancet Oncol*. **2009**, *10*, 2960-5.
35. Moret V, Laras Y, Cresteil T, Aubert G, Ping DQ, Di C, et al. Discovery of a new family of bis-8-hydroxyquinoline substituted benzylamines with pro-apoptotic activity in cancer cells: Synthesis, structure–activity relationship, and action mechanism studies. *European Journal of Medicinal Chemistry*. **2009**, *44*, 558-67.
36. Kraus J-L, Conti F, Madonna S, Tchoghandjian A, Beclin C Alternative responses of primary tumor cells and glioblastoma cell lines to N,N-bis-(8-hydroxyquinoline-5-yl- methyl)-benzyl substitutes amines: Cell death versus P53-independent senscence. *International Journal of Oncology*.
37. Madonna S, Maher P, Kraus J-L N,N-Bis-(8-hydroxyquinoline-5-yl methyl)-benzyl substituted amines (HQNBA): Peroxisome proliferator-activated receptor (PPAR-γ) agonists with neuroprotective properties. *Bioorganic & Medicinal Chemistry Letters*. **2010**, *20*, 6966-8.
38. Bruyere C JLK1486, a Bis 8-Hydroxyquinoline-Substituted Benzylamine, Displays Cytostatic Effects in Experimental Gliomas through MyT1 and STAT1 Activation and, to a Lesser Extent, PPARy Activation. *Translational Oncology*. **2011**, *4*, 126-37.
39. Healy SJM, Gorman AM, Mousavi-Shafaei P, Gupta S, Samali A Targeting the endoplasmic reticulum-stress response as an anticancer strategy. *European Journal of Pharmacology*. **2009**, *625*, 234-46.
40. Yamamori T, Meike S, Nagane M, Yasui H, Inanami O ER stress suppresses DNA double-strand break repair and sensitizes tumor cells to ionizing radiation by stimulating proteasomal degradation of Rad51. *FEBS Letters*. **2013**, *587*, 3348-53.
41. Bindra RS, Schaffer PJ, Meng A, Woo J, Maseide K, Roth ME, et al. Down-Regulation of Rad51 and Decreased Homologous Recombination in Hypoxic Cancer Cells. *Molecular and Cellular Biology*. **2004**, *24*, 8504-18.
42. Nagelkerke A, Bussink J, van der Kogel AJ, Sweep FCGJ, Span PN The PERK/ATF4/LAMP3-arm of the unfolded protein response affects radioresistance by interfering with the DNA damage response. *Radiotherapy and Oncology*. **2013**, *108*, 415-21.
43. Dungey FA, Caldecott KW, Chalmers AJ Enhanced radiosensitization of human glioma cells by combining inhibition of poly(ADP-ribose) polymerase with inhibition of heat shock protein 90. *Molecular Cancer Therapeutics*. **2009**, *8*, 2243-54.
44. Premkumar DR, Jane EP, Agostino NR, DiDomenico JD, Pollack IF Bortezomib-induced sensitization of malignant human glioma cells to vorinostat-

induced apoptosis depends on reactive oxygen species production, mitochondrial dysfunction, Noxa upregulation, Mcl-1 cleavage, and DNA damage. *Molecular Carcinogenesis*. **2013**, *52*, 118-33.
45. Cron KE, Zhu Kea Proteasome Inhibitors Block DNA Repair and Radiosensitize Non-Small Cell Lung Cancer. *PLOS one*. **2013**, *8*.
46. Evans SM, Jenkins KW, Jenkins WT, Dilling T, Judy KD, Schrlau A, et al. Imaging and Analytical Methods as Applied to the Evaluation of Vasculature and Hypoxia in Human Brain Tumors. *Radiation Research*. **2008**, *170*, 677-90.
47. Rivera M, Wu Q, Hamerlik P, Hjelmeland AB, Bao S, Rich JN Acquisition of meiotic DNA repair regulators maintain genome stability in glioblastoma. *Cell Death and Disease*. **2015**, *6*, e1732.
48. Shimada M, Nakanishi M DNA Damage Checkpoints and Cancer. *Journal of Molecular Histology*. **2006**, *37*, 253-60.
49. Zhou B-BS, Elledge SJ The DNA damage response: putting checkpoints in perspective. *Nature*. **2000**, *408*.
50. Velic D, Couturier A, Ferreira M, Rodrigue A, Poirier G, Fleury F, et al. DNA Damage Signalling and Repair Inhibitors: The Long-Sought-After Achilles' Heel of Cancer. *Biomolecules*. **2015**, *5*, 3204-59.
51. Baumann P, West SC Role of the human RAD51 protein in homologous recombination and double-stranded-break repair. *TIBS*. **1998**.
52. Chapman JR, Taylor Martin RG, Boulton Simon J Playing the End Game: DNA Double-Strand Break Repair Pathway Choice. *Molecular Cell*. **2012**, *47*, 497-510.
53. Paull TT, al e A critical role for histone H2AX in recruitment of repair factors to nuclear foci after DNA damage. *Current Biology*. **2000**.
54. Lim YC, Roberts TL, Day BW, Stringer BW, Kozlov S, Fazry S, et al. Increased sensitivity to ionizing radiation by targeting the homologous recombination pathway in glioma initiating cells. *Molecular Oncology*. **2014**, *8*, 1603-15.
55. Lukas J, Lukas C, Bartek J More than just a focus: The chromatin response to DNA damage and its role in genome integrity maintenance. *Nature Cell Biology*. **2011**, *13*, 1161-9.
56. Rogakou EP, Pilch DR, Orr AH, Ivanova VS, Bonner WM DNA Double-stranded Breaks Induce Histone H2AX Phosphorylation on Serine 139. *Journal of Biological Chemistry*. **1998**, *273*, 5858-68.
57. Rhind N, Russell P Signaling Pathways that Regulate Cell Division. *Cold Spring Harbor Perspectives in Biology*. **2012**, *4*, a005942-a.
58. Klein HL The consequences of Rad51 overexpression for normal and tumor cells. *DNA Repair*. **2008**, *7*, 686-93.
59. Linke SP, Sengupta S, Khabie N, Jeffries BA, Buchhop S, Miska S, et al. p53 Interacts with hRAD51 and hRAD54, and Directly Modulates Homologous Recombination. *Cancer Research*. **2003**, *63*, 2596-605.

60. Henning W, Stürzbecher H-W Homologous recombination and cell cycle checkpoints: Rad51 in tumour progression and therapy resistance. *Toxicology*. **2003**, *193*, 91-109.
61. Short SC, Giampieri S, Worku M, Alcaide-German M, Sioftanos G, Bourne S, et al. Rad51 inhibition is an effective means of targeting DNA repair in glioma models and CD133+ tumor-derived cells. *Neuro-Oncology*. **2011**, *13*, 487-99.
62. Tsuzuki t, Fujii Y, Sakumi K, Tominaga Y, Nakao K, Sekiguchi M, et al. Targeted disruption of the Rad51 gene leadsto lethality in embryonic mice. *PNAS*. **1996**, *93*, 6236-40.
63. Calderon IL, Contopoilou CR, Mortimer RK Isolation and Characterization of Yeast DNA Repair Genes. *Current Genetics*. **1983**, *7*, 93-100.
64. Basile G, Aker M, Mortimer RK Nucleotide Sequence and Transciptional Regulation of the Yeast Recombinational Repair Gene Rad51. *Molecular and Cellular Biology*. **1992**, *12*, 3235-46.
65. Aboussekhra A, Chanet R, Adjiri A, Francis F Semidominant Suppressors of Srs2 Helicase Mutations of Saccharomyces cerevisiae Map in the RAD51 Gene, Whose Sequence Predicts a Protein with Similarities to Procaryotic RecA Proteins. *Molecular and Cellular Biology*. **1992**, *12*, 3224-34.
66. Welsh JW, Ellsworth RK, Kumar R, Fjerstad K, Martinez J, Nagel RB, et al. Rad51 Protein Expression and Survival in Patients with Glioblastoma Multiforme. *International Journal of Radiation Oncology*Biology*Physics*. **2009**, *74*, 1251-5.
67. Zhang N, Wu X, Yang L, Xiao F, Zhang H, Zhou A, et al. FoxM1 Inhibition Sensitizes Resistant Glioblastoma Cells to Temozolomide by Downregulating the Expression of DNA-Repair Gene Rad51. *Clinical Cancer Research*. **2012**, *18*, 5961-71.
68. Hall EJ, Giaccia AJ *Radiobiology for the Radiologist*. 6th ed., Lippincott Williams & Wilkins: Philadelphia 2006.
69. Quiros S, Roos WP, Kaina B Rad51 and BRCA2 - New Molecular Targets for Sensitizing Glioma Cells to Alkylating Anticancer Drugs. *PLOS one*. **2011**, *6*, e27183.
70. Sturzbecher H-W, Donzelmann B, Henning W, Knippschild U, Buchhop S p53 is linked directly to homologous recombination processes via RAD51/RecA protein interaction. *EMBO Journal*. **1996**, *15*, 1992-2002.
71. Yoon D, Wang Y, Stapleford K, Wiesmüller L, Chen J p53 Inhibits Strand Exchange and Replication Fork Regression Promoted by Human Rad51. *Journal of Molecular Biology*. **2004**, *336*, 639-54.
72. Russell JS, Brady K, Burgan WE, Cerra MA, Oswald KA, Camphausen K, et al. Gleevec-Mediated Inhibition of Rad51 Expression and Enhancement of Tumor Cell Radiosensitivity. *Cancer Research*. **2003**, *63*, 7377-783.
73. Dungey FA, Löser DA, Chalmers AJ Replication-Dependent Radiosensitization of Human Glioma Cells by Inhibition of Poly(ADP-Ribose) Polymerase: Mechanisms and Therapeutic Potential. *International Journal of Radiation Oncology*Biology*Physics*. **2008**, *72*, 1188-97.

74. Gorman AM, Healy SJM, Jäger R, Samali A Stress management at the ER: Regulators of ER stress-induced apoptosis. *Pharmacology & Therapeutics*. **2012**, *134*, 306-16.
75. Rutkowski DT, Kaufman RJ A trip to the ER: coping with stress. *Trends in Cell Biology*. **2004**, *14*, 20-8.
76. Ma Y Delineation of a Negative Feedback Regulatory Loop That Controls Protein Translation during Endoplasmic Reticulum Stress. *Journal of Biological Chemistry*. **2003**, *278*, 34864-73.
77. Diehl JA, Fuchs SY, Koumenis C The Cell Biology of the Unfolded Protein Response. *Gastroenterology*. **2011**, *141*, 38-41.e2.
78. Munro S, Pelham HRB An Hsp70-like Protein in the ER: Identity with the 78kd Glucose-Regulated Protein and the Immunoglobulin Heavy Chain Binding Protein. *Cell*. **1986**, *46*, 291-300.
79. Bertolotti A, Zhang Y, Hendershot LM, Harding HP, Ron D Dynamic interation of BiP and ER stress tranducers in the unfolded-protein response. *Nature Cell Biology*. **2000**, *2*.
80. Harding HP, Zhang Y, Bertolotti A, Zeng H, Ron D Perk is essential for Translational Regulation and Cell Survival during the Unfolded Protein Response. *Molecular Cell*. **2000**, *5*, 897-904.
81. Sood R, Porter AC, Ma K, Quilliam LA, Wek RC Pancreatic eukaryotic initiation factor-2 alpha kinase (PEK) homologues in humans, Drosophila melangaster and Caenorhabditis elegans that mediate translational control in repsonse to enoplasmic reticulum stress. *Biochem J*. **2000**, *346*, 281-93.
82. Harding HP, Novoa I, Zhang Y, Zeng H, Wek R, Schapira M, et al. Regulated Translational Initiation Controls Stress-Induced Gene Expression in Mammalian Cells. *Molecular Cell*. **2000**, *6*, 1099-108.
83. Szegezdi E Bcl-2 family on guard at the ER. *Am J Phsiol Cell Physiol*. **2009**, *296*.
84. Zhang L, Tong X, Zhang J, Huang J, Wang J DAW22, a natural sesquiterpene coumarin isolated from Ferula ferulaeoides (Steud.) Korov. that induces C6 glioma cell apoptosis and endoplasmic reticulum (ER) stress. *Fitoterapia*. **2015**, *103*, 46-54.
85. Lurlaro R, Muñoz-Pinedo C Cell death induced by endoplasmic reticulum stress. *FEBS Journal*. **2015**, n/a-n/a.
86. Tian X, Ye J, Alonso-Basanta M, Hahn SM, Koumenis C, Dorsey JF Modulation of CCAAT/Enhancer Binding Protein Homologous Protein (CHOP)-dependent DR5 Expression by Nelfinavir Sensitizes Glioblastoma Multiforme Cells to Tumor Necrosis Factor-related Apoptosis-inducing Ligand (TRAIL). *Journal of Biological Chemistry*. **2011**, *286*, 29408-16.
87. Hetschko H, Voss V, Seifert V, Prehn JHM, Kögel D Upregulation of DR5 by proteasome inhibitors potently sensitizes glioma cells to TRAIL-induced apoptosis. *FEBS Journal*. **2008**, *275*, 1925-36.

88. Li Z, Li Z Glucose regulated protein 78: A critical link between tumor microenvironment and cancer hallmarks. *Biochimica et Biophysica Acta (BBA) - Reviews on Cancer*. **2012**, *1826*, 13-22.
89. Lee AS The glucose-rgulated proteins: stress induction and clinical applications. *TRENDS in Biochemical Sciences*. **2001**, *26*, 504-9.
90. Morris JA, Dorner AJ, Edwards CA, Hendershot LM, Kaufman RJ Immunoglobulin Binding Protein (BiP) Function Is Required to Protect Cells from Endoplasmic Reticulum Stress but Is Not Required for the Secretion of Selective Proteins. *The Journal of Biological Chemistry*. **1997**, *272*, 4327-34.
91. Davidson DJ, Haskell C, Majest S, Kherzai A, Egan DA, Walter KA, et al. Kringle 5 of Human Plasminogen Induces Apoptosis of Endothelial and Tumor Cells through Surface-Expressed GLucose-Regulated Protein 78. *Cancer Research*. **2005**, *65*, 4663-72.
92. Dorner AJ, Wasley LC, Kaufman RJ Overexpression of GRP78 mitigates stress induction of glucose regulated proteins and blocks secretion of selective proteins in Chinese hamster ovary cells. *EMBO Journal*. **1992**, *11*, 1563-71.
93. Lee J, Kotliarova S, Kotliarov Y, Li A, Su Q, Donin NM, et al. Tumor stem cells derived from glioblastomas cultured in bFGF and EGF more closely mirror the phenotype and genotype of primary tumors than do serum-cultured cell lines. *Cancer Cell*. **2006**, *9*, 391-403.
94. Quick QA, Faison MO CHOP and caspase 3 induction underlie glioblastoma cell death in response to endoplasmic reticulum stress. *Experimental and Therapeutic Medicine*. **2012**.
95. Dong D, Ni M, Li J, Xiong S, Ye W, Virrey JJ, et al. Critical Role of the Stress Chaperone GRP78/BiP in Tumor Proliferation, Survival, and Tumor Angiogenesis in Transgene-Induced Mammary Tumor Development. *Cancer Research*. **2008**, *68*, 498-505.
96. Koong AC, Chauvan V, Romero-Ramirez L Targeting XBP-1 as a novel anti-cancer strategy. *Cancer Biol Ther*. **2006**, *5*, 756-90.
97. Carrasco D, Sukhdeo K, Protopopova M, Sinha R, Enos M, Carrasco D, et al. The differentiation and stress response factor XBP-1 drives multiple myeloma pathogenesis. *Cancer Cell*. **2007**, *11*, 349-60.
98. Romero-Ramirez L, Cao H, Nelson D, Hammond E, Lee A, Yoshida H, et al. XBP1 is essential for survival under hypoxic conditions and is required for tumor growth. *Cancer Research*. **2004**, *64*, 5943-7.
99. Lin J, Li H, Zhang Y, Ron D, Walter P Divergent effects of PERK and IRE1 signaling on cell viability. *PLOS One*. **2009**, *4*.
100. Harding HP, Zhang Y, Ron D Protein translation and folding are coupled by an endoplasmic-reticulum-resident kinase. *Nature*. **1999**, *397*, 271-4.
101. Abastado J, Miller P, Jackson B, KHinnebusch A Suppresion of ribosomal reinitiaion at upstream open reading frames in amino acid straved cells forms the basis for GCN4 translational control. *Molecular and Cellular Biology*. **1991**, *11*, 486-96.

102. Dever TE, Feng L, Wek RC, Cigan AM, Donahue TF, Hinnebusch AG Phosphorylation of Initiation Factor 2 apha by protein kinase GCN2 mediates gene-specific translational control of GCN4 in yeast. *Cell*. **1992**, *68*, 585-96.
103. De Haro C, Mendez R, Santoyo J The eIF-2alpha kinase and the control of protein synthesis. *FASEB J*. **1996**, *12*, 1378-87.
104. Chen J, London I Regulation of protein synthesis by heme-regulated eIF-2 alpha kinase. *Trends Biochem Sci*. **1995**, *20*, 105-8.
105. Berry M, Knutson G, Lasky S, Munemitsu S, Samuel C Mechanism of inteferon action, Purifcation and substrate specificities of the double -stranded RNA-dependent protein kinase form untreated and inteferson-treated mouse fibroblasts. *J Biol Chem*. **1985**, *20*, 11240-7.
106. Shi Y, Vattem KM, Sood R, An J, Liang J, Stramm L, et al. Identification and Characterization of Pancreatic Eukaryotic Initiation Factor 2 alpha-Subunit Kinase, PEK, Involved in Translational Control. *Molecular and Cellular Biology*. **1998**, *18*, 7499-509.
107. Harding HP, Zeng H, Zhang Y, Jungries R, Chung P, Plesken H, et al. Diabetes Mellitus and Exocrine Dysfunction in Perk -/- Mice Reveals a Role for Translational Control in Secreretory Cell Survival. *Molecular Cell*. **2001**, *7*, 1153-63.
108. Bi M, Naczki C, Koritzinsky M, Fels D, Blain J, Hu N, et al. ER stress-regulated translation increases tolerance to extreme hypoxia and promotes tumor growth. *EMBO Journal*. **2005**, *24*, 3470-81.
109. Blais JD, Addison CL, Edge R, Falls T, Zhao H, Wary K, et al. Perk-Dependent Translational Regulation Promotes Tumor Cell Adaptation and Angiogenesis in Response to Hypoxic Stress. *Molecular and Cellular Biology*. **2006**, *26*, 9517-32.
110. Avivar-Valderas A, Salas E, Bobrovnikova-Marjon E, Diehl JA, Nagi C, Debnath J, et al. PERK integrates autophay and oxidative stress responses to promote survival during extracellular matrix. *Mol Cell Biol*. **2011**, *31*, 3616-29.
111. Dey S, Sayers CM, Verginadis II, Lehman SL, Cheng Y, Cerniglia GJ, et al. ATF4-dependent induction of heme oxygenase 1 prevents anoikis and promotes metastasis. *Journal of Clinical Investigation*. **2015**, *125*, 2592-608.
112. Bobrovnikova-Marjon E, Grigoriadou C, Pytel D, Zhang F, Ye J, Koumenis C, et al. PERK promotes cancer cell proliferation and tumor growth by limiting oxidative DNA damage. *Oncogene*. **2010**, *29*, 3881-95.
113. Tanaka T, Tsujimura T, Takeda K, Sugihara A, Maekawa A, Terada N, et al. Targeted disruption of the ATF4 discloses its essential role in the formation of eye lens fibres. *Genes to Cells*. **1998**, *3*, 801-10.
114. Hai T, Liu F, Coukos WJ, Green MR Transcription factor ATF cDNA clones: an extensive family of leucine zipper proteins able to selectively form DNA-binding heterodimers. *Genes and Development*. **1989**, *3*, 2083-90.
115. Vallejo M, Ron D, Miller CP, Habener JF C/ATF, a member of the activating transcription factor family of DNA-binding proteins, dimerizes with

CAAT/enhancer-binding proteins and directs their binding to cAMP response elements. *Proceedings of the National Academy of Sciences*. **1993**, *90*, 4679-83.
116. Podust LM, Krezel AM, Kim Y Crystal Structure of the CCAAT Box/Enhancer-binding Protein beta Activating Transcription Factor-4 Basic Leucine Zipper Heterodimer in the Absence of DNA. *Journal of Biological Chemistry*. **2001**, *276*, 505-13.
117. Karpinski BA, Morle GD, Huggenvik J, Uhler MD, Leiden JM Molecular cloning of human CREB-2: An ATF/CREB transcription factor that can negatively regulate transcription from the cAMP response element. *Proceedings of the National Academy of Sciences*. **1992**, *89*, 4820-4.
118. Tsujimotot A, Nyunoya H, Morita T, Sato T, Shimotohno K Isolation of cDNAs for DNA-Binding Proteins Which Specifically Bind to a tax-Responsive Enhancer Element in the Long Terminal Repeat of Human T-Cell Leukemia Virus Type I. *Journal of Virology*. **1991**, *65*, 1420-6.
119. Hettmann T, Barton K, Leiden JM Microphthalmia due to p53-mediated apoptosis of anterior lens epithelial cells in mice lacking the CREB-2 transcription factor. *Developmental Biology*. **2000**, *222*, 110-23.
120. Mueller PP, Hinnebusch AG Multiple upstream AUG codons mediate translational control of GCN4. *Cell*. **1986**, *45*, 201-7.
121. Sonenberg N, Hinnebusch AG Regulation of translation initiation in eukaryotes: mechanisms and biological targets. *Cell*. **2009**, *136*.
122. Chan C-P, Kok K-H, Tang H-MV, Wong C-M, Jin D-Y Internal ribosome entry site-mediated translational regulation of ATF4 splice variant in mammalian unfolded protein response. *Biochimica et Biophysica Acta (BBA) - Molecular Cell Research*. **2013**, *1833*, 2165-75.
123. Luo S, Baumeister P, Yang S, Abcouwer SF, Lee AS Induction of Grp78/BiP by Translational Block: ACTIVATION OF THE Grp78 PROMOTER BY ATF4 THROUGH AN UPSTREAM ATF/CRE SITE INDEPENDENT OF THE ENDOPLASMIC RETICULUM STRESS ELEMENTS. *Journal of Biological Chemistry*. **2003**, *278*, 37375-85.
124. Ma Y, Brewer JW, Alan Diehl J, Hendershot LM Two Distinct Stress Signaling Pathways Converge Upon the CHOP Promoter During the Mammalian Unfolded Protein Response. *Journal of Molecular Biology*. **2002**, *318*, 1351-65.
125. Fawcett TW, Martindale JL, Guyton KZ, Ha T, Holbrook NJ Complexes containing activating transcription factor (ATF)/cAMP-responsive element-binding proein (CREB) interact with the CCAAT/enhancer-binding protein (C/EBP)-ATF composite site to regulate Gadd153 expression during the stress response. *Biochem J*. **1999**, *339*, 135-41.
126. Alexandre S, Nakaki T, Vanhamme L, Lee AS A Binding Site for the Cyclic Adenosine 3',5'-Mononphosphate-Response Element-Binding Protein as a Regulatory Element in the grp78 Promoter. *Molecular Endocrinology*. **1991**, *5*, 1862-72.

127. Hope IA, Struhl K GCN4 Protein, Synthesized In Vitro, Binds HIS3 Regulatory Sequences: Implication for General Control of Amino Acid Biosynthetic Genes in Yeast. *Cell*. **1985**, *43*.
128. Siu F, Bain PJ, LeBlanc-Chaffin R, Chen H, Kilberg MS ATF4 Is a Mediator of the Nutrient-sensing Response Pathway That Activates the Human Asparagine Synthetase Gene. *Journal of Biological Chemistry*. **2002**, *277*, 24120-7.
129. Rzymski T, Milani M, Pike L, Buffa F, Mellor HR, Winchester L, et al. Regulation of autophagy by ATF4 in response to severe hypoxia. *Oncogene*. **2010**, *29*, 4424-35.
130. Zhu H, Xia L, Zhang Y, Wang H, Xu W, Hu H, et al. Activating Transcription Factor 4 Confers a Multidrug Resistance Phenotype to Gastric Cancer Cells through Transactivation of SIRT1 Expression. *PLOS one*. **2012**, *7*, e31431.
131. Wang Z, Chen W Emerging Roles of SIRT1 in Cancer Drug Resistance. *Genes & Cancer*. **2013**, *4*, 82-90.
132. Jr. F, Albert J., Jr A, Isaac, Hollander MC DNA damage-inducible transcripts in mammalian cells. *Proceedings of the National Academy of Sciences*. **1988**, *85*, 8800-4.
133. Ghosh AP, Klocke BJ, Ballestas ME, Roth KA CHOP Potentially Co-Operates with FOXO3a in Neuronal Cells to Regulate PUMA and BIM Expression in Response to ER Stress. *PLOS one*. **2012**, *7*, e39586.
134. Barone MV, Crozat A, Tabaee A, Philipson L, Ron D CHOP(GADD153) and its oncogenic variant, TLS-CHOP, have opposing effects on the induction of G1/S arrest. *Genes & Development*. **1994**, *8*, 453-64.
135. Wang X-Z, Lawson B, Brewer JW, Zinszner H, Sanjay A, Mi L-J, et al. Signals from the Stressed Endoplasmic Reticulum Induce C/EBP-Homologous Protein (CHOP/GADD153). *Molecular and Cellular Biology*. **1996**, *16*, 4273-80.
136. Zinszner H, Kuroda M, Wang X, Batchvarova N, Lightfoot RT, Remotti H, et al. CHOP is implicated in programmed cell death in response to impaired function of the endoplasmic reticulum. *Genes and Development*. **1998**, *12*, 982-95.
137. Jiang S, Zhang E, Zhang R, Li X Altered activity patterns of transcription factors induced by endoplasmic reticulum stress. *BMC Biochemistry*. **2016**, *17*.
138. Shen L, Wen N, Xia M, Zhang Y, Liu W, Xu Y, et al. Calcium efflux from the endoplasmic reticulum regulates cisplatin-induced apoptosis in human cervical cancer HeLa cells. *Oncology Letters*. **2016**.
139. Ma J, Qiu Y, Yang L, Peng L, Xia Z, Hou L-N, et al. Desipramine induces apoptosis in rat glioma cells via endoplasmic reticulum stress-dependent CHOP pathway. *Journal of Neuro-Oncology*. **2011**, *101*, 41-8.
140. Zang C, Liu H, Bertz J, Possinger K, Koeffler HP, Elstner E, et al. Induction of endoplasmic reticulum stress response by TZD18, a novel dual ligand for peroxisome proliferator-activated receptor / , in human breast cancer cells. *Molecular Cancer Therapeutics*. **2009**, *8*, 2296-307.

141. Kim IY, Kang YJ, Yoon MJ, Kim EH, Kim SU, Kwon TK, et al. Amiodarone sensitizes human glioma cells but not astrocytes to TRAIL-induced apoptosis via CHOP-mediated DR5 upregulation. *Neuro-Oncology*. **2011**, *13*, 267-79.
142. Liu WT, Huang CY, Lu IC, Gean PW Inhibition of glioma growth by minocycline is mediated through endoplasmic reticulum stress-induced apoptosis and autophagic cell death. *Neuro-Oncology*. **2013**, *15*, 1127-41.
143. Marciniak SJ, Yun CY, Oyadomari S, al e CHOP induces death by promoting protein synthesis and oxidation in the stressed endoplasmic reticulum. *Genes & Development*. **2004**, *18*, 3066-77.
144. McCullough KD, Martindale JL, Klotz LO, Aw TY, Holbrook NJ Gadd153 Sensitizes Cells to Endoplasmic Reticulum Stress by Down-Regulating Bcl2 and Perturbing the Cellular Redox State. *Molecular and Cellular Biology*. **2001**, *21*, 1249-59.
145. Kim EH, Yoon MJ, Kim SU, Kwon TK, Sohn S, Choi KS Arsenic Trioxide Sensitizes Human Glioma Cells, but not Normal Astrocytes, to TRAIL-Induced Apoptosis via CCAAT/Enhancer-Binding Protein Homologous Protein Dependent DR5 Up-regulation. *Cancer Research*. **2008**, *68*, 266-75.
146. Kim JY, Kim EH, Kim SU, Kwon TK, Choi KS Capsaicin sensitizes malignant glioma cells to TRAIL-mediated apoptosis via DR5 upregulation and survivin downregulation. *Carcinogenesis*. **2009**, *31*, 367-75.
147. Woo JS, Kim SM, Jeong CH, Ryu CH, Jeun S-S Lipoxygenase inhibitor MK886 potentiates TRAIL-induced apoptosis through CHOP- and p38 MAPK-mediated up-regulation of death receptor 5 in malignant glioma. *Biochemical and Biophysical Research Communications*. **2013**, *431*, 354-9.
148. Cao L, Lei H, Chang M-Z, Liu Z-Q, Bie X-H Down-regulation of 14-3-3β exerts anti-cancer effects through inducing ER stress in human glioma U87 cells: Involvement of CHOP–Wnt pathway. *Biochemical and Biophysical Research Communications*. **2015**, *462*, 389-95.
149. Han J, Back SH, Hur J, Lin Y-H, Gildersleeve R, Shan J, et al. ER-stress-induced transcriptional regulation increases protein synthesis leading to cell death. *Nature Cell Biology*. **2013**, *15*, 481-90.
150. Gilbert CA, Daou MC, Moser RP, Ross AH Gamma-secretase inhibitors enhance temozolomide treatment of human gliomas by inhibiting neurosphere repopulation and xenograft recurrence. *Cancer Res*. **2010**, *70*, 6870-9.
151. Tabas I, Ron D Integrating the mechanisms of apoptosis induced by endoplasmic reticulum stress. *Nature cell biology*. **2011**, *13*, 184-90.
152. Wang Q, Mora-Jensen H, Weniger MA, Perez-Galan P, Wolford C, Hai T, et al. ERAD inhibitors integrate ER stress with an epigenetic mechanism to activate BH3-only protein NOXA in cancer cells. *Proc Natl Acad Sci U S A*. **2009**, *106*, 2200-5.
153. Han J, Back SH, Hur J, Lin YH, Gildersleeve R, Shan J, et al. ER-stress-induced transcriptional regulation increases protein synthesis leading to cell death. *Nat Cell Biol*. **2013**, *15*, 481-90.

154. Rhind N, Russell P Signaling pathways that regulate cell division. *Cold Spring Harb Perspect Biol*. **2012**, *4*.
155. Uziel T, Lerenthal Y, Moyal L, Andegeko Y, Mittelman L, Shiloh Y Requirement of the MRN complex for ATM activation by DNA damage. *EMBO J*. **2003**, *22*, 5612-21.
156. Kobayashi J, Tauchi H, Chen B, Burma S, Tashiro S, Matsuura S, et al. Histone H2AX participates the DNA damage-induced ATM activation through interaction with NBS1. *Biochem Biophys Res Commun*. **2009**, *380*, 752-7.
157. Wang R, Chadalavada K, Wilshire J, Kowalik U, Hovinga KE, Geber A, et al. Glioblastoma stem-like cells give rise to tumour endothelium. *Nature*. **2010**, *468*, 829-33.
158. Moret V, Laras Y, Cresteil T, Aubert G, Ping DQ, Di C, et al. Discovery of a new family of bis-8-hydroxyquinoline substituted benzylamines with pro-apoptotic activity in cancer cells: synthesis, structure-activity relationship, and action mechanism studies. *Eur J Med Chem*. **2009**, *44*, 558-67.
159. Madonna S, Beclin C, Laras Y, Moret V, Marcowycz A, Lamoral-Theys D, et al. Structure-activity relationships and mechanism of action of antitumor bis 8-hydroxyquinoline substituted benzylamines. *Eur J Med Chem*. **2010**, *45*, 623-38.
160. Ramirez YP, Mladek AC, Phillips RM, Gynther M, Rautio J, Ross AH, et al. Evaluation of novel imidazotetrazine analogues designed to overcome temozolomide resistance and glioblastoma regrowth. *Mol Cancer Ther*. **2015**, *14*, 111-9.
161. Stupp R, Brada M, van den Bent MJ, Tonn JC, Pentheroudakis G High-grade glioma: ESMO Clinical Practice Guidelines for diganosis, treatment and follow-up. *Annals of Oncology*. **2014**.
162. Wong ET, Hess KR, Gleason MJ, Jeackle KA, Kyritsis AP, Prados MD, et al. Outcomes and Prognostic Factoes in Recurrent Glioma Patients Enrolled Onto Phase II Clinical Trials. *Journal of Clinical Oncology*. **1999**, *17*, 2572-8.
163. Singh SK, Clarke ID, Terasaki M, Bonn VE, Hawkins C, Squire J, et al. Identification of a Cancer Stem Cell in Human Brain Tumors. *Cancer Research*. **2003**, *63*, 5821-8.
164. Singh SK, Hawkins C, Clarke ID, Squire JA, Bayani J, Hide T, et al. Identification of human brain tumour initiating cells. *Nature*. **2004**, *432*, 396-400.
165. Liu X, Han EK, Anderson M, Shi Y, Semizarov D, Wang G, et al. Acquired Resistance to Combination Treatment with Temozolomide and ABT-888 Is Mediated by Both Base Excision Repair and Homologous Recombination DNA Repair Pathways. *Molecular Cancer Research*. **2009**, *7*, 1686-92.
166. Chakravarti A, Erkkinen MG, Nestler U, Stupp R, Mehta M, Aldape K, et al. Temozolomide-Mediated Radiation Enhancement in Glioblastoma: A Report on Underlying Mechanisms. *Clinical Cancer Research*. **2006**, *12*, 4738-46.
167. Ramirez Y, Weatherbee J, Wheelhouse R, Ross A Glioblastoma Multiforme Therapy and Mechanisms of Resistance. *Pharmaceuticals*. **2013**, *6*, 1475-506.

168. Cahill DP, Levine KK, Betensky RA, Codd PJ, Romany CA, Reavie LB, et al. Loss of the Mismatch Repair Protein MSH6 in Human Glioblastomas Is Associated with Tumor Progression during Temozolomide Treatment. *Clinical Cancer Research*. **2007**, *13*, 2038-45.
169. Friedman HS, McLendon Roger E, Kerby T, Dugan M, Bigner SH, Henry AJ, et al. DNA Mismatch Repair and O6-Alkylguanine-DNA Alkyltransferase Analysis and Response to Temodal in Newly Diagnosed Maligant Glioma. *Journal of Clinical Oncology*. **1998**, *16*, 3851-7.
170. Felsberg J, Thon N, Eigenbrod S, Hentschel B, Sabel MC, Westphal M, et al. Promoter methylation and expression of MGMT and the DNA mismatch repair genes MLH1, MSH2, MSH6 and PMS2 in paired primary and recurrent glioblastomas. *International Journal of Cancer*. **2011**, *129*, 659-70.
171. Stark AM, Witzel P, Strege RJ, Hugo H-H, Mehdorn HM p53, mdm2, EGFR, and msh2 expression in paired initial and recurrent glioblastoma multiforme. *J Neurol Neurosurg Psychiatry*. **2003**, *74*, 779-83.
172. Kurz EU, Lees-Miller SP DNA damage-induced activation of ATM and ATM-dependent signaling pathways. *DNA Repair*. **2004**, *3*, 889-900.
173. Meir EGV, Kikuchi T, Tada M, Li H, Diserens A-C, Wojcik BE, et al. Analysis of the p53 Gene and Its Expression in Human Glioblastoma Cells. *Cancer Research*. **1994**, *54*, 649-52.
174. Bonnet D, Dick J Human acute myeloid leukemia is organized as a hierarachy that originates from a primitive hematopoietic cell. *Nature Medicine*. **1997**, *7*, 730-7.
175. Lapidot Tea, Sirard C, Vormoor J, Murdoch B, Hoang T, Caceres-Cortes J, et al. A cell initiating human acute myeloid leukemia after transplantation into SCID mice. *Nature*. **1994**, *367*, 645-8.
176. Gupta PB, Chaffer CL, Weinberg RA Cancer stem cells: mirage or reality? *Nature Medicine*. **2009**, *15*.
177. Pattabiraman DR, Weinberg RA Tackling the cancer stem cells — what challenges do they pose? *Nature Reviews Drug Discovery*. **2014**, *13*, 497-512.
178. Reynolds BA, Weiss S Generation of Neurons and Astrocytes from Isolated Cells of the Adult Mammalian Central Nervous System. *Science*. **1992**, *255*, 1707-10.
179. Morshead CM, Reynolds BA, Craig CC, McBurnet MW, Staines WA, Morassutti D, et al. Neural Stem Cells in the Adult Mammalian Forebrain: A Relativly Quiescent Subpopulation of Subependymal Cells. *Neuron*. **1994**, *13*, 1071-82.
180. Okano H, Sawamoto K Neural stem cells: involvement in adult neurogenesis and CNS repair. *Philosophical Transactions of the Royal Society B: Biological Sciences*. **2008**, *363*, 2111-22.
181. Temple S, Alvarez-Buylla A Stem cells in the adult mammalian central nervous system. *Current Opinion in Neurobiology* **1999**, *9*, 135-41.

182. Bao S, Wu Q, McLendon RE, Hao Y, Shi Q, Hjelmeland AB, et al. Glioma stem cells promote radioresistance by preferential activation of the DNA damage response. *Nature*. **2006**, *444*, 756-60.
183. Borovski T, Verhoeff JJC, ten Cate R, Cameron K, de Vries NA, van Tellingen O, et al. Tumor microvasculature supports proliferation and expansion of glioma-propagating cells. *International Journal of Cancer*. **2009**, *125*, 1222-30.
184. Chen R, Nishimura MC, Bumbaca SM, Kharbanda S, Forrest WF, Kasman IM, et al. A Hierarchy of Self-Renewing Tumor-Initiating Cell Types in Glioblastoma. *Cancer Cell*. **2010**, *17*, 362-75.
185. Beier D, Hau P, Proescholdt M, Lohmeier A, Wischhusen J, Oefner PJ, et al. CD133+ and CD133- Glioblastoma-Derived Cancer Stem Cells Show Differential Growth Characteristics and Molecular Profiles. *Cancer Research*. **2007**, *67*, 4010-5.
186. Joo KM, Kim SY, Jin X, Song SY, Kong D-S, Lee J, II, et al. Clinical and biological implications of CD133-positive and CD133-negative cells in glioblastomas. *Laboratory Investigation*. **2008**, *88*, 808-15.
187. Wang J, Sakariassen PØ, Tsinkalovsky O, Immervoll H, Bøe SO, Svendsen A, et al. CD133 negative glioma cells form tumors in nude rats and give rise to CD133 positive cells. *International Journal of Cancer*. **2008**, *122*, 761-8.
188. Shmelkov SV CD133 expression is not restricted to stem cells, and both CD133+ and CD133- metastatic colon cancer cells initiate tumors. *The Journal of Clinical Invesitigation*. **2008**, *118*, 2111-20.
189. Cheng J-X, Liu B-L, Zhang X How powerful is CD133 as a cancer stem cell marker in brain tumors? *Cancer Treatment Reviews*. **2009**, *35*, 403-8.
190. Venere M, Fine HA, Dirks PB, Rich JN Cancer stem cells in gliomas: Identifying and understanding the apex cell in cancer's hierarchy. *Glia*. **2011**, n/a-n/a.
191. Bachoo RM, Maher EA, Ligon KL, Sharpless NE, Chan SS, You MJ, et al. Epidermal growth factor receptor and Ink4a/Arf: Convergent mechanisms governing terminal differentiation and transfomration along the neural stem cell to astrocyte axis. *Cancer Cell*. **2002**, *1*.
192. Uhrbom L, Kastemar M, Johansson FK, Westermark B, Holland EC Cell Type-Specific Tumor Suppression by Ink4a and Arf in Kras-Induce Mouse Gliomagenesis. *Cancer Research*. **2005**, *65*.
193. Jacques TS, Swales A, Brzozowski MJ, Henriquez NV, Linehan JM, Mirzadeh Z, et al. Combinations of genetic mutations in the adult neural stem cell compartment determine brain tumour phenotypes. *The EMBO Journal*. **2009**, *29*, 222-35.
194. Rich RJGaJN Making a tumour's bed-glioblastoma stem cells and the vascualr niche.pdf. *nature*. **2007**, *7*, 733-6.
195. Takahashi K, Yamanaka S Induction of Pluripotent Stem Cells from Mouse Embryonic and Adult Fibroblast Cultures by Defined Factors. *Cell*. **2006**, *126*, 663-76.

196. Utikal J, Polo JM, Stadtfeld M, Maherali N, Kulalert W, Walsh RM, et al. Immortalization eliminates a roadblock during cellular reprogramming into iPS cells. *Nature*. **2009**, *460*, 1145-8.
197. Alcantara Llaguno S, Chen J, Kwon C-H, Jackson EL, Li Y, Burns DK, et al. Malignant Astrocytomas Originate from Neural Stem/Progenitor Cells in a Somatic Tumor Suppressor Mouse Model. *Cancer Cell*. **2009**, *15*, 45-56.
198. Park C-K The changes in MGMT promoter methylation status in initial and recurrent glioblastomas. *Translational Oncology*. **2012**, *5*, 393-7.
199. Pegg A Repair of O(6)-alkylguanine by alkyltransferases. *Mutation Research*. **2000**, *462*, 83-100.
200. Kanzawa T, Bedwell J, Kondo Y, Kondo S, Germano IM Inhibition of DNA repair for sensitizing resistance glioma cells to temozolomide. *J Neurosurg*. **2003**, *99*, 1047-52.
201. Quinn JA, Desjardins A, Weingart J, Brem H, Dolan ME, Delaney SM, et al. Phase I trial of temozolomide plus O6-benzylguanine for patients with recurrent or progressive malignant glioma. *J Clin Oncol*. **2005**, *28*, 7178-87.
202. Friedman HS, Prados MD, Wen PY, Mikkelsen T, Schiff D, Abrey LE, et al. Bevacizumab Alone and in Combination With Irinotecan in Recurrent Glioblastoma. *Journal of Clinical Oncology*. **2009**, *27*, 4733-40.
203. Vredenburgh JJ, Desjardins A, Herndon JE, Dowell JM, Reardon DA, Quinn JA, et al. Phase II Trial of Bevacizumab and Irinotecan in Recurrent Malignant Glioma. *Clinical Cancer Research*. **2007**, *13*, 1253-9.
204. Jain RK, di Tomaso E, Duda DG, Loeffler JS, Sorensen AG, Batchelor TT Angiogenesis in brain tumours. *Nature Reviews Neuroscience*. **2007**, *8*, 610-22.
205. Karpel-Massler G, Westhoff MA, Zhou S, Nonnenmacher L, Dwucet A, Kast RE, et al. Combined Inhibition of HER1/EGFR and RAC1 Results in a Synergistic Antiproliferative Effect on Established and Primary Cultured Human Glioblastoma Cells. *Molecular Cancer Therapeutics*. **2013**, *12*, 1783-95.
206. Caravita T, de Fabritiis P, Palumbo A, Amadori S, Boccadoro M Bortezomib: efficacy comparisons in solid tumors and hematologic malignancies. *Nature Clinical Practice Oncology*. **2006**, *3*, 374-87.
207. Bota DA, Alexandru D, Keir ST, Bigner D, Vredenburgh J, Friedman HS Proteasome inhibition with bortezomib induces cell death in GBM stem-like cells and temozolomide-resistant glioma cell lines, but stimulates GBM stem-like cells' VEGF production and angiogenesis. *Journal of Neurosurgery*. **2013**, *119*, 1415-23.
208. Williamson MJ, Silva MD, Terkelsen J, Robertson R, Yu L, Xia C, et al. The relationship among tumor architecture, pharmacokinetics, pharmacodynamics, and efficacy of bortezomib in mouse xenograft models. *Molecular Cancer Therapeutics*. **2009**, *8*, 3234-43.
209. Vlachostergios PJ, Papandreou CN Efficacy of low dose temozolomide in combination with bortezomib in U87 glioma cells: a flow cytometric analysis. *Archives of Medical Science*. **2015**, *2*, 307-10.

210. Jacquemont C, Taniguchi T Proteasome Function Is Required for DNA Damage Response and Fanconi Anemia Pathway Activation. *Cancer Research*. **2007**, *67*, 7395-405.
211. Murakawa Y, Sonoda E, Barber LJ, Zeng W, Yokomori K, Kimura H, et al. Inhibitors of the Proteasome Suppress Homologous DNA Recombination in Mammalian Cells. *Cancer Research*. **2007**, *67*, 8536-43.
212. Pyrko P, Kardosh A, Liu YT, Soriano N, Xiong W, Chow RH, et al. Calcium-activated endoplasmic reticulum stress as a major component of tumor cell death induced by 2,5-dimethyl-celecoxib, a non-coxib analogue of celecoxib. *Molecular Cancer Therapeutics*. **2007**, *6*, 1262-75.
213. Kardosh A, Golden EB, Pyrko P, Uddin J, Hofman FM, Chen TC, et al. Aggravated Endoplasmic Reticulum Stress as a Basis for Enhanced Glioblastoma Cell Killing by Bortezomib in Combination with Celecoxib or Its Non-Coxib Analogue, 2,5-Dimethyl-Celecoxib. *Cancer Research*. **2008**, *68*, 843-51.
214. White MC, Johnson GG, Zhang W, Hobrath JV, Piazza GA, Grimaldi M Sulindac sulfide inhibits sarcoendoplasmic reticulum Ca2+ATPase, induces endoplasmic reticulum stress response, and exerts toxicity in glioma cells: Relevant similarities to and important differences from celecoxib. *Journal of Neuroscience Research*. **2013**, *91*, 393-406.
215. Booth L, Roberts JL, Cruickshanks N, Tavallai S, Webb T, Samuel P, et al. PDE5 Inhibitors Enhance Celecoxib Killing in Multiple Tumor Types. *Journal of Cellular Physiology*. **2015**, *230*, 1115-27.
216. Gupta AK, Li B, Cerniglia GJ, Ahmed MS, Hahn SM, Maity A The HIV protease ihibitor nelfinavir downregulates Akt phosphorylation by inhibiting proteasomal activity and inducing the unfolded protein response. *Neoplasia*. **2007**, *9*, 271-8.
217. Xipell E, Aragón T, Martínez-Velez N, Vera B, Idoate MA, Martínez-Irujo JJ, et al. Endoplasmic reticulum stress-inducing drugs sensitize glioma cells to temozolomide through downregulation of MGMT, MPG, and Rad51. *Neuro-Oncology*. **2016**, now022.
218. Westphal M, Yia-Herttuala S, Martin J, Warnke P, Menei P, Eckland D, et al. Adenovirus-mediated gene therapy with sitimagene ceradenovec followed by intravenous ganciclovir for patients with operable high-grade glioma (ASPECT): a randomised, open-label, phase 3 trial. *Lancet Oncol*. **2013**, *14*, 823-33.
219. Castro MG, Lowenstein PR Neuro-oncology: The long and winding road—gene therapy for glioma. *Nature Reviews Neurology*. **2013**, *9*, 609-10.